Pacific Northwest
NATIONAL LABORATORY

PNNL-38154

Integrated Multi-Fidelity Model and Co-Simulation Platform for Distribution System Transient and Dynamic Analysis—DistribuDyn

August 2025

Wei Du
Sheik M. Mohiuddin
Udoka C. Nwaneto
Francis K. Tuffner
Xiaonan Lu
Yaosuo S. Xue
Hanchao Liu
Zhe Chen
Roshan Sharma

U.S. DEPARTMENT of ENERGY

Prepared for the U.S. Department of Energy
under Contract DE-AC05-76RL01830

DISCLAIMER

PACIFIC NORTHWEST NATIONAL LABORATORY
operated by
BATTELLE
for the
UNITED STATES DEPARTMENT OF ENERGY
under Contract DE-AC05-76RL01830

Printed in the United States of America

Available to DOE and DOE contractors from
the Office of Scientific and Technical Information,
P.O. Box 62, Oak Ridge, TN 37831-0062
www.osti.gov
ph: (865) 576-8401
fox: (865) 576-5728
email: reports@osti.gov

Available to the public from the National Technical Information Service
5301 Shawnee Rd., Alexandria, VA 22312
ph: (800) 553-NTIS (6847)
or (703) 605-6000
email: info@ntis.gov
Online ordering: http://www.ntis.gov

PNNL-38154

Integrated Multi-Fidelity Model and Co-Simulation Platform for Distribution System Transient and Dynamic Analysis—DistribuDyn

August 2025

Wei Du
Sheik M. Mohiuddin
Udoka C. Nwaneto
Francis K. Tuffner
Xiaonan Lu
Yaosuo S. Xue
Hanchao Liu
Zhe Chen
Roshan Sharma

Prepared for
the U.S. Department of Energy
under Contract DE-AC05-76RL01830

Pacific Northwest National Laboratory
Richland, Washington 99354

Final Technical Report (FTR)

a. Federal Agency	Department of Energy	
b. Award Number	38453	
c. Project Title	Integrated Multi-Fidelity Model and Co-Simulation Platform for Distribution System Transient and Dynamic Analysis—DistribuDyn	
d. Recipient Organization	Pacific Northwest National Laboratory	
e. Project Period	Start: 10/21/2021	End: 3/31/2025
f. Principal Investigator (PI)	Wei Du Staff Research Engineer Wei.du@pnnl.gov (509) 371-6609	
g. Business Contact (BC)	Kathleen Judd Project Management Office Director kathleen.judd@pnnl.gov (206) 528-3330	
h. Certifying Official (if different from the PI or BC)	Name Title Email address Phone number	

Wei Du *5/15/2025*

Signature of Certifying Official Date

By signing this report, I certify to the best of my knowledge and belief that the report is true, complete, and accurate. I am aware that any false, fictitious, or fraudulent information, misrepresentations, half-truths, or the omission of any material fact, may subject me to criminal, civil or administrative penalties for fraud, false statements, false claims or otherwise. (U.S. Code Title 18, Section 1001, Section 287 and Title 31, Sections 3729-3730). I further understand and agree that the information contained in this report are material to Federal agency's funding decisions and I have any ongoing responsibility to promptly update the report within the time frames stated in the terms and conditions of the above referenced Award, to ensure that my responses remain accurate and complete.

Acknowledgement: This material is based upon work supported by the U.S. Department of Energy's Office of Energy Efficiency and Renewable Energy (EERE) under the Solar Energy Technologies Office Award Number 38453.

Executive Summary:

As inverter-based, distributed energy resources (DERs) and variable loads continue to proliferate across distribution systems, it is increasingly important to understand their impacts on system stability and reliability. However, most commercially available simulation tools for distribution planning primarily focus on steady-state and quasi-steady-state analysis, offering limited capabilities to study transient and dynamic behaviors.

To address this gap, the project team developed an integrated multi-fidelity modeling and co-simulation platform that enables simulating the transient and dynamic behavior of distribution systems featuring a high penetration of inverter-based DERs and variable loads. The project team achieved the following accomplishments. First, the network solver of the DOE-funded open-source tool GridLAB-D has been updated to handle short-circuit fault simulations, enabling it to simulate large-signal fault scenarios of distribution systems. Second, the co-simulation between GridLAB-D and the commercial electromagnetic transient (EMT) simulation tool PSCAD has been achieved by using the DOE-funded co-simulation engine HELICS™. This allows the integration of black-box PSCAD inverter models developed by manufacturers into realistic distribution feeder models to examine their impact at the system level. Third, physics-based and data-driven machine learning approaches have been used to develop white-/black-/gray-box models of grid-forming and grid-following inverters and variable loads. These models have been validated using field measurements, hardware experiments, controller-hardware-in-the-loop testing, or EMT simulations. These models have been integrated into GridLAB-D. Finally, the enhanced GridLAB-D simulation platform and the validated inverter models were used to model a distribution feeder in the ComEd territory for planning studies. The impact of grid-forming and grid-following inverters on the transients and dynamics of distribution systems has been thoroughly studied under the realistic distribution feeder environment.

The outcomes of this project significantly advance transient and dynamic modeling capabilities for distribution systems and increase the confidence of utilities and operators

in planning and operating systems with high levels of inverter-based DERs and variable loads.

Table of Contents

1 Background

Modern power systems are experiencing a major transition with increasing penetration of distributed inverter-based resources (IBRs) and variable loads (VLs) connected at the distribution level. This paradigm shift will result in a more active interaction between transmission and distribution (T&D) systems and pose new challenges in power system modeling and simulation. Most existing power system simulation tools simulate transmission and distribution systems separately, which may not be suitable for future highly T&D-interactive power systems. Prior DOE efforts have developed relevant models and tools through different programs. For example, SETO-funded programs (e.g., SHINES, SuNLaMP, and ENERGISE) have significantly advanced the steady-state and quasi-steady-state modeling and simulation of different sections among the overall integrated power grids, ranging from transmission to distribution systems. The OE Microgrid R&D program has also facilitated the dynamic simulation of distribution-level microgrids using open-source tools (e.g., GridLAB-D). Other DOE programs, such as GMLC and NAERM, also funded the T&D co-simulation work in different aspects. Although the developed models and tools significantly advanced the modeling and co-simulation of integrated power grids, there is still a lack of accurate models and tools to simulate the transient and dynamic behaviors of full-size, three-phase unbalanced distribution systems that feature high penetration of IBRs and VLs.

2 Project Objectives

The DistribuDyn project team proposes to develop multi-fidelity IBR and variable load models and an integrated co-simulation platform to accurately simulate the transient and dynamic behaviors of distribution systems and their interactions with transmission systems. Physics-based and data-driven machine learning (ML) approaches will be developed collaboratively to realize a balance between model fidelity and computational efficiency. The co-simulation platform will be built by leveraging open-source tools, such as GridLAB-D and HELICS. The existing capabilities of HELICS will be expanded to interface GridLAB-D with other simulators to enable various types of co-simulation such as the electromagnetic transient and three-phase phasor co-simulation for unbalanced distribution systems. Finally, field μPMU and point-on-wave data will be used to validate the models. The success of this project will advance the transient and dynamic modeling of distribution systems and increase the confidence of utilities and system operators in operating distribution systems with high penetration of IBRs and VLs.

The project includes five major tasks, including 1) physics-based and data-driven ML modeling (white-/black-/gray-box), 2) integrated co-simulation platform development, 3) data generation and collection, 4) distribution feeder model validation and calibration, and 5) model validation, integration, and evaluation in a realistic feeder environment in GridLAB-D. Each task has defined multiple subtasks. In addition, 16 milestones were developed to ensure all the tasks were successfully executed, as shown in Table 2-1.

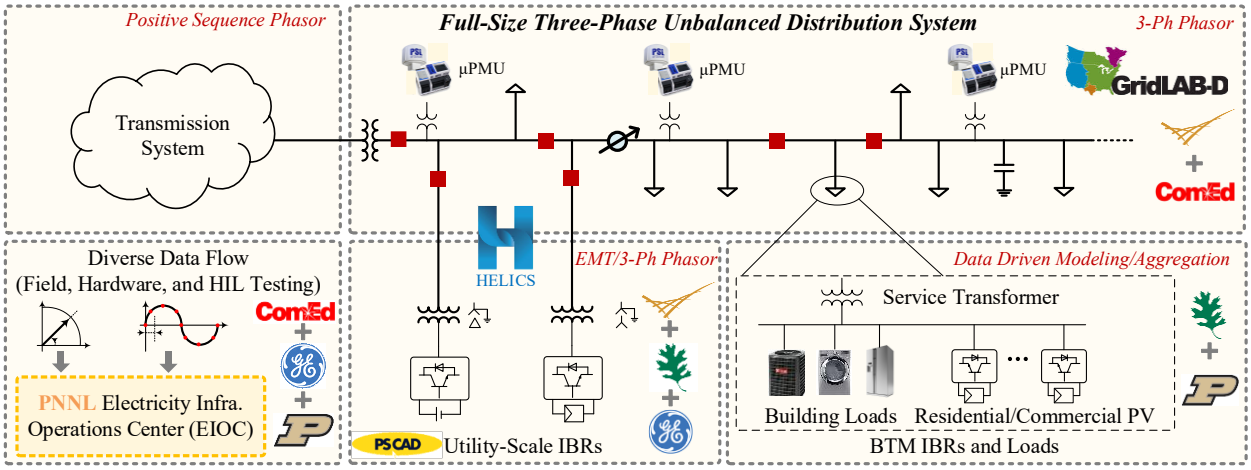

Fig. 2-1 Project overview

Table 2-1 Milestone table

Year #	Task #	Milestone #	Milestone Name/Description	End Date	Milestone Type
1	1	1	Conform IAB members for this project. The IAB should include at least two ISOs, two utilities, and one vendor.	12/31/2021	Quarterly
			Project Evaluation Criteria: Include at least two ISOs, two utilities, and one vendor in the IAB. **Metric Justification:** Six members from ISOs, utilities, and vendors should be enough to guarantee the diversity of IAB. **State-of-the-art baseline:** Typically an IAB will include 3-5 members.		
1	2	2	A. Convert the feeder model from the utility partner from CYME to GridLAB-D and assure the average error of node voltages is less than 0.1% in the power flow analysis based on the summer peak load scenario. B. Update the network solver in GridLAB-D to successfully handle faults, including line-to-ground, line-to-line, and open-phase faults. C. Evaluate different black-box model structures and nonlinear estimators through literature review and necessary simulation and determine the most appropriate black-box modeling approach for large distribution-connected IBRs.	3/30/2022	Quarterly
			Project Evaluation Criteria: A. Assure the average error of node voltages between CYME and GridLAB-D is less than 0.1% in power flow analysis based on the summer peak load scenario. B. Assure GridLAB-D solver is able to solve both balanced and unbalanced short circuit faults by utilizing the fixed-point-iterative approach. The IEEE 13-Node Test Feeder will be selected		

			to test the short circuit currents, and the error between GridLAB-D calculation results and the results from the IEEE PES Test Feeder Working Group[1] will be ensured less than 0.2%. C. Evaluate at least three black-box modeling methods. Necessary literature review and simulation analysis will be performed to determine which modeling method to use considering both model accuracy and simulation efficiency. **Metric Justification:** A. A 0.1% average error in power flow analysis should be small enough for futher dynamic simulation. B. One main purpose of this project is to study the response of IBRs to faults. Therefore, it is important to assure that GridLAB-D can handle both balanced and unbalanced faults. A 0.2% error in short circuit current calculation should be small enough for further large-signal transient simulation. C. There are three commonly used black-box modeling approaches, 1) nonlinear autoregressive exogeneous modeling method, 2) Hammerstein-Wiener modeling method, and 3) artificial intelligence-based modeling method. **State-of-the-art baseline:** A. PNNL has sufficient experience on feeder model conversion, and a 0.1% average error is typically used to evaluate the accuracy of model conversion. B. Currently GridLAB-D does not support fault studies. C. There are multiple black-box modeling methods proposed in literature, but their advantages and disadvantages are not clearly understood.		
1	**1**	**3**	Develop the generic three-phase phasor models of large distribution-connected IBRs with grid-support functions specified in IEEE Std. 1547 in GridLAB-D. Compare with the EMT IBR model with an error less than 5% for IBR output P and Q under an unbalanced disturbance. The disturbance should be added at the terminal of the IBR. P and Q should be normalized based on the device rating. The IBR output voltages and currents will also be compared and the errors will be minimized.	6/30/2023	Quarterly
			Project Evaluation Criteria: the normalized root mean squared error (NRMSE) is used to evaluate the accuracy of the generic large distribution-connected IBR model, which is defined as: $NRMSE = \sqrt{\frac{1}{N}\sum_{k=1}^{N}\left[\left(y_k - z_k\right)/z_k\right]^2}$ where y_k is the output of the phasor IBR model, and z_k is the output of the EMT IBR model. The NRMSE should be less than 5% for P and Q. **Metric Justification:** NRMSE has been widely used for dynamic model validation. Therefore, it is selected to compare the EMT and phasor models of IBRs. **State-of-the-art baseline:** Currently there are not many references that study the differences between three-phase phasor and EMT models of IBRs during faults.		
1	**2**	**4**	Develop APIs to assure GridLAB-D can exchange information with PSCAD and GridPACK through HELICS. Perform initial co-simulation with one generic IBR model in PSCAD and an IEEE 34-node test feeder in GridLAB-D using the conventional FFT waveform-phasor conversion technique. Assure the computation time is improved by at least 50% compared to the full-EMT simulation. The full-EMT model will be based on the PSCAD model of the IEEE 34-node test feeder developed by the IEEE PES Test Feeder Working Group[2].	9/30/2022	Annual

[1] https://site.ieee.org/pes-testfeeders/resources/

[2] https://site.ieee.org/pes-testfeeders/resources/

			Project Evaluation Criteria: HELICS can synchronize GridLAB-D and PSCAD during the co-simulation, and the computation time is improved by at least 50% compared to the full-EMT simulation for the studied case. **Metric Justification:** Synchronization between different simulation platforms is important to guarantee the accuracy of EMT & phasor co-simulation. The main purpose of co-simulation is to improve the computational efficiency. Therefore, it is important to evaluate whether the co-simulation can improve computational efficiency or not. **State-of-the-art baseline:** Currently, the EMT & phasor co-simulation has not been achieved using HELICS.		
1	**3**	**5**	Set up the RTDS HIL testing platform for testing large distribution-connected IBRs. Set up the laboratory testing platforms for testing residential IBRs and VLs. Set up the communication link and stream the field data from the utility partner to PNNL EIOC.	12/31/2022	Annual
			Project Evaluation Criteria: A. The RTDS HIL platform for testing the large distribution-connected IBRs should be set up at the vendor partner's lab. B. The laboratory testing platform for testing residential IBRs and motors should be set up at the university partner's lab. C. The laboratory testing platform for testing air conditioners and variable-frequency drive motors should be set up at the utility partner's lab. D. The communication link should be set up, and the field data of the feeder should be streamed from the utility partner to PNNL EIOC. **Metric Justification:** With the laboratory testing platform set up and field data collected, the team can start to collect the required data for developing and validating the models. **State-of-the-art baseline:** The team partners already have some of the devices that will be tested in their labs, and they will expand the setup to satisfy the needs of this project. The field data at the transmission level has already been streamed from the utility partner to PNNL EIOC, but the distribution field data has not been streamed to PNNL EIOC yet.		
2	**1**	**6**	Develop direct-connected motor and inverter-driven motor models with representative mechanical torque characteristics and protection of residential/commercial building loads. Achieve a less than 5% mismatch between simulation outputs and Modelica-based building library model[3]. Draw conclusions on how different mechanical torque characteristics affect motor stalling.	12/31/2022	Quarterly
			Project Evaluation Criteria: The representative loads should include at least air conditioners and refrigerators with different thermal protection settings. The model accuracy should achieve a less than 5% mismatch between simulation and Modelica-based building library model. **Metric Justification:** The Modelica-based building library developed by Lawrence Berkeley National Laboratory has been widely used in the building research area. A less than 5% mismatch can assure the accuracy of the developed load models. **State-of-the-art baseline:** Currently, studies mainly focus on modeling motors, with less attention paid to modeling various mechanical torque characteristics behind the motors in residential and commercial buildings. Moreover, the comparison between the load models used in the power system dynamic simulation have not been compared to the load models used in the building research area.		

[3] DOE/LBNL, Modelica Building Library, https://simulationresearch.lbl.gov/modelica/

2	**2**	**7**	Interface five PSCAD models of large distribution-connected IBRs provided by the vendor partner to GridLAB-D through HELICS. Perform the co-simulation in an IEEE 34-node test feeder with the developed waveform-phasor conversion technique. Compare the EMT & phasor co-simulation with the full EMT simulation; assure that the NRMSE at IBR output P and Q are within 2%. In addition to P and Q, the IBR output voltages and currents will also be compared, and the errors will be minimized.	3/30/2023	Quarterly
			Project Evaluation Criteria: Assure HELICS has the capability to interface black-box IBR models developed by OEMs. The NRMSE should be less than 2% for P and Q under a voltage disturbance. **Metric Justification:** One of the main purposes of this project is to assure the PSCAD IBR models developed by OEMs can be interfaced to the distribution network solver to allow co-simulation. A less than 2% NRMSE can assure the accuracy of the EMT & phasor co-simulation approach. **State-of-the-art baseline:** The positive sequence phasor & EMT co-simulation platform has been developed by many software vendors such as Electranix and ETAP. However, currently there are not many studies about the three-phase phasor & EMT co-simulation.		
2	**3**	**8**	Complete the laboratory testing of large distribution-connected IBRs, residential IBRs and VLs. Collect the laboratory testing data, field μPMU data, and point-on-wave data from PQ analyzers.	3/30/2023	Quarterly
			Project Evaluation Criteria: A. For the RTDS HIL testing, the test cases specified in Table 1 should be completed by the vendor partner. The test results will be shared with PNNL, the other lab partner. B. For the laboratory testing of BTM IBRs and motors, the test cases specified in Table 1 should be completed by the university partner. The test results will be shared with PNNL. C. For the laboratory testing of air conditioners and variable frequency drive motors, the test cases specified in Table 1 should be completed by the utility partner. The test results will be shared with PNNL and the other lab partner. D. The fault events recorded by the μPMU and PQ analyzers installed in the studied feeder during the data collection stage should be transferred to PNNL EIOC. E. For the voltage change testing, it should at least include ±5%, ±10%, and ±20% step changes; for the frequency change testing, it should at least include ±1 Hz/s and ±3 Hz/s changes in the rate of change of frequency. F. All the testing procedures will follow the common engineering practice to assure the experiments are correctly conducted. For the RTDS HIL testing, the digital/analog signal conversion should be calibrated to assure the error is less than 0.1%. For the laboratory hardware testing, the automatic calibration will be performed for the oscilloscopes before using them to capture the waveforms. **Metric Justification:** The laboratory testing data and field data are critical for the modeling work. All the tests listed in Table 1 should be completed, and the data should be shared with relevant partners. **State-of-the-art baseline:** The data collection process will start once the laboratory testing platforms are set up.		
2	**1**	**9**	Develop the aggregated gray-box model of BTM IBRs and VLs in GridLAB-D. Compare simulation outputs with lab testing results and assure the NRMSE is less than 2% for P and Q. In addition to P and Q, the voltages and currents will also be compared, and the errors will be minimized.	6/30/2023	Quarterly
			Project Evaluation Criteria: The NRMSE between the outputs P and Q from simulation and the lab testing results should be less than 2% under a voltage disturbance.		

			Metric Justification: NRMSE has been widely used for model validation. Therefore, it is selected to compare the gray-box model and lab testing results. A less than 2% NRMSE should assure the accuracy of the developed models. **State-of-the-art baseline:** In the bulk power system simulation, the aggregation is typically at the distribution substation (e.g., the composite load model). For this project, we will aggregate BTM IBRs and VLs behind a service transformer in a distribution feeder. Such kind of work has not been well studied in the past.		
2	**1**	**10**	Develop an IBR model library and a load model library in GridLAB-D to hold the developed IBR and load models. Validate and calibrate the developed white-, black-, and gray-box models of large distribution-connected and BTM IBRs and VLs. Assure the NRMSE between the output P and Q of simulation and field measurements and/or laboratory testing is less than 2% for each model with a confidence level higher than 95%. In addition to P and Q, the voltages and currents will also be compared, and the errors will be minimized.	9/30/2023	Annual
			Project Evaluation Criteria: A. The IBR model library should include both GFMs and GFLs. For GFMs, both droop control and virtual synchronous machine controls should be modeled. For GFLs, the grid-support functions including volt-var, frequency-watt, and different ride-through and tripping settings will be modeled. The IBR model library should also include the phasor-based IBR models provided by the vendor partner. B. The load model library should include representative building loads, including at least air conditioners, refrigerators, heaters, and coolers. C. The NRMSE between the output P and Q of simulation and field measurements and/or laboratory testing results should be less than 2% with a confidence level higher than 95% for for the developed models. P and Q should be normalized based on the device rating. D. For the selected black-box modeling method, it should be tested by at least two different IBR designs. **Metric Justification:** One of the main goal of this project is to develop a tool that enables dynamic and transient simulation of distribution systems, and the IBR and load model libraries are important for running simulation. A less than 2% NRMSE can assure the accuracy of the developed models. **State-of-the-art baseline:** The existing distribution system planning software tools such as CYME and OpenDSS do not have dynamic models of IBRs and loads, and there is not too much model validation work performed at the distribution level. P and Q are typically used to validate the IBR models at the transmission level [4].		
3	**4**	**11**	Compare simulation results of the GridLAB-D feeder model with field measurements. Calibrate the feeder model to assure that the NRMSE of the voltage and frequency of the 25 nodes equipped with μPMUs are less than 5% with a confidence level higher than 90%.	12/30/2023	Quarterly
			Project Evaluation Criteria: The NRMSE of the voltage and frequency of the 25 nodes equipped with μPMUs should be less than 5% for captured fault events. **Metric Justification:** It is beneficial to investigate how the field μPMU data can be used to calibrate the distribution feeder model. The calibrated distribution feeder model will be used to integrate different IBR models developed by the team. **State-of-the-art baseline:** The comparison of simulation results and multiple field μPMU data for a distribution feeder has not been well studied in the past.		

[4] P. Pourbeik et al., "Generic Dynamic Models for Modeling Wind Power Plants and Other Renewable Technologies in Large-Scale Power System Studies," in IEEE Transactions on Energy Conversion, vol. 32, no. 3, pp. 1108-1116, Sept. 2017

3	**5**	**12**	Complete the literature review on the current industry practice for model testing and establish standard test cases for testing and validating the white-/black-/gray-box models developed under this project.	3/31/2024	Quarterly
			Project Evaluation Criteria: A. The literature review should at least cover the ERCOT model quality test, WECC criteria for acceptance of new dynamic models, UNIFI specification, NERC Grid Forming Functional Specifications for BPS-Connected Battery Energy Storage Systems, and the IEEE P2800.2 under development. B. The standard test cases should at least include the test cases used by ERCOT and WECC, and new test cases should also be included as necessary for IBRs connected in distribution systems. **Metric Justification:** Establish standard test cases are important, and will be used as reference to facilitate testing and validating the models developed under this project (i.e., MS 3.5.13, MS 3.5.14 and MS 3.5.15) **State-of-the-art baseline:** Currently, there are no standard test cases for testing the IBR models for distribution systems. Review and reference the standard test cases used by transmission systems are helpful to test the IBR models for distribution system simulations.		
3	**5**	**13**	Complete the white-box IBR model validation in GridLAB-D against other commercial IBR products.	3/31/2024	Quarterly
			Project Evaluation Criteria: A. The test data of at least one additional commercial IBR beyond the GE LV5 inverter should be used to validate the model. The model validation and testing will be conducted against the standard test cases established under MS 3.5.12. B. The P and Q should match the steady-state and dynamic performances of the commercial IBR reasonably, and the NRMSE should be provided. **Metric Justification:** Validate the white-box IBR model against other commercial IBR products is important to assure that the developed model can be generalized to represent some typical control functions used by many IBR manufacturers. **State-of-the-art baseline:** So far, the white-box IBR model is only validated against the GE LV5 inverter. It is important validate the model against other IBR products.		
3	**5**	**14**	Complete the black-box and gray-box model testing and validation in GridLAB-D with additional commercial IBR products.	9/30/2024	Quarterly
			Project Evaluation Criteria: A. For the black-box IBR model, the test data of at least one commercial IBR other than the GE LV5 inverter should be used to validate the model. B. For the gray-box IBR model, the test data of at least one commercial BTM IBR should be used to validate the model. C. The black- and gray-box model validation and testing will be conducted against the standard test cases established under MS 3.5.12. C. The P and Q should match the steady-state and dynamic performances of the commercial IBR reasonably, and the NRMSE should be provided. **Metric Justification:** Validate the black-/gray-box models against other commercial IBR products is important to assure that the developed model can be generalized to represent some typical control functions used by many IBR manufacturers. **State-of-the-art baseline:** Currently, the black-box IBR model is only validate against the GE LV5 IBR product, and the gray-box model has not been validated against commercial BTM IBR products yet.		
3	**5**	**15**	Complete the integration and evaluation of the white-/black-/gray-box models in the ComEd feeder model in GridLAB-D.	12/31/2024	Quarterly
			Project Evaluation Criteria: A. For the white-box IBR models, at least 5 GFM and GFL IBR models in total should be integrated into the ComEd feeder model. The GridLAB-D feeder model together with the IBR		

			models should be used to simulate typical disturbance events such as balanced and unbalanced faults and load switching, and no numerical stability issues should be identified in the simulation. B. For the black- and gray-box models, at least one black-box model and one gray-box model should be integrated into the ComEd feeder model in GridLAB-D. Typical disturbance events such as balanced and unbalanced faults and switching should be simulated to identify any potential issues such as the model inaccuracy and the numerical instability. Identified issues should be documented and analyzed. C. The utility partner should perform simulations of the ComEd feeder model integrated with IBR models in GridLAB-D and provide user experience to the team. The corresponding validation and testing will be conducted against the standard test cases established under MS 3.5.12. **Metric Justification:** The white-, black-, and gray-box modeling approaches are at different technology readiness levels (TRLs). The white-box modeling is a mature technology so that the white-box models developed under this project should be directly used for typical contingency analysis for distribution systems without causing any numerical stability issues. The black- and gray-box models are still at relatively low TRLs, so it is important to investigate whether these models can used for simulation of a typical size of distribution feeder and identify any potential issues. Such evaluation in a typical distribution feeder model would help identify the applicability and limitations of the white-/black-/gray-box modeling approaches. **State-of-the-art baseline:** Currently, all the white-/black-/gray-box models are being developed and tested in a single-inverter infinite-bus system. These models have not been evaluated in a realistic feeder model yet.		
3	**5**	**16**	Dissemination and tech transfer for the developed white/black/gray-box models	3/31/2025	Quarterly
			Project Evaluation Criteria: A. A user guide should be developed to clarify the intended applications, pros and cons, and limitations of the white-/black-/gray-box modeling approaches. The user guide will also streamline the basic steps and information that can helps third party users to deploy the developed models for their applications, e.g., inputs/outputs interface, configurable coefficients, training data requirements for black- and gray-box models, etc. B. The source codes of the developed white-/black-/gray-box models should be uploaded to GridLAB-D on Github for public use. C. At least one panel/tutorial proposal should be submitted to conferences such as PESGM and ESIG to socialize the project outcome. D. Coordinate with OEDI-SI to establish use cases for distribution dynamics and transients analysis using the developed models. **Metric Justification:** The development of user guide and tutorial materials are important for project outcome dissemination and technology transfer. The source codes should also be uploaded to latest version of GridLAB-D in Github for public use. **State-of-the-art baseline:** Dissemination and technology transfer are important for all projects.		

3 Project Results and Discussion

3.1 High-Level Summary of Project Results

This subsection provides a high-level summary of major projects results and discusses how the milestones were accomplished. For easier reference, the relevant milestones were added after each major accomplishment. The later subsections provide a more detailed discussion on the project results.

Integrated Co-Simulation Platform for Studying Distribution Systems Transients and Dynamics

(a) GridLAB-D Network Solver Enhancement

To enable GridLAB-D to simulate the transients and dynamics of distribution systems, the network solver needs to be updated to handle short-circuit faults. The project team has enhanced the GridLAB-D solver's capabilities to handle both balanced and unbalanced faults by updating the solver with a fixed-point iterative approach. The solver's performance was benchmarked against results provided by the IEEE PES Test Feeder Working Group for the IEEE 13-Node Test Feeder. The following milestone has been accomplished.

[**M 1.2.2.B**] Assure GridLAB-D solver is able to solve both balanced and unbalanced short circuit faults by utilizing the fixed-point-iterative approach. The IEEE 13-Node Test Feeder will be selected to test the short circuit currents, and the error between GridLAB-D calculation results and the results from the IEEE PES Test Feeder Working Group[5] should be less than 0.2%.

(b) EMT & Per-Phase Phasor Co-Simulation

EMT & per-phase phasor co-simulation is critical to allow the integration of the EMT inverter models developed by manufacturers into the GridLAB-D solver to evaluate their impact in a realistic distribution feeder environment. For this project, a high-fidelity co-simulation platform was developed integrating PSCAD, HELICS, and GridLAB-D to achieve the EMT & per-phase phasor co-simulation. This approach enables the EMT & phasor co-simulation to study the distribution system transients and dynamics, which is different from the conventional EMT & positive-sequence phasor co-simulation approach. Specifically, five black-box PSCAD inverter models were connected to the IEEE 34-Node Test Feeder modeled in GridLAB-D to achieve co-simulation. HELICS functioned as the communication middleware, enabling synchronized data exchange between the two simulation environments. To ensure accurate coupling at the simulation boundary, a novel interface model was developed to prevent false tripping of the vendor-specific inverter models during disturbances. Additionally, an initialization algorithm was developed to properly initialize interface model variables, ensuring a seamless transition from power flow to dynamic simulation mode in the co-simulation workflow. The platform's accuracy was validated against a full EMT simulation of the test system. Results showed strong correlation, with the Normalized Root Mean Square Error (NRMSE) for inverter active and

[5] https://site.ieee.org/pes-testfeeders/resources/

reactive power outputs remaining within 2%, confirming the reliability and fidelity of the co-simulation approach. The following milestones have been accomplished. It is important to note that although EMT and per-phase phasor co-simulation can be used to study transient stability in distribution systems, it is not intended for analyzing harmonics or high-frequency oscillations due to the phasor assumptions in the GridLAB-D solver. Pure EMT simulations are recommended for studying such phenomena.

[M1.2.4]: Develop APIs to assure GridLAB-D can exchange information with PSCAD and GridPACK through HELICS.

[M2.2.7]: Interface five PSCAD models of large distribution-connected IBRs provided by the vendor partner to GridLAB-D through HELICS.

Physics-Based and Data-Driven ML Modeling for Distribution-Connected IBRs

The project team has used physics-based and data-driven ML approaches to develop white-/black-/gray-box models of grid-forming and grid-following inverters and variable loads. These models are essential for studying the transients and dynamics of distribution systems.

(a) White-Box Per-Phase Phasor Grid-Forming and Grid-Following Inverter Models

This project has developed the white-box per-phase phasor models of large distribution-connected IBRs. The developed IBR model is embedded with grid-support functions including volt-var and frequency-watt that can be modeled based on the IEEE Std. 1547 specification. The white-box IBR phasor models have been validated against either with RTDS control hardware in loop (CHIL) tests or EMT simulations. The tests include both normal operation and grid faults. To ensure the developed model can generally represent some typical control functions used by many IBR manufacturers, this project also used the data from multiple commercial IBRs to validate the white-box model. From the results, P and Q from the model match well with the steady-state and dynamic performances of the commercial IBR test data, and the NRMSEs in these tests are under 2%. Additionally, tests from model validation test procedures outlined in ERCOT, WECC, NERC, and IEEE-P2800 standards have also been used to validate white-box GFL and VSM-based GFM IBR phasor models. The following milestones have been accomplished.

[M1.1.3]: Develop the generic three-phase phasor models of large distribution-connected IBRs with grid-support functions specified in IEEE Std. 1547 in GridLAB-D.

[M2.1.10]: Develop an IBR model library and a load model library in GridLAB-D to hold the developed IBR and load models. Validate and calibrate the developed white-, black-, and gray-box models of large distribution-connected and BTM IBRs and VLs.

[M3.5.13]: Complete the white-box IBR model validation in GridLAB-D against other commercial IBR products.

[M3.5.16.A]: A user guide should be developed to clarify the intended applications, pros and cons, and limitations of the white-/black-/gray-box modeling approaches.

[M3.5.16.B]: The source codes of the developed white-/black-/gray-box models should be uploaded to GridLAB-D on Github for public use.

(b) Black-Box Grid-Following Inverter Model

The project team developed a convolutional neural network (CNN)-based deep learning model for GFL-controlled IBRs. The model was trained on data from commercial IBRs under diverse grid conditions, including voltage and frequency ride-through events, and it was successfully integrated into GridLAB-D for large-scale stability simulations. The model was validated against ERCOT standards, achieving an NRMSE under 5% for P and Q while meeting steady-state and dynamic performance expectations. This marks the first successful integration of a data-driven, ML-based IBR model into GridLAB-D, demonstrating its potential for power system stability and planning studies. It should be noted that the accuracy and robustness of black-box models depend on diverse training datasets, especially for extreme events like frequency jumps. This work paves the way for more advanced data-driven, ML-based grid modeling and simulation frameworks. The following milestones have been achieved.

[M1.2.2.C]: Evaluate different black-box model structures and nonlinear estimators through literature review and necessary simulation, and determine the most appropriate black-box modeling approach for large distribution-connected IBRs.

[M2.1.10]: Develop an IBR model library and a load model library in GridLAB-D to hold the developed IBR and load models. Validate and calibrate the developed white-, black-, and gray-box models of large distribution-connected and BTM IBRs and VLs.

[M3.5.14]: Complete the black-box and gray-box model testing and validation in GridLAB-D with additional commercial IBR products.

[M3.5.16 A]: A user guide should be developed to clarify the intended applications, pros and cons, and limitations of the white-/black-/gray-box modeling approaches.

[M3.5.16 B]: The source codes of the developed white-/black-/gray-box models should be uploaded to GridLAB-D on Github for public use.

(c) Gray-Box BTM Feeder Models with IBRs and Loads

The project team developed a gray-box behind-the-meter (BTM) feeder model that incorporates IBRs and loads by integrating physics-based modeling with data-driven neural networks (NNs). The physics-based component, represented by ordinary differential equations, captures the fundamental control characteristics of inverters residing within the BTM feeder and serves as the structural backbone of the model. The data-driven component, implemented via simplified NNs, corrects the discrepancies between measured data and the physical model outputs, significantly enhancing overall model accuracy while enabling fast training. The resulting hybrid model achieves a normalized root NRMSE of less than 5%. Its effectiveness has been validated under various grid conditions, including voltage and frequency ride-through events, fault scenarios, and dynamic voltage and frequency variations. All validated models have been integrated into the open-source GridLab-D platform, combining the strengths of physics-based and data-driven ML approaches to ensure high fidelity with manageable computational overhead. The following milestones have been achieved.

[M2.1.9]: Develop the aggregated gray-box model of BTM IBRs and VLs in GridLAB-D. Compare simulation outputs with lab testing results and assure the NRMSE is less than 2% for P and Q.

[M3.5.14]: Complete the black-box and gray-box model testing and validation in GridLAB-D with additional commercial IBR products.

[M3.5.16 A]: A user guide should be developed to clarify the intended applications, pros and cons, and limitations of the white-/black-/gray-box modeling approaches.

[M3.5.16 B]: The source codes of the developed white-/black-/gray-box models should be uploaded to GridLAB-D on Github for public use.

Model Validation, Integration, and Evaluation in a Realistic Feeder Environment in GridLAB-D

To evaluate the IBR models in a realistic feeder environment, ten IBR models, including white-, black-, and gray-box models for GFMs and GFLs, were added to the ComEd feeder model, which has about 565 nodes. The IBRs models were tested under various fault events, including balanced and unbalanced faults, load changes, and voltage and frequency step changes at different feeder locations. No numerical stability issues were observed in the simulations and the simulation results met the expected requirements**.** The results show that the developed co-simulation platform and IBR models allow to simulate the transients and dynamics of distribution systems with a high penetration of distributed energy resources. Notably, the simulation speed is significantly improved compared to the EMT simulations. The following milestones have been achieved.

[**M 1.2.2.A**] Convert the feeder model from the utility partner from CYME to GridLAB-D and assure the average error of node voltages are less than 0.1% in the power flow analysis based on the summer peak load scenario

[**M 3.5.15**] Complete the integration and evaluation of the white-/black-/gray-box models in the ComEd feeder model in GridLAB-D.

3.2 Integrated Co-Simulation Platform Development

3.2.1 Update GridLAB-D Solver for Short-Circuit Fault Simulation

The fixed-point-iterative (FPI) method has been successfully implemented into GridLAB-D, enabling better solution stability in faulted conditions. This code update has been pushed to the public repository and merged into the mainline GridLAB-D. The basics of the fixed-point-iterative method can be found in the footnoted references[6,7].

It is useful to note the main variation in the FPI method against the existing “current injection method” implemented in GridLAB-D is the infinite bus becomes a current injection on the model and loads are the primary content of the current injections vector.

To test and validate the performance of the FPI solver, the IEEE 13-node test feeder is considered. In this test feeder, the percentage error in the short-circuit current computations under balanced and unbalanced short-circuit faults is computed and compared with the results reported by the IEEE PES Test Feeder Working Group. The percent difference for the fault values was calculated as follows:

$$\%difference = \left| \frac{I_{GLD} - I_{BASE}}{I_{BASE}} \right| \cdot 100$$

where I_{GLD} is the fault current computed from GridLAB-D and I_{BASE} is the reference solution from the IEEE 13-node model.

The values of the comparison for fault currents on the IEEE 13-node feeder are shown in Table 3-1. It is worth noting that for multi-phase nodes, only the maximum difference is shown in the table (e.g., if the Phase A difference was 0.01% and Phase B was 0.02%, the table lists 0.02% as the entry). Fig. 3-1 provides a visual representation of the maximum error. The required 'metric of performance,' according to Milestone 1.2.2, was to have the error magnitude below 0.2%. Figure 3.1 shows that all error magnitudes are well below the threshold needed for the implementation to be considered a success.

3.2.2 Subsection Conclusion and Discussion

In this subsection, the updated GridLAB-D solver, incorporating the fixed-point iterative approach, is presented. This update enables the solver to address both balanced and unbalanced short-circuit faults. The performance of the updated solver was compared with data from the IEEE PES Test Feeder Working Group for the IEEE 13-Node Test Feeder, verifying that the requirements of milestone **[M 1.2.2.B]** have been met.

---

[6] *Dugan, R. and T. McDermott, “An Open Source Platform for Collaborating on Smart Grid Research” in* Proceedings of the 2011 IEEE Power and Energy Society Meeting*, DOI: 10.1109/PES.2011.6039829.*

[7] *Zhang, Z., M. Mo, and C. Wu, “Improved Phase-coordinate Fixed-point Iterative Method Based on Equivalence Admittance Approximation for Power Flow Calculation in Three-phase Distribution Systems” in* Proceedings of the 2020 4th International Conference on HVDC. *DOI: 10.1109/HVDC50696.2020.9292801.*

Table 3-1 Magnitude of maximum percent error for fault currents on IEEE 13-node system – GridLAB-D compared to baseline (Unit: %).

	Fault Type							
Node	***LLL***	***LLL-G***	***LL-AB***	***LL-BC***	***LL-CA***	***SLG-A***	***SLG-B***	***SLG-C***
611								*0.003*
632	*0.019*	*0.018*	*0.011*	*0.018*	*0.016*	*0.006*	*0.010*	*0.006*
633	*0.016*	*0.017*	*0.012*	*0.016*	*0.015*	*0.006*	*0.007*	*0.006*
634	*0.007*	*0.006*	*0.049*	*0.049*	*0.047*	*0.000*	*0.005*	*0.003*
645				*0.015*			*0.007*	*0.007*
646				*0.013*			*0.009*	*0.004*
650	*0.030*	*0.031*	*0.030*	*0.030*	*0.030*	*0.020*	*0.020*	*0.020*
652						*0.001*		
670	*0.016*	*0.015*	*0.008*	*0.014*	*0.015*	*0.006*	*0.006*	*0.006*
671	*0.014*	*0.013*	*0.004*	*0.010*	*0.014*	*0.002*	*0.002*	*0.003*
675	*0.023*	*0.020*	*0.013*	*0.021*	*0.019*	*0.005*	*0.012*	*0.010*
680	*0.011*	*0.012*	*0.003*	*0.011*	*0.011*	*0.002*	*0.007*	*0.000*
684					*0.011*	*0.001*		*0.000*
692	*0.023*	*0.023*	*0.014*	*0.019*	*0.024*	*0.008*	*0.009*	*0.009*

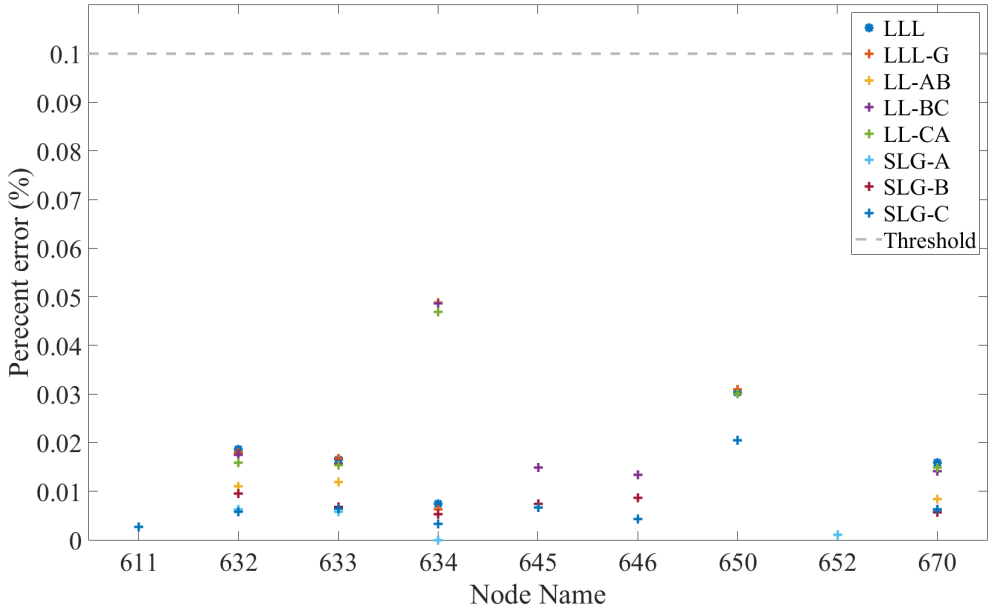

Fig. 3-1: Magnitude of percent error for fault currents on IEEE 13-node – GridLAB-D results compared against baseline.

3.2.3 PSCAD/HELICS/GridLAB-D Co-Simulation

To reduce the simulation execution time while maintaining a reasonable level of accuracy when studying a large-scale distribution system with a high penetration of inverter-based resources, the team developed a co-simulation platform based on PSCAD (as the EMT simulator), GridLAB-D (as the three-phase phasor simulator) and HELICS (as the communication protocol that coordinates information exchange between the EMT simulator and the three-phase phasor simulator). In the following subsections, the co-simulation platform will be described, used to run case-studies, and subsequently validated against results from a full EMT simulation model. Modifications that were made to make the co-simulation platform more accurate and efficient, will also be discussed.

3.2.3.1 Co-Simulation Approach

The co-simulation platform is built on PSCAD (a commercial EMT simulation solver), GridLAB-D (an open-source three-phase phasor solver), and HELICS (an open-source serial communication protocol). The choice of GridLAB-D as the phasor solver is due to its per-phase phasor modeling feature which allows unbalanced power systems such as distribution grids to be studied accurately. For this co-simulation platform, the detailed inverter model is implemented in PSCAD, the distribution feeder model is represented in GridLAB-D, and HELICS is used to facilitate interactions between GridLAB-D and PSCAD. To electrically connect PSCAD to GridLAB-D, an electrical interface model is developed as shown in Fig. *3-2*. This electrical interface model links the points of interconnection (interface buses) between the PSCAD and GridLAB-D.

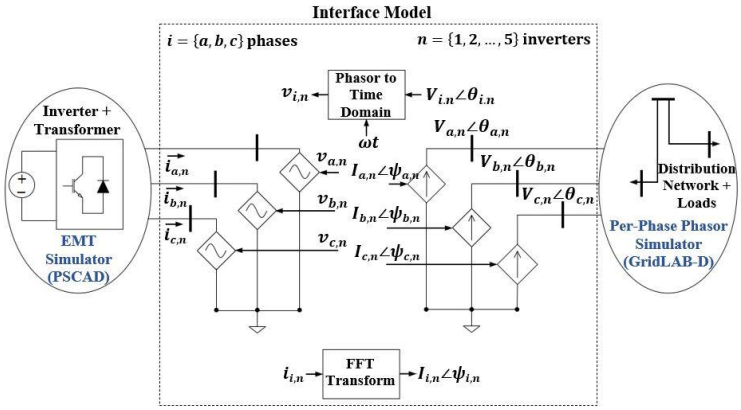

Fig. 3-2 Electrical interface model for the EMT & three-phase phasor co-simulation platform.

In PSCAD, the interface bus in GridLAB-D is represented as a controllable voltage source whereas in GridLAB-D, the interface bus is represented as a controllable current source. On one hand, the three-phase point-on-wave currents flowing into the interconnection bus in PSCAD is converted into phasor currents using fast-Fourier transform (FFT) blocks in the PSCAD simulation domain. On the other hand, the three-phase phasor interface bus voltages in GridLAB-D, which are in magnitude-angle form, are converted into three-phase point-on-wave voltages by using sinusoidal blocks in PSCAD. The current injection from PSCAD is treated as a negative load in GridLAB-D.

As mentioned before, HELICS controls the flow of information (time, voltage, current) between GridLAB-D and PSCAD. HELICS is an open-source tool that integrates simulators across diverse simulation domains. This integration is facilitated by HELICS through the creation of federates and a broker. A federate is an instance of a simulation executable that represents either an individual object or a collection of objects. The broker coordinates multiple federates, ensuring synchronization and facilitating data exchange among them. The sequence of data exchange between the simulators is given in Fig. 3-3.

Fig. 3-4 shows the flow of information between PSCAD and GridLAB-D via HELICS. The PSCAD federate is represented via a python API. The GridLAB-D federate is defined via a JSON file. The HELICS broker coordinates the federates. The co-simulation is initiated from the PSCAD side of the platform. To enable this, Windows executables of the Python API, GridLAB-D, HELICS, and PSCAD case files are organized into a simulation set, which is then executed.

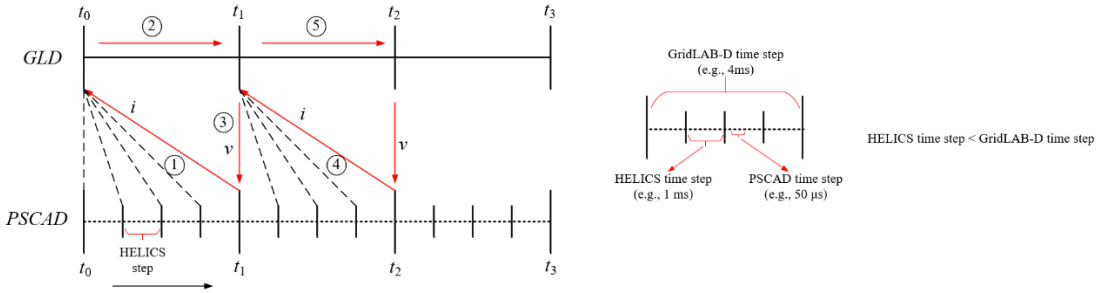

Fig. 3-3 The co-simulation protocol.

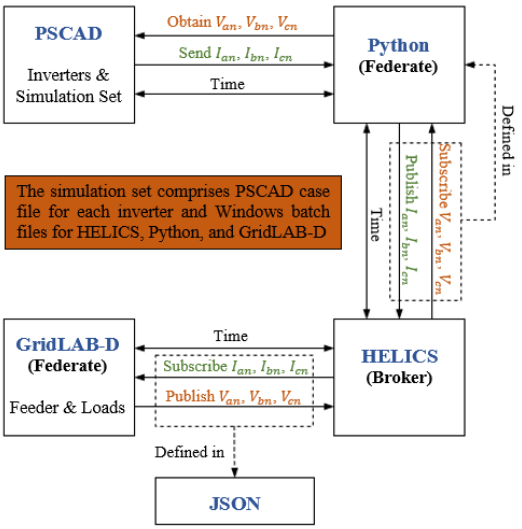

Fig. 3-4 The co-simulation framework and workflow.

The co-simulation process operates as follows: GridLAB-D receives phasor values of current injections from PSCAD (an EMT simulator) via HELICS, conducts a power flow simulation, and updates the phasor voltages at its interface buses. These updated

voltages are then transmitted to the EMT simulator through HELICS. The PSCAD simulator, in turn, receives the instantaneous voltages at its interface buses from GridLAB-D, performs a time-domain simulation, and updates the instantaneous current injections at its interface buses. These currents are then converted into phasor form before being sent back to GridLAB-D via HELICS.

To ensure a seamless transition from the power-flow mode to the dynamic (co-simulation) mode, the (current and voltage) variables of the interface model are initialized. The initial values are obtained from the phasor simulation of the entire system (both the inverters and the feeder).

3.2.3.2 Validation in the IEEE 34-Node Test Feeder

To validate the co-simulation platform, 5 black-box grid-following (GFL) inverter models, from an inverter manufacturer, are connected to the IEEE 34-Node Test Feeder as shown in Fig. 3-5. The black-box inverters are connected to Nodes 806, 812, 850, 816 and 830, which are all three-phase nodes. In the full EMT case, the feeder along with the 5 black-box inverters are entirely modeled in PSCAD. In the co-simulation case, the 5 black-box inverter models are implemented in PSCAD, and the rest of the feeder is modeled in GridLAB-D. The parallel simulation feature of PSCAD is leveraged, and thus each black-box inverter model runs in a separate CPU core, which largely increases the simulation speed.

Two simulation case studies are presented:

- Case 1: LLL-G fault at Node 806 at the PSCAD side
- Case 2: SLG-A fault at Node 844 at the GridLAB-D side

A rigorous comparison between the full EMT and co-simulation was performed for the above two cases. The results are presented in Sections 3.1.2.2.1 – 3.1.2.2.2.

3.2.3.2.1 Case 1: LLL-G Fault in PSCAD

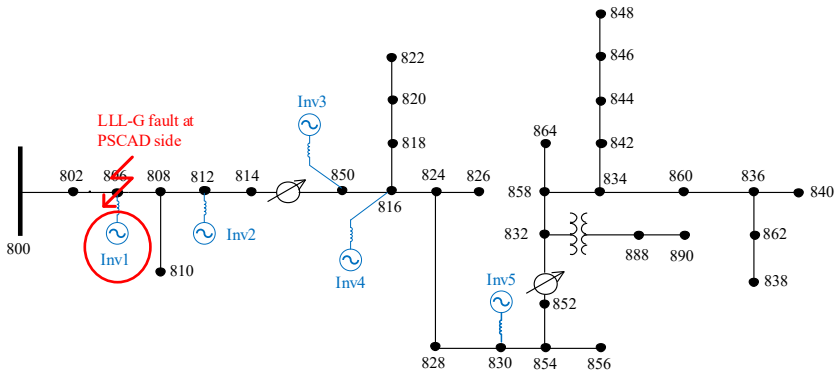

Fig. 3-5 LLL-G fault on the PSCAD side and measurements at the terminals of inverter 1.

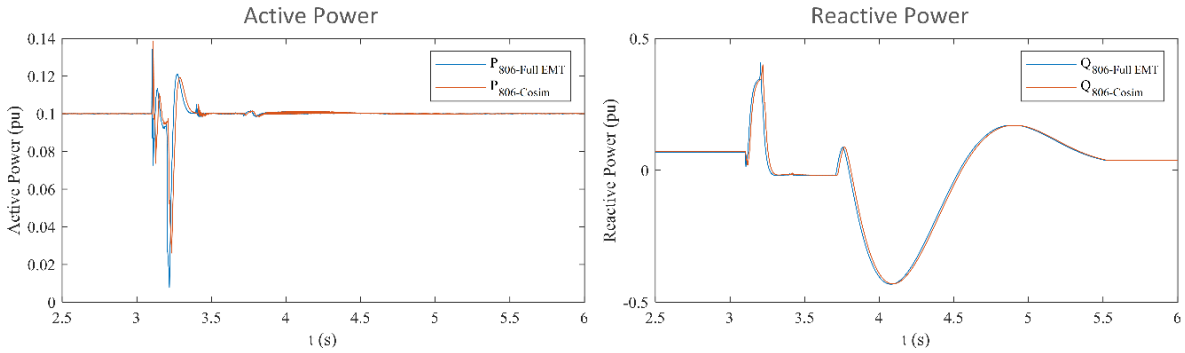

Fig. 3-6 Active and reactive power responses at Node 806.

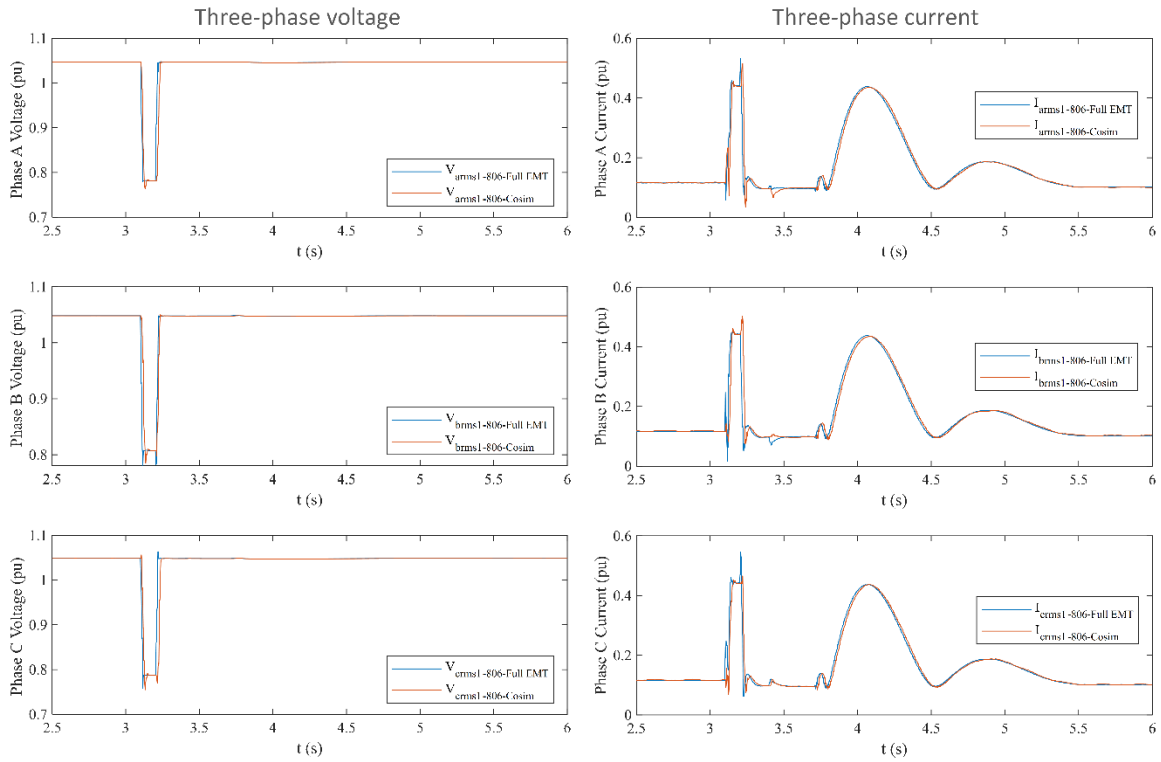

Fig. 3-7 Three-phase voltage and current responses at Node 806.

For the 3-phase-to-ground fault on the PSCAD side, all the 5 black-box inverters exhibit very similar responses to the fault according to some of the results shown in Fig. *3-5* - Fig. *3-7*. The P&Q normalized root mean square error (NRMSE) for each inverter in this case is summarized in Table *3-2*.

Table 3-2 NRMSE of inverters during LLL-G fault in PSCAD.

Inverter Name	NRMSE of P (%)	NRMSE of Q (%)
Inverter 1	0.63	1.83
Inverter 2	0.58	1.42
Inverter 3	0.59	1.46
Inverter 4	0.59	1.46
Inverter 5	0.58	1.36

3.2.3.2.2 Case 2: SLG-A Fault in GridLAB-D

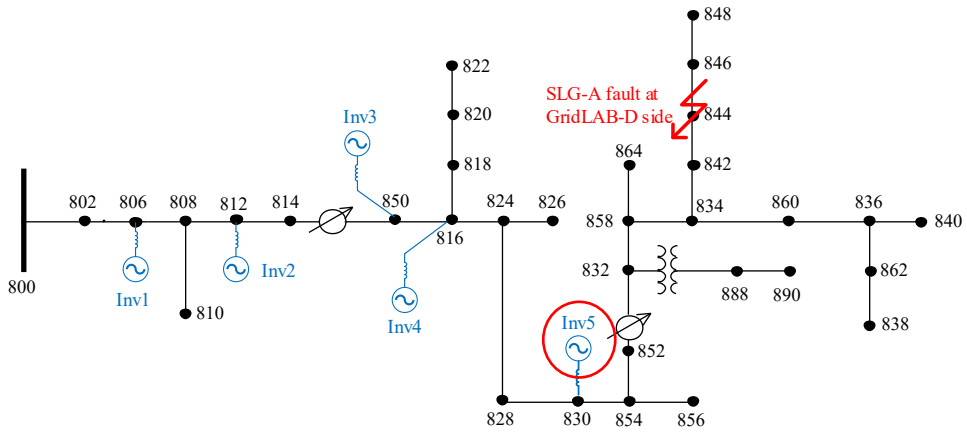

Fig. 3-8 SLG-A fault on the GridLAB-D side and measurements at the terminals of inverter 5.

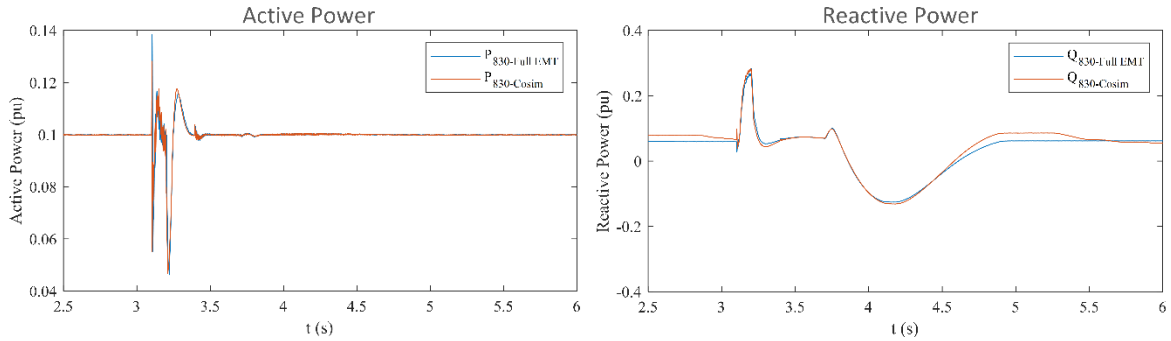

Fig. 3-9 Active and reactive power responses at Node 830.

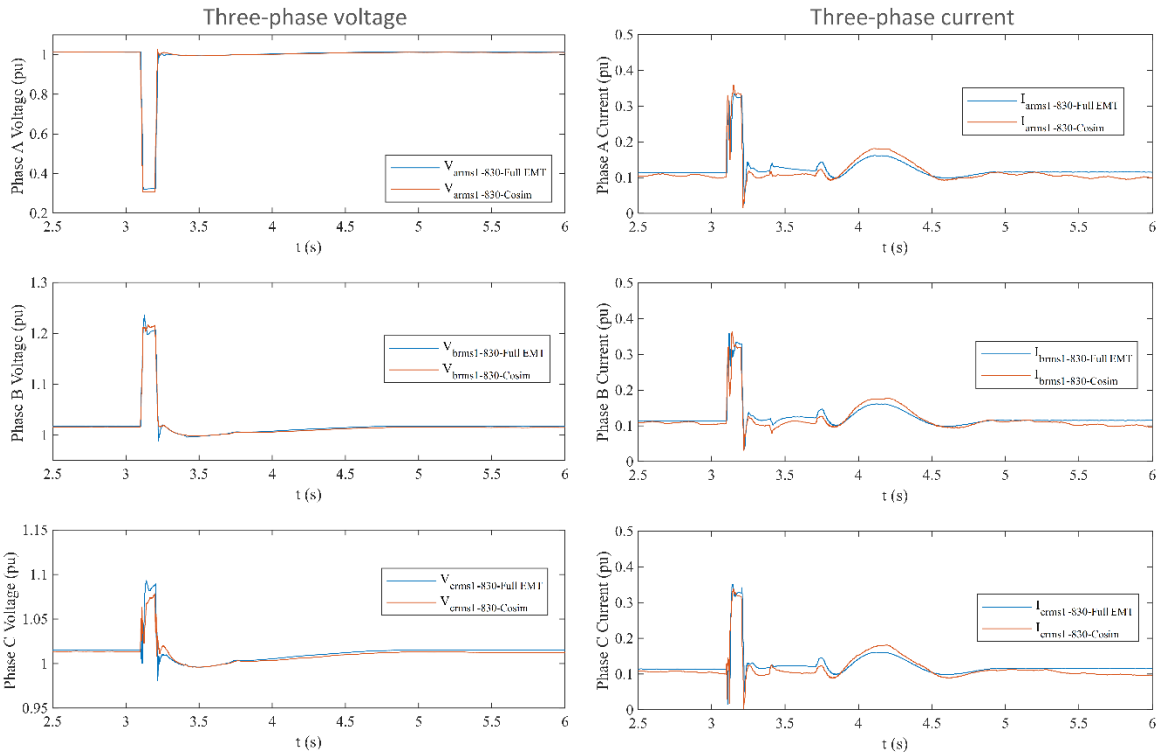

Fig. 3-10 Three-phase voltage and current responses at Node 830.

For the single-line-to-ground fault applied on the GridLAB-D side, some of the comparison results between full-EMT and co-simulation are presented in Fig. *3-9* - Fig. *3-10*. The P&Q NRMSE for each inverter in this case is outlined in Table *3-3*. The mismatch in Q for Inverter 2 is caused by the steady-state error of power flow solved by two different simulators.

Table 3-3 NRMSE of inverters during SLG-A fault in GridLAB-D.

Inverter Name	**NRMSE of P (%)**	**NRMSE of Q (%)**
Inverter 1	0.02	0.40
Inverter 2	0.26	7.36
Inverter 3	0.24	1.28
Inverter 4	0.24	1.31
Inverter 5	0.28	1.36

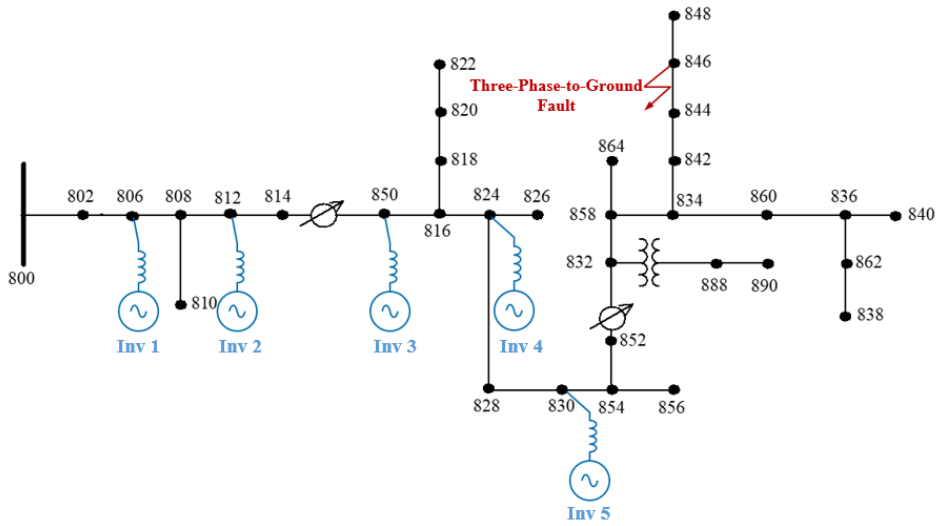

Fig. 3-11 An LLL-G fault at Node 846 in the GridLAB-D side of the co-simulation model.

3.2.3.3 Discussion of the IBR Tripping Issue

During the process of validating the PSCAD/HELICS/GridLAB-D co-simulation platform, it was observed that in some fault scenarios, the co-simulation model results do not match with the full EMT model results. For instance, when a severe fault (e.g., three-phase-to-ground fault) that lasts for 0.1s, is applied in the Full-EMT (PSCAD) and PSCAD/HELICS/GridLAB-D co-simulation models containing 5 black-box inverter models, there is a discrepancy in results obtained from the Full-EMT simulation and co-simulation models. Whereas the Full-EMT model predicts that all the inverters rode through the 0.1s fault, however, the co-simulation model predicts that only one inverter rode through the fault. A setup of the case scenario is illustrated in Fig. *3-11*. More details about the scenario setup are outlined below:

- 5 black-box GFL inverters are connected at Nodes 806, 812, 850, 824, & 830.
- For the co-simulation model, the GridLAB-D model starts exchanging information with the PSCAD model at t = 4 s.
- The time step for the PSCAD/HELICS/GridLAB-D model is 10 μs/1 ms/4 ms
- The time step for the Full-EMT model is 10 μs
- A Three-Phase-to-Ground Fault occurs at Bus 846 at 5.1 s and then cleared at 5.2 s. The per-phase fault impedance is 1 ohm.

3.2.3.3.1 What is responsible for the tripping?

Fig. *3-12* shows results depicting the scenario. The co-simulation model predicted that the inverter at Node 812 did not ride through the fault whereas the Full-EMT (PSCAD) model predicted that the inverter at Node 812 rode through the fault.

To locate the source of the issue, fault codes generated by the black-box inverter were analyzed. The analysis suggested that AC overvoltage induced by high dv/dt during fault-clearing was responsible for the tripping. Fig. *3-13* shows the voltage at Node 812 and the corresponding inverter output current. It is evident that there is a spike in the node

voltage obtained from the co-simulation model during the fault clearing time. The reason for the spike is due to the inability of GridLAB-D to clear the fault at the zero-crossing of current/voltage. Note that the black-box inverter is configured to trip when there is a fats voltage transient.

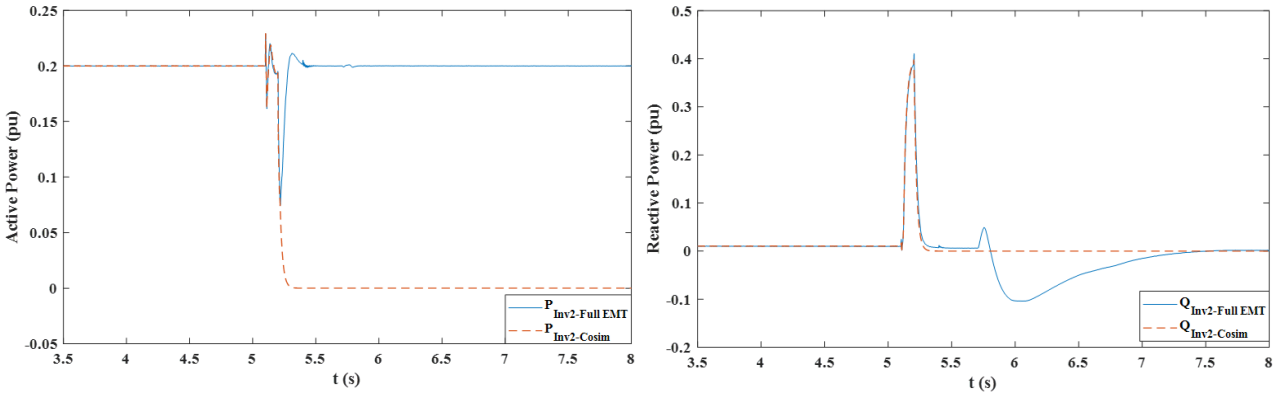

Fig. 3-12 Active and reactive power output of the inverter at Node 812 for a three-phase-to-ground fault at Node 846.

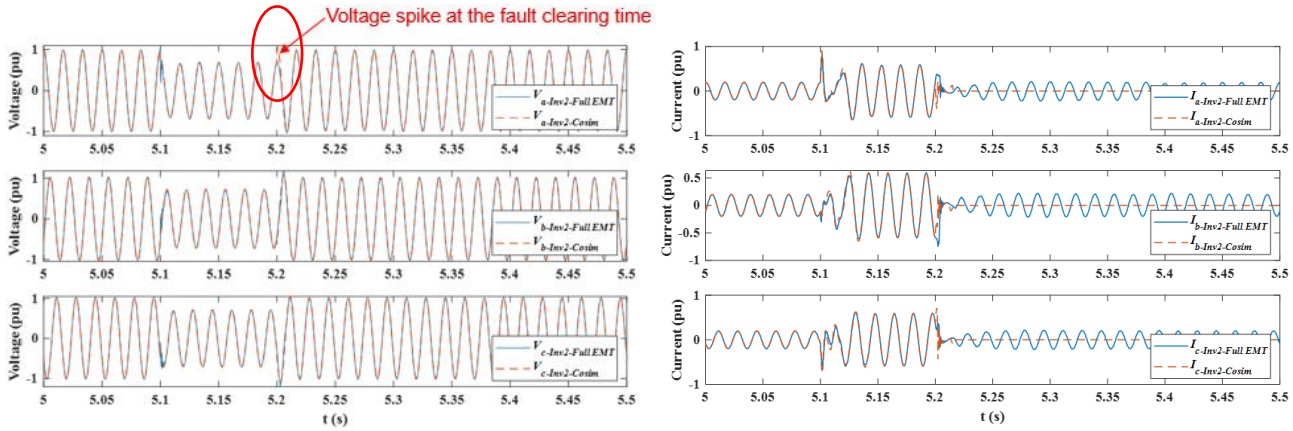

Fig. 3-13 Node voltage and output current for the inverter at Node 812.

To resolve the false-tripping issue associated with the co-simulation model, the electrical interface model is modified by including a rate limiter. Fig. *3-14* shows the improved version of the electrical interface model. The three-phase phasor voltages from GridLAB-D are passed through a rate limiter before being converted to sinusoids that are fed to the controllable voltage source in the PSCAD side of the co-simulation platform. The maximum decrease and increase rates of the rate limiter were selected to restrict the *dv/dt* rise only during fault clearing (at the rising edge) while allowing natural high *dv/dt* at the falling edge, as real faults can occur at any point on the waveform.

Fig. *3-15* – Fig. *3-16* depict some of the results obtained with or without rate limiters. The results indicate that the inclusion of the rate limiter in the co-simulation model did not only prevent the tripping of the black-box inverters during fault clearing, but also

increased the level of correlation between the Full-EMT model results and the co-simulation results. It is important to note that the selection of rate limiter parameters relies on knowledge of the inverter's control algorithms and settings. Selecting incorrect rate limiter parameters can potentially exaggerate or understate the inverter's performance, leading to misleading simulation results.

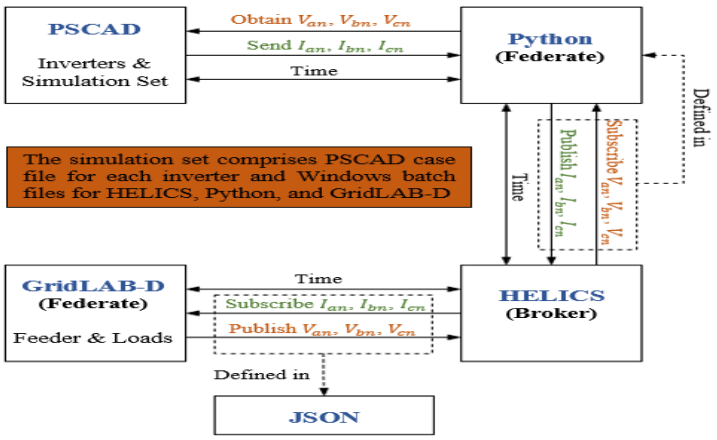

Fig. 3-14 Improved electrical interface model for the EMT & three-phase phasor co-simulation platform.

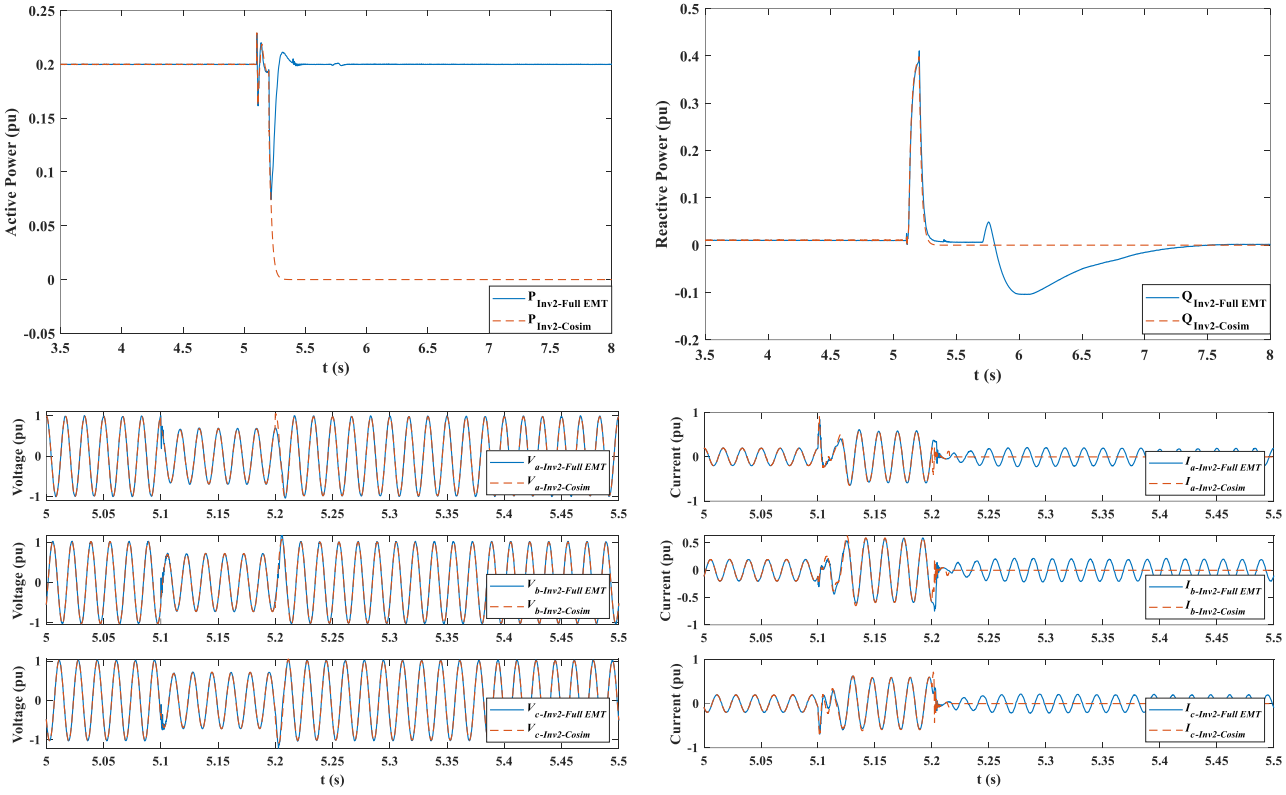

Fig. 3-15 Response of the inverter at Node 812 without rate limiters included.

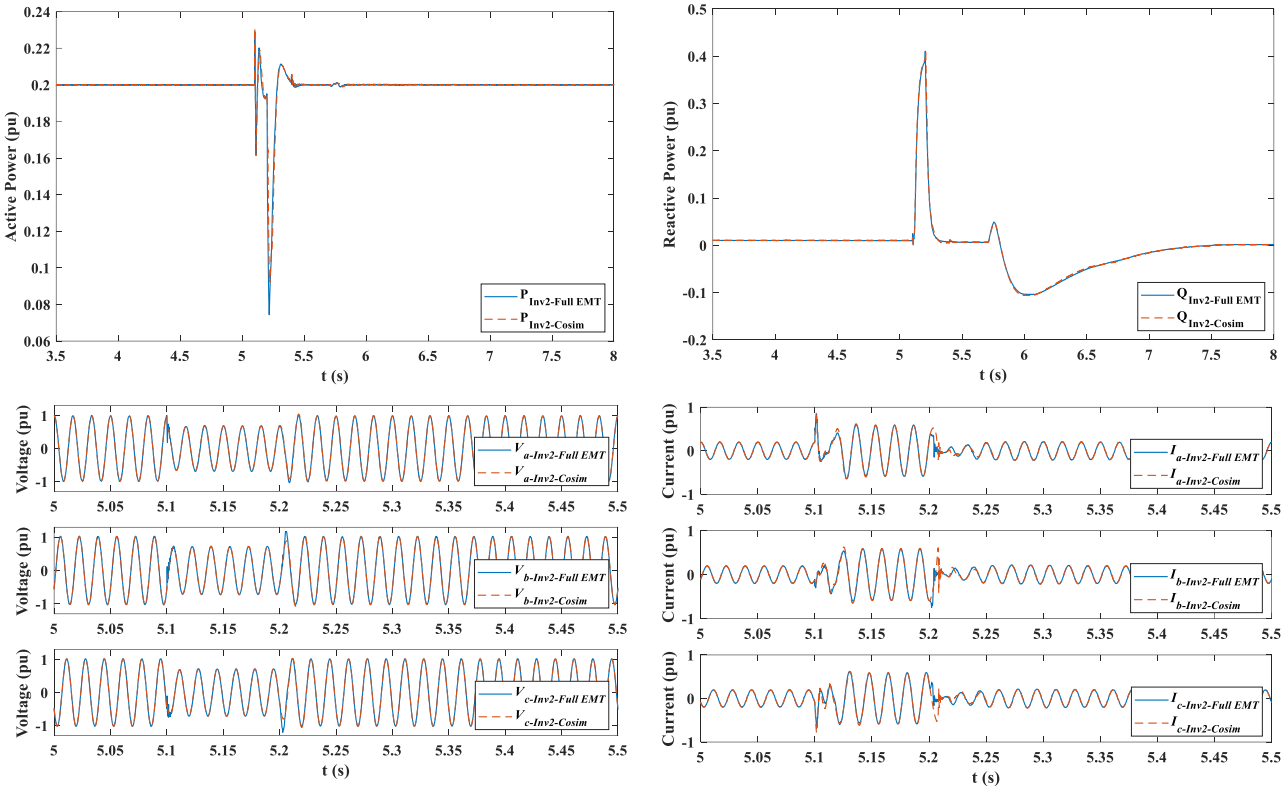

Fig. 3-16 Response of the inverter at Node 812 with rate limiters included.

3.2.3.3.2 Performance Evaluation of the Improved Co-Simulation Platform

The fidelity of the improved co-simulation model is verified through error analysis and simulation execution time comparison with respect to the Full-EMT model.

Error Analysis:

Table 3-4 shows the NMRSE results obtained from comparing the co-simulation model results with the full-EMT results. We can see that the NRMSE of all inverters are approximately within the 2% threshold.

Table 3-4 NRMSE of Inverters in a Co-Simulation Model with Rate Limiters for a Three-Phase-to-Ground Fault in GridLAB-D.

Inverter Name	NRMSE of P (%)	NRMSE of Q (%)
Inverter 1	0.01	0.14
Inverter 2	0.23	0.31
Inverter 3	0.45	1.44
Inverter 4	0.49	1.79
Inverter 5	0.42	2.03

Simulation Execution Time Comparison:
Table 3-5 illustrates the simulation execution times of the Full-EMT model and the co-simulation model. We can see that the co-simulation model is about 2 times faster than the full-EMT model for the same simulation runtime. It can be envisioned that with larger size feeder model and even more inverter models, the simulation efficiency can be further improved.

Table 3-5 Simulation Execution Time Comparison (runtime: 8 s).

Model	Execution Time (s)	Speed-Up Factor
Full-EMT	896	1
Co-Simulation	485	1.85

3.2.4 Subsection Conclusion and Discussion

In this subsection, a high-fidelity co-simulation platform based on PSCAD, HELICS, and GridLAB-D has been described and validated against a full EMT (PSCAD) simulation model via a case study involving the study of transient dynamics of a large-scale (IEEE 34-Node Test System) distribution system with 5 vendor-based inverter models **(M 2.2.7)**. The proposed co-simulation platform enables critical transients in a high DER-penetrated distribution grids to be studied in a shorter timeframe compared to full-EMT simulation without a significant degradation in accuracy levels (NMRSE < 2%). It is found that accurate results from the co-simulation platform depend on the use of electrical interface models that accurately represent transients without exaggeration or underestimation. More research is needed to improve the accuracy and reduce the complexity of the co-simulation platform.

3.3 Physics-Based and Data-Driven ML Modeling (White-/Black-/Gray-box)

This section presents the physics-based and data-driven ML modeling of white-/black-/gray-box IBRs.

3.3.1 Data Sources and Test Cases

To support the development and validation of these models, data from various sources, including commercial IBRs, were obtained. *Table 3-6* lists the data sources and the corresponding models.

Table 3-6 List of data source and corresponding models.

Data Source	Corresponding Model					
	White-box GFL	White-box GFM	Black-box GFL	Gray-box BTM IBR	Motor	ComED feeder
CHIL testing of GE LV5 IBR	✓		✓			
One commercial IBR experimental results	✓					
EMT simulation of REGFM_B1		✓				
NREL 1MW testbed that includes two GFMs and one GFL	✓		✓	✓		
VFD motor load testing					✓	
μPMU and PQ meter data of ComED feeder						✓

In addition, to test and validate the quality of the developed models, the following tests were performed, as recommended by the procedures outlined in the ERCOT, WECC, NERC, and IEEE P2800 standards. Table *3-7* summarizes the list of tests conducted to evaluate the quality of the developed models.

Table 3-7 Summary of the model quality tests.

Test	Expectation/Success Criteria	Tested model
Flat-Start Test	Voltage, active power, reactive power, and frequency are expected to remain very close to the initial system condition	GFM and GFL
Phase-Angle-Jump Test	Oscillations should be well damped	GFM and GFL
System Strength Test	Model should be stable for SCR of 3 and higher. If the model is unstable for an SCR of 1.5, then technical reasons for the discrepancy should be given and the IBR model should be enhanced	GFM and GFL
Small Voltage Disturbance Test	Oscillations should be well damped and real power output should be sustained throughout the test	GFM and GFL
High Voltage Disturbance Test	Model exhibits appropriate dynamic reactive and AVR responses. No momentary cessation	GFM and GFL
Low Voltage Disturbance Test	Model exhibits appropriate dynamic reactive and AVR responses. No momentary cessation	GFM and GFL

Small Frequency Disturbance Test	The governor or frequency controller should lower or raise the real power dispatch as per the droop and dead-band characteristic	GFM and GFL
Change of Parameter Test	The output active and reactive power should follow the commands	GFM and GFL
Fault Test	Should be able to ride-through typical faults and maintain stability post faults	GFM and GFL
Loss of Last Synchronous Generator Test	Should maintain the voltage and frequency stability after going into the islanded mode	GFM

3.3.2 Discussion on White-/Black-/Gray-Box Modeling Approaches

Before introducing the white-/black-/gray-box models, the table below summarizes their strengths, limitations, technology maturity, and typical use cases, so that users can understand the pros and cons of each modeling approach and select them for appropriate use.

Table 3-8 Summary of Strengths, Limitations, and Use Cases of White-/Black-/Gray-Box Modeling Approaches

Type	**Description**	**Strengths**	**Limitations**	**Technology Maturity**	**Use Cases**
White-Box	Detailed mathematical models derived from first principles (circuit equations, control block diagrams, device physics).	- Transparent, readable, and understandable - Parameters typically have physical meanings	- Require detailed knowledge of the actual equipment - Parameter tuning can be difficult if the model structure does not accurately represent the actual equipment - Simulation could be slow when performing large-scale EMT simulations	-High. Matured technology used in power industry	- IBR Interconnection studies - System-level stability studies
Black-Box	Uses machine learning models (e.g., neural networks) trained on input-output data, without explicit physical equations.	- No need to disclose internal design - May accelerate simulation once trained	- Require large, high-quality datasets - No clear physical meaning - May violate physical laws	-Low. Not used in power industry yet.	- Could be used for modeling unknown or proprietary device behavior from measured data
Gray-Box	Combines physical equations with data-driven components; physical laws constrain the learning process while ML captures unknown parts.	- Can embed constraints to ensure physical feasibility - May requires less data than black-box - May accelerate simulation once trained	- Still require some physical knowledge - Could be more complex to develop and tune - May be limited by both physical model accuracy and data quality	-Low. Not used in power industry yet.	- Could be used for situations where partial physics is known but some dynamics are unknown

3.3.3 White-Box IBR Model and Validation

3.3.3.1.1 Phasor Model Development of Grid-Following (GFL) Inverter

In this work, the grid-following (GFL) inverter model developed for distribution performance studies is based upon solar photovoltaic (PV) plant models[8]. The GFL inverter model in Fig. 3-17 is a controlled-current source injecting currents into the network in response to the real and reactive current commands under both balanced and unbalanced grid disturbances.

The inverter supports the frequency-based active power droop and voltage-based reactive power droop functions that could impact the power commands, P_{cmd} and Q_{cmd}, separately. The model also incorporates voltage ride through capability to prevent the combination of the active and reactive currents from exceeding inverter capability.

The inverter overcurrent caused by faults could be relieved by limiting the current commands. Reactive current injection could be suppressed to help limit excess voltage on the terminals. The current limiting function is included to prevent the combination of the real and reactive currents from exceeding inverter capability. Priority of active power or reactive power can be chosen. When active power has priority, the active power command is limited to the hardware current limit. The limit applied to the reactive current command is calculated based on the remaining inverter current capability and the voltage dependent current limit. Similarly, when reactive power has the priority, the limit on the reactive current command is determined as the minimum of the hardware current limit and the voltage dependent limit, and the remaining inverter current capability becomes the limit applied to the active power current command.

Besides positive sequence, the GFL control in Fig. 3-17 extends to also cover transient dynamics under unbalanced grid disturbances. The negative sequence current is regulated. In this work, both the negative sequence active and reactive current components are regulated to be zero. This can be furtherly programed to user-defined negative sequence control as well. When interfacing the phasor model with the distribution network power flow solver, the internal negative sequence voltage output of a GFL controlled inverter is converted to its Norton equivalent current source and both positive and negative sequence current sources are summed together. Also, it should be noted that the negative sequence current magnitude impacts the inverter capability in the positive sequence current limiting block.

[8] K. Clark, R. A. Walling and N. W. Miller, "Solar photovoltaic (PV) plant models in PSLF," *2011 IEEE Power and Energy Society General Meeting*, Detroit, MI, USA, 2011, pp. 1-5.

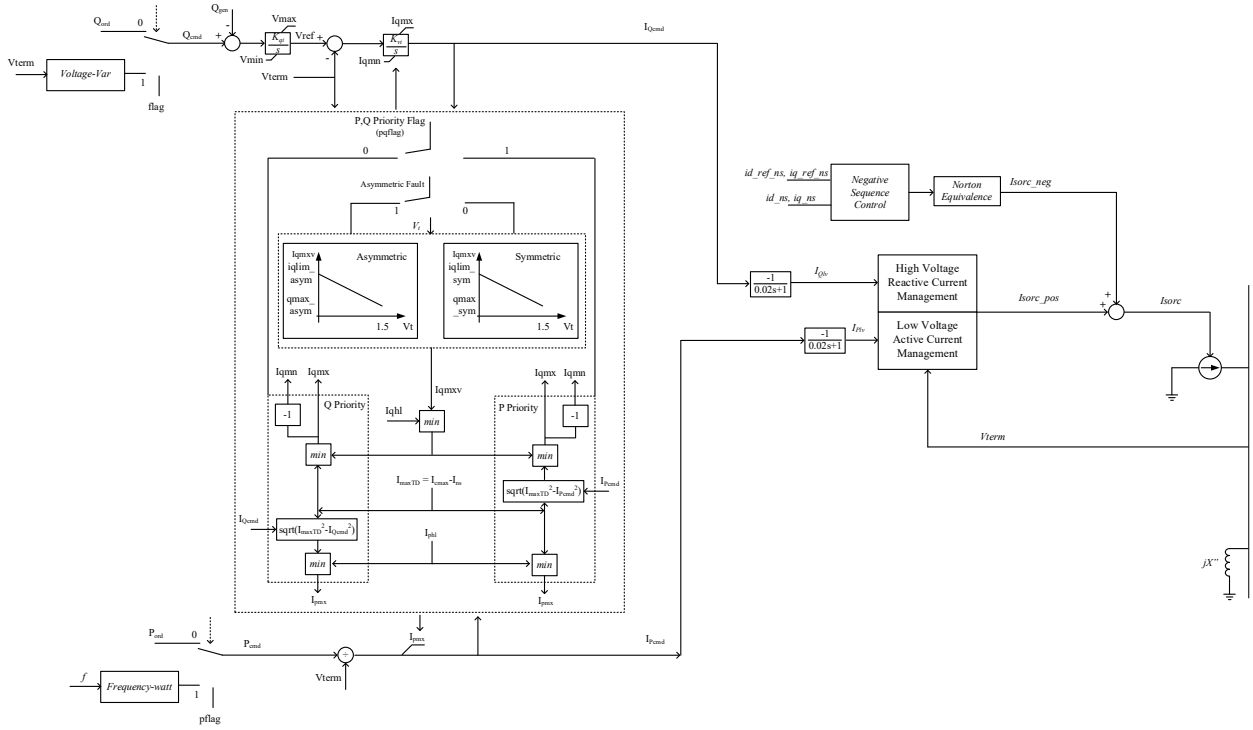

Fig. 3-17 GFL Inverter Model Developed Based on [9] .

3.3.3.1.2 Simulation Results & Validation

GFL inverter is simulated with per-phase phasor model representation developed in GridLAB-D. Table *3-9* shows the GFL inverter parameters used throughout the simulation. To ensure the veracity of dynamic simulations that can inform utility planning, GridLAB-D results are compared with results from CHIL simulation platform and phasor model in MATLAB/Simulink. The CHIL simulation platform includes a controller hardware and power circuits are modeled in real-time digital simulator (RTDS) including the inverter power stage, transformer, grid model, DC source and load. The controller takes current and voltage feedbacks from the simulated plant inside RTDS, and generated PWM pulses given to switches are sent from the controller to RTDS.

Table 3-9 GFL Inverter Parameters.

Parameter	**Value**	**Parameter**	**Value**
Rating (MVA)	1	k_{qp} (pu)	0.5
Rated RMS Voltage (V)	550	k_{qi} (pu)	0.5
Grid reactance (mH)	5	k_{vp} (pu)	1
Grid resistance (mΩ)	0.501	k_{vi} (pu)	50

[9] Clark, Kara, Nicholas W. Miller, and Reigh Walling. "Modeling of GE solar photovoltaic plants for grid studies." *General Electric International. Inc, Schenectady, NY* 12345 (2010).

In CHIL platform, voltage and current measurements after the inverter output LC filter and at the dc bus side are recorded. Fault scenarios, such as balanced and unbalanced grid voltage drops, are investigated to calibrate the developed GFL model in this reporting period.

Frequency - power Droop and ROCOF Tests

Fig. 3-18 shows the simple model used here to capture inverter frequency-watt dynamics. The frequency-watt function is modeled as a lookup table indexed by the measured frequency of the system. A low pass filter is used to model the frequency measurement dynamics from the PLL. The inverter is modeled by a first order transfer function with a time constant which represents the response speed of the power control. The frequency-watt function is modeled using droop and dead-band values as shown in Fig. 3-19.

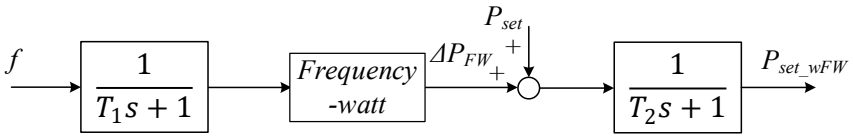

Fig. 3-18 Distributed inverter model including frequency-watt function.

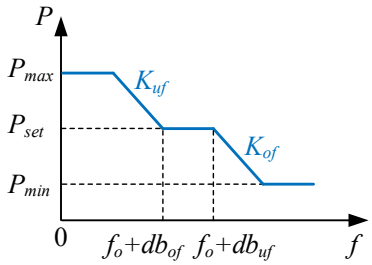

Fig. 3-19 Frequency-watt function parameters.

Fig. 3-20 shows a plot of the time response of GFL inverter to a fast frequency change. The inverter's active power response is fast and well-damped within about 0.4 s. The inverter's reactive power response does show some unexpected dynamics during and immediately after the frequency event. Similar fluctuations could also be seen in q-axis voltage and current, indicating slight voltage variation could be caused by high ROCOF event and possible reactive power control loop could be improved for these.

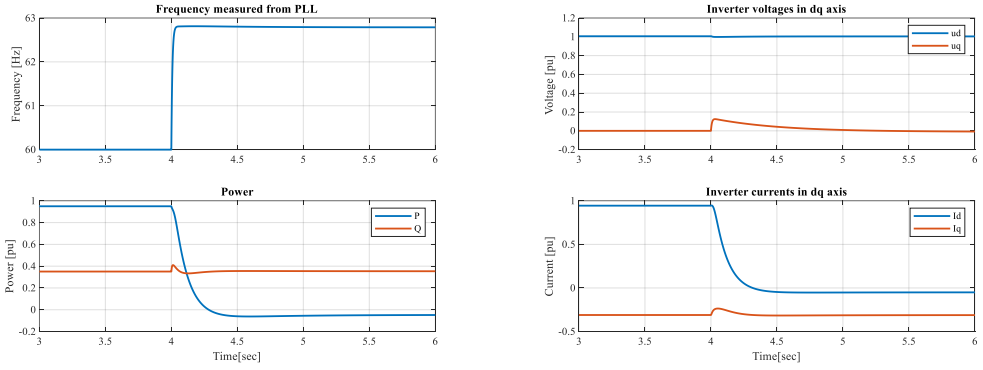

(a) Frequency, P and Q (b) Voltage and current in dq axis

Fig. 3-20 Inverter frequency-watt response to grid frequency step change.

In Fig. 3-21, the grid frequency is adjusted upwards and then back downwards between 60 and 62.33 Hz. The ROCOF is about 1.165 Hz/s. The frequency-watt droop is 5%. The results have shown the relationship between frequency and active power, indicating the measured droop curve matches the expected droop curve very well.

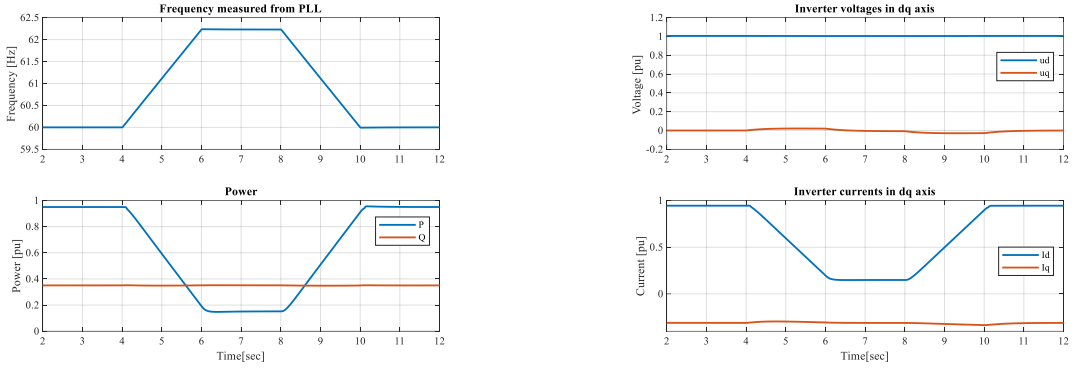

(a) Frequency, P and Q (b) Voltage and current in dq axis

Fig. 3-21 ROCOF test. Frequency changes between 60 and 62.33 Hz. 5% Droop Slope, Apparent power = 100%, and Power Factor = 0.95.

In Fig. 3-22, the grid frequency is adjusted downwards to 58.3 Hz and then back upwards to 60 Hz. The frequency-watt droop is still 5%. The apparent power is 0.5 pu and power factor is 0.95. When the grid frequency decreases to a certain level, the active power reaches to the maximum value and the reactive power is regulated to be zero. After the grid frequency upwards to 60 Hz, the reactive power reference changes back to the pre-set value.

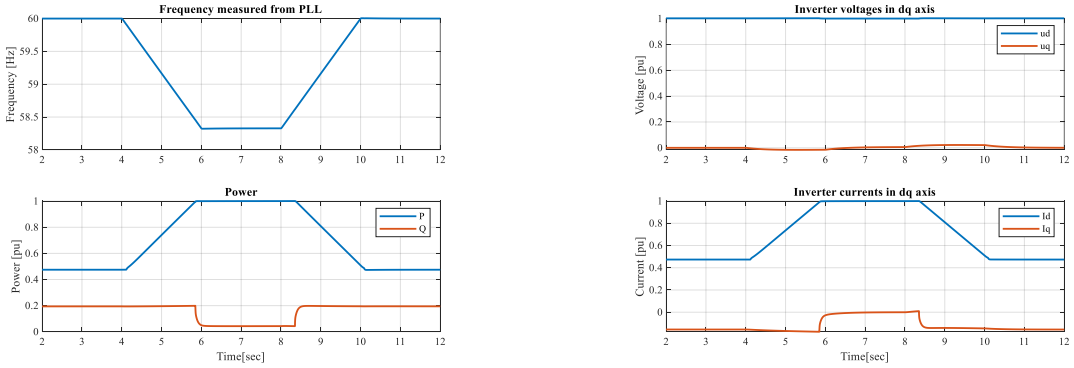

(a) Frequency, P and Q (b) Voltage and current in dq axis

Fig. 3-22 ROCOF test. Frequency changes between 60 and 58.3 Hz. 5% Droop Slope, Apparent power = 50%, and Power Factor = 0.95.

Fig. 3-23 represents the battery inverter dynamics. During this ROCOF event, the inverter provides about 0.2 pu reactive while the active power is changed based on frequency-watt function, which could mimic the charging and discharging of the battery inverter.

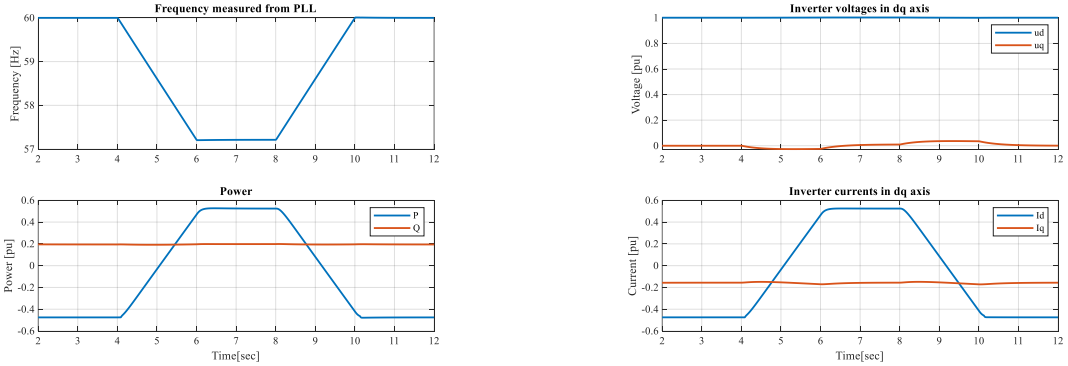

(a) Frequency, P and Q (b) Voltage and current in dq axis

Fig. 3-23 ROCOF test. Frequency changes between 60 and 57.2 Hz. 5% Droop Slope, Apparent power = 50%, and Power Factor = 0.95.

Volt - Var Support

In this test case, the active power reference is 0.5 pu and reactive power reference is 0 pu. The volt-var slope is 4%. Fig. 3-24 shows result of grid voltage staircase from 1.05 to 0.95 pu. The power is measured before the inverter's filter such that the reactive power is nonzero at the rated grid voltage. The reactive power increase is proportional to the grid voltage drop with the defined slope.

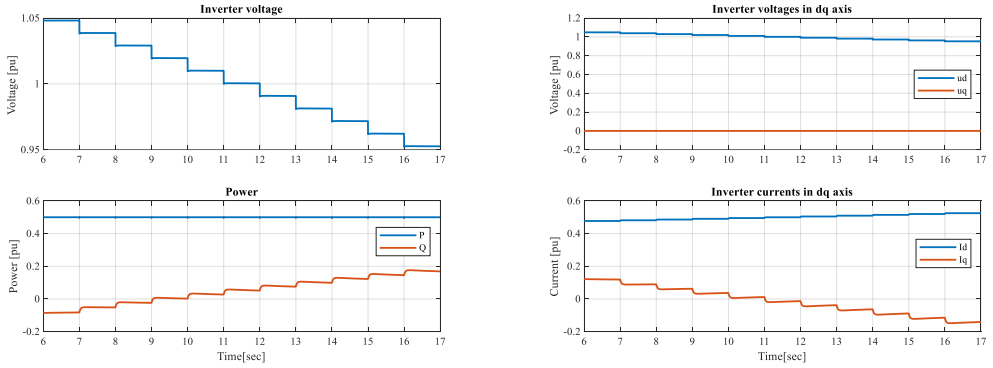

(a) Voltage, P and Q (b) Voltage and current in dq axis

Fig. 3-24 Voltage-var test.

LVRT with P = 1.05 pu Before Faults

Fig. 3-25 (a) shows 30% LVRT waveforms in GridLAB-D, Simulink and CHIL platforms. The inverter is with Q priority. The peak inverter output current is kept the same before and after the event. Active power is decreased from 1.05 to 0.635 pu while reactive power increases to 0.435 pu to support the grid voltage. Both power and current results are matched well among different platforms.

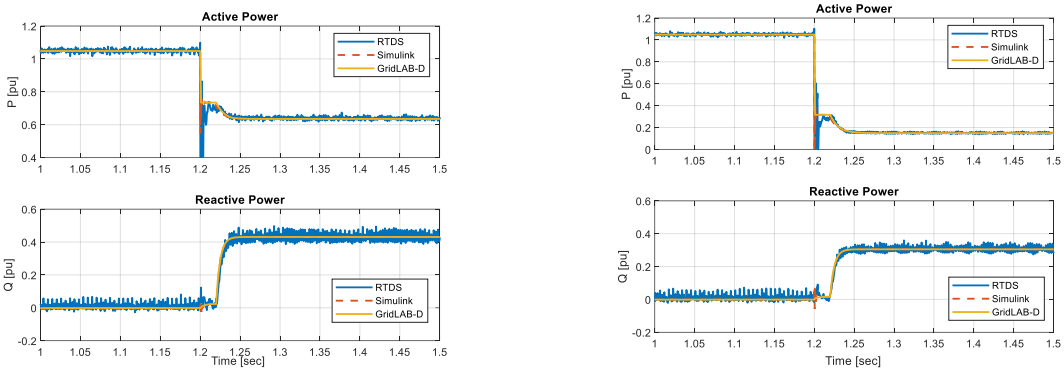

(a) 30% balanced grid voltage drop *(b) 70% balanced grid voltage drop*

Fig. 3-25 Results of balanced grid voltage drops in CHIL, Simulink, GridLAB-D platforms. P = 1.05 pu and Q = 0 before the fault.

Fig. 3-25 (b) shows 70% LVRT waveforms. Due to deeper voltage drop, the inverter with Q priority provides the reactive power of 0.3 pu based on the pre-defined Q vs voltage dip relationship. The remaining inverter current capacity supports the active power, which is 0.15 pu after the fault.

LVRT with different P and Q

Fig. 3-26 shows 70% LVRT waveforms when P = 0.5 pu and Q = 0.5 pu. As seen in the dq-axis current plot, when the reduction of the transient reactive power is decreased, the increase of active power correspondingly becomes smaller. Transient P and Q behaviors has demonstrated a closer matching with RTDS results.

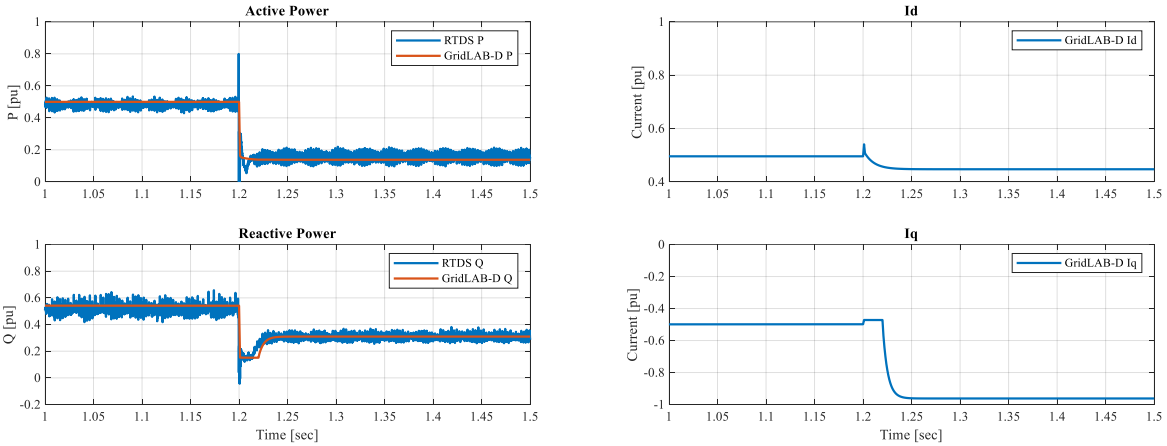

(a) P and Q (b) Currents in dq reference frame

Fig. 3-26 Results of 70% balanced grid voltage drops in CHIL, GridLAB-D, and improved GridLAB-D models. The grid voltage drops from 1 to 0.3 pu. P = 0.5 pu and Q = 0.5 pu before the fault.

Unbalanced Grid Voltage Faults

Fig. 3-27 shows the results when 50% grid phase A voltage drop is applied. During the faults, the positive sequence Q is regulated to follow the Q priority control algorithm and the remain inverter capacity is used to export positive sequence P to the grid. Both negative sequence P and Q are regulated to be zeros. Both steady-state P and Q in GridLAB-D match with the CHIL results. The negative sequence currents transiently impact on the positive sequence P which results in the positive sequence P discrepancy at the first 50 ms after the faults as shown in the figure. It should be noted that the negative sequence component control can be further modified with other control strategy as well.

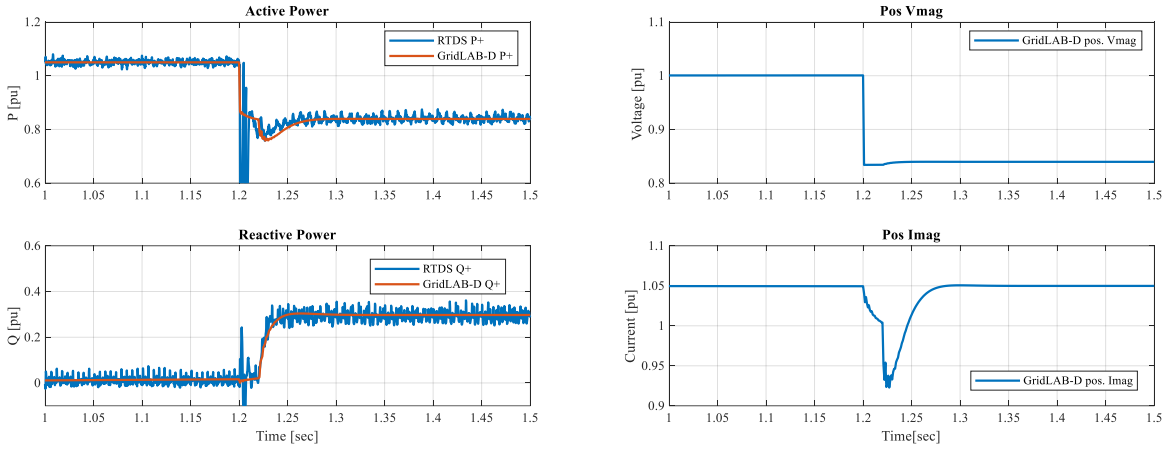

(a) P and Q (b) Positive voltage and current magnitudes

Fig. 3-27 Results of unbalanced grid voltage drop in CHIL, GridLAB-D, and improved GridLAB-D models. The grid phase A voltage drops from 1 to 0.5 pu. P = 1.05 pu and Q = 0 pu before the fault.

3.3.3.2 Grid-Forming IBR

3.3.3.1 Phasor Model Development of Grid-Forming (GFM) Inverter

The baseline positive sequence phasor model is based on the generic dynamic model approved by Western Electricity Coordinating Council (WECC), i.e., REGFM_B1.

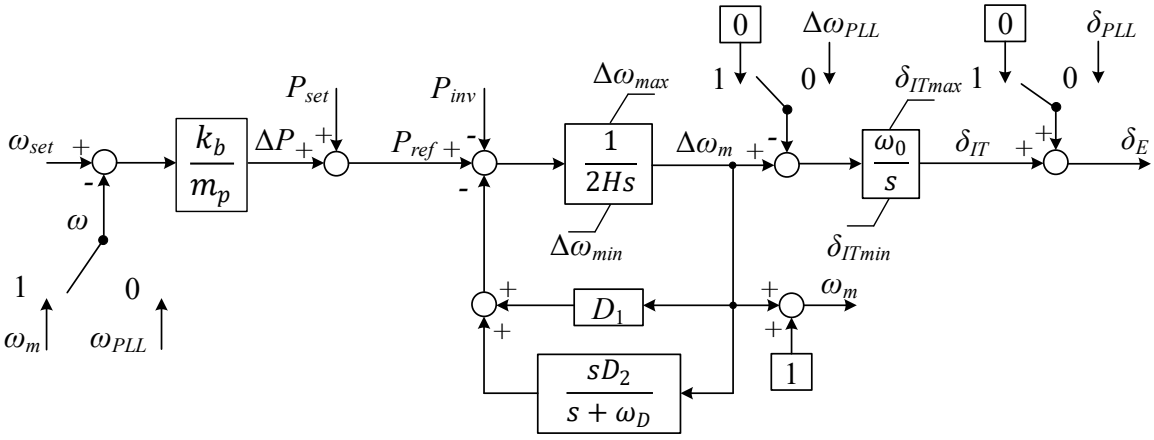

(a) VSM frequency control block

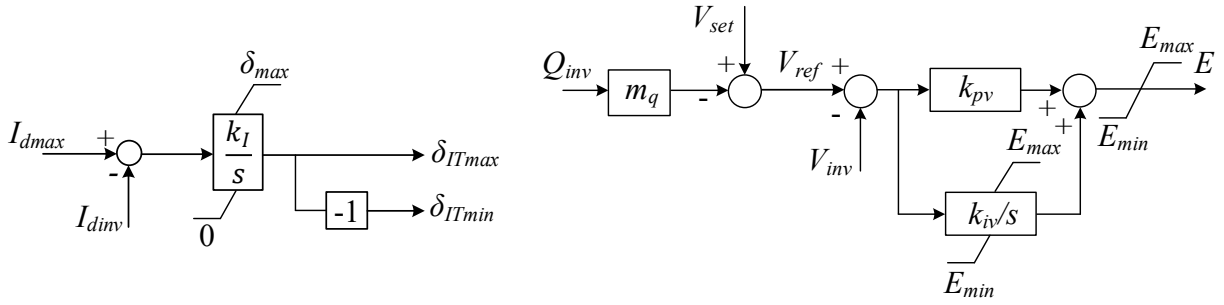

(b) Active power limiting block (c) VSM voltage control block

Fig. 3-28 VSM control implemented in phasor domain for GFM inverter.

As shown in Fig. 3-28, the grid-forming (GFM) inverter model is a controlled-voltage source controlling the frequency and voltage amplitude. A generic VSM control is used to implement the GFM concept. This model also considers protection functions such as the active power limiting and voltage saturations The controlled-current source incorporates protection functions such as low voltage ride through and high voltage ride through capabilities. This generic model can be updated for future GFM technologies later. This task mainly focuses on the performance of this representative GFM inverter model used for bulk system performance studies.

The mathematical model of a synchronous generator is implemented in the inverter's control to obtain an output voltage $E\angle\delta_E$. The internal voltage amplitude E is implemented by a reactive power voltage (Q-V) droop followed by a classic PI voltage regulator mimicking a simplified excitation system, as shown in Fig. 3-28 (c). On the other hand, the VSM-oriented angle, δ_E, is achieved via active power frequency (P-f) droop. For the implementation shown in Fig. 3-28 (a), the angular frequency setpoint, ω_{set}, could be compared with either virtual angular speed, ω_m, or frequency from PLL, ω_{PLL}, and the difference is divided by droop coefficient, m_p. k_b determines if this droop is enabled or not. The power reference, P_{ref}, is achieved by adding ΔP to the nominal power setpoint, P_{set}. Governed by the virtual rotor inertia, the change in power reflects to the change in the angular frequency, $\Delta\omega_m$, which is the difference between the nominal angular frequency and the virtual angular speed, ω_m. The frequency-droop characteristics on the virtual rotor is implemented by a damping power proportional to $\Delta\omega_m$ with a slope of D_1. It should be noted that the combination of $1/m_p$ and D_1 contributes to the steady-state P-f droop. The transient damping is also introduced by using a high-pass filter with cutoff frequency of ω_D and the high-pass filtered $\Delta\omega_m$ is multiplied by a gain of D_2.

The saturation limits of δ_{IT} are controlled by the active power limiting block in Fig. 3-28 (b). The d-axis maximum current, I_{dmax}, and the maximum angle, δ_{max}, can be calculated via

$$I_{dmax} = k_{PF} I_{max}$$
$$\delta_{max} = \sin^{-1}(X_L I_{max})$$

where k_{PF} is a factor to determine I_{dmax}, I_{max} is the steady-state current limit, and X_L is the coupling reactance. On the other hand, saturation limits applied to E are calculated as

$$E_{min} = \sqrt{\left(V_{inv} - I_{qmax}X_L\right)^2 + (I_{dinv}X_L)^2}$$

$$E_{max} = \sqrt{\left(V_{inv} + I_{qmax}X_L\right)^2 + (I_{dinv}X_L)^2}$$

$$I_{qmax} = \sqrt{{I_{max}}^2 - {I_{dinv}}^2}$$

where V_{inv} is the voltage amplitude at the connection point and I_{dinv} is the d-axis current. When faults occur in the system, $E\angle\delta_E$ can be saturated. The active power is dependent on k_{PF} while remaining capability provides reactive support to the grid.

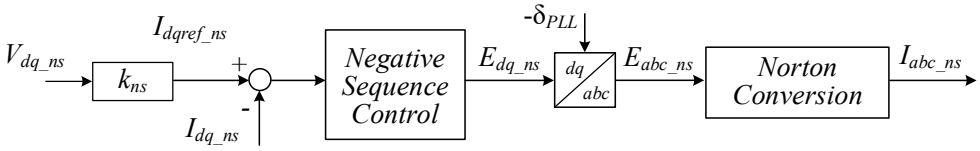

Fig. 3-29 Negative sequence block implemented in phasor domain for GFM inverter.

This work extends the inverter-based phasor models to have unbalanced control capabilities for distribution system performance studies during unbalanced grid voltage faults. One of existing unbalanced control methods is employed to generate negative sequence voltage reference as expected. In the negative sequence control, it includes PI controllers and decoupling of the α and β components in the stationary αβ frame. By actively regulating the negative sequence current components to zero, the inverter only delivers balanced positive sequence currents under unbalanced conditions. Therefore, the pulsating terms in the active and reactive power are solely dependent on negative sequence voltage components. This unbalanced control method is employed to generate negative sequence voltage reference as expected in GFM inverter. Besides regulating the negative sequence current components being zero, the inverter also has the flexibility to regulate the negative sequence currents proportional to negative sequence voltage components.

Compensation of negative sequence currents in an inverter with unbalanced voltages is incorporated into the generation of the modulation index in Fig. 3-29 as an addition to the main control loop that regulates the positive sequence components.

3.3.3.2 Simulation Results & Validation

The phasor model of a virtual synchronous machines VSM-based GFM inverter is developed in GridLAB-D. Table 3.3-10 shows the GFL inverter parameters. Dispatch points change and fault events are studied.

Table 3.3-10 GFM Inverter Parameters.

Parameter	Value	Parameter	Value
Rating (MVA)	1	H (s)	0.5
Rated RMS Voltage (V)	550	D_1 (pu)	0
ω_o (rad/s)	376.99	D_2 (pu)	100
X_L (pu)	0.15	ω_D (pu)	50
k_b	1	I_{max} (pu)	1.2
m_p (pu)	0.02	k_{PF}	0.875
$\Delta\omega_{max}$, $\Delta\omega_{min}$ (pu)	0.05, -0.05	k_I (pu/s)	2

For validation, an equivalent inverter EMT switching model is built and simulated in PSCAD with the same test cases.

Active Power Dispatch Point Step Change

Fig. 3-30 shows the grid frequency response to a step change in active power setpoint and also shows the VSM active power injection. The 0.4 pu step is applied at 1.2 s. It can be seen that the VSM system is obviously able to maintain the grid frequency within its operating boundaries. It is noted that the time to reach set-point frequency is 0.5 s. This response time will be increased when the inertial response is added.

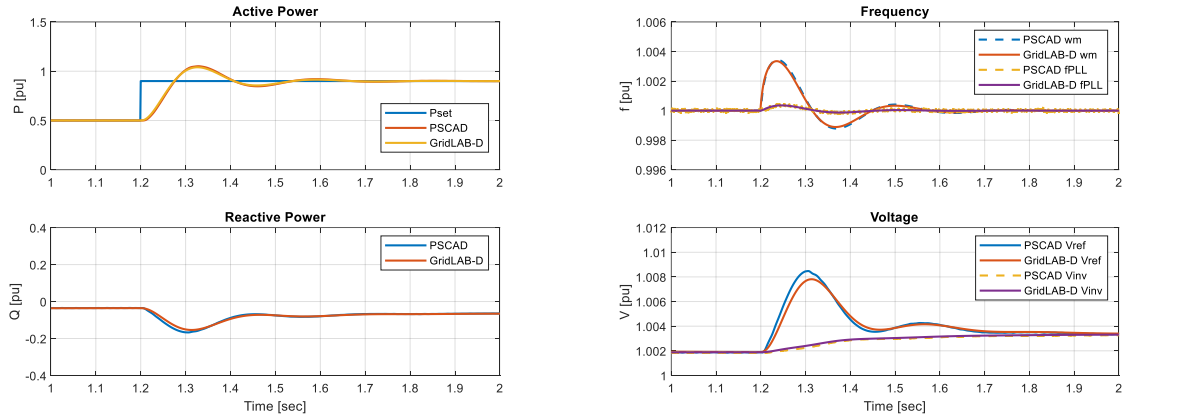

(a) P and Q

(b) Commands and measurements of frequency and voltage

Fig. 3-30 Results of active power step change in PSCAD and GridLAB-D models. The active power setpoint changes from 0.5 pu to 0.9 pu.

Voltage Dispatch Point Step Change

Fig. 3-31 shows the voltage response to a step change in voltage setpoint. After the setpoint changes from 1.0002 pu to 0.98 pu, the capacitive power is increased, and the voltage reference is updated based on the Q-V droop gain. The inverter voltage is regulated with the updated reference. GridLAB-D results match very well with PSCAD results.

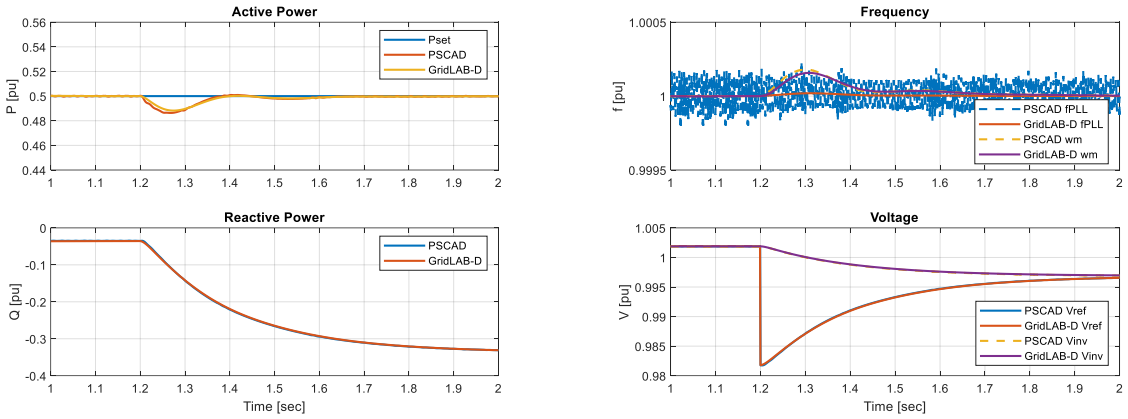

(a) P and Q

(b) Commands and measurements of frequency and voltage

Fig. 3-31 Results of a voltage setpoint step change in PSCAD and GridLAB-D platforms. The voltage setpoint changes from 1.0002 pu to 0.98 pu.

LVRT

After the fault, the saturation limits are updated with the dq-axis currents. And the angle difference between the inverter and the grid is saturated to the saturation limit. Similarly, the inverter internal voltage E_{mag} is saturated to maximum limit E_{max}. With these limiting blocks activated, the inverter becomes stable at new operating points. Fig. 3-32 shows 30% LVRT waveforms in PSCAD and GridLAB-D platforms. After the fault is applied at t = 1.2 s, the angle difference and the internal voltage are saturated to 0.18 rad/s and 0.833 pu, respectively. P decreases to 0.69 pu and Q increases to 0.44 pu.

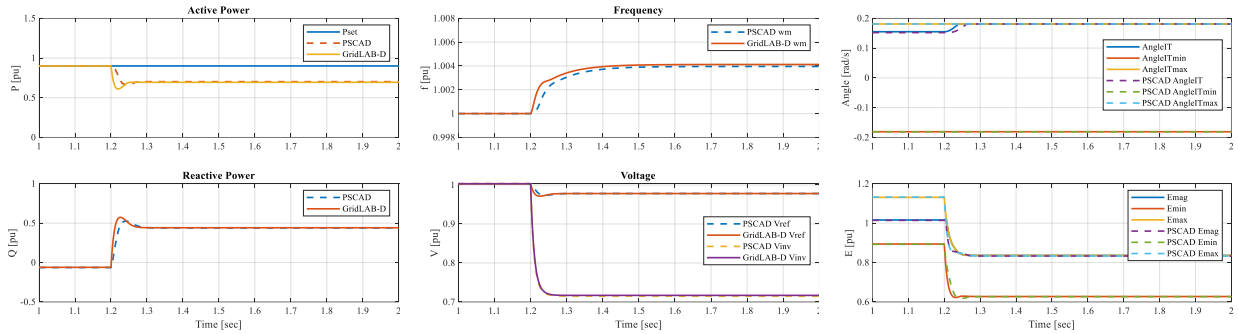

(a) P and Q

(b) Frequency and voltage

(c) Angle difference and internal voltage

Fig. 3-32 Results of 30% balanced grid voltage drops in PSCAD and GridLAB-D platforms. The grid voltage drops from 1 to 0.7 pu. P_{set} = 0.9 pu and Q_{set} = 0 pu before the fault.

Fig. 3-33 shows 70% LVRT waveforms. As the grid voltage drop becomes severe, more active power is reduced and more reactive power is regulated to support the grid voltage. In this case, active power is decreased from 0.9 pu to 0.2 pu while reactive power increases to 0.32 pu. Both power and control variable results are matched well among different platforms.

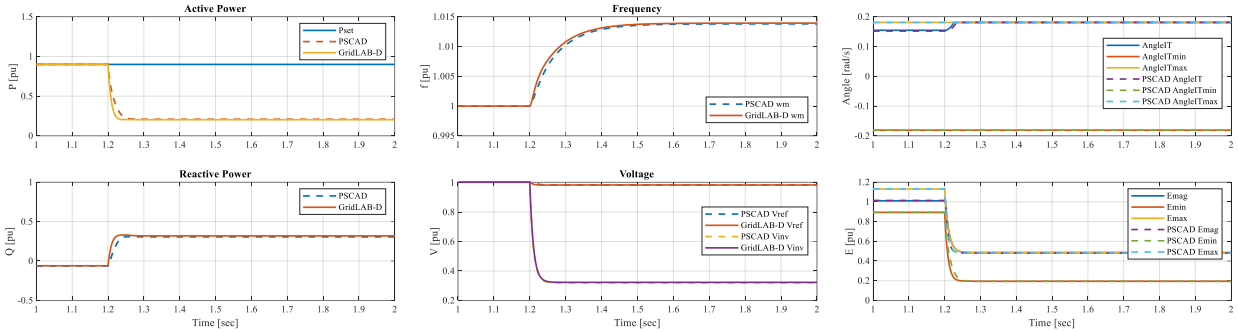

(a) P and Q

(b) Frequency and voltage

(c) Angle difference and internal voltage

Fig. 3-33 Results of 70% balanced grid voltage drops in PSCAD and GridLAB-D platforms. The grid voltage drops from 1 to 0.3 pu. P_{set} = 0.9 pu and Q_{set} = 0 pu before the fault.

Table 3.3-11 is the list of NRMSE values of GFM inverter phasor model under the balanced grid fault events. All NRMSE for P and Q in the table are kept under 2%.

Table 3.3-11 NRMSEs of GFM inverter phasor model under balanced grid voltage fault events.

Event		*Per-phase phasor model*
30% LVRT, P_{set} = 0.9 pu, Q_{set} = 0 pu	*P*	*1.82%*
	Q	*1.97%*
70% LVRT, P_{set} = 0.9 pu, Q_{set} = 0 pu	*P*	*1.52%*
	Q	*1.6%*

Unbalanced Grid Voltage Faults

This case is an unbalanced voltage sag. In this scenario, grid voltage v_{ga} falls to 0.7 pu at t = 2.2 s. The negative sequence currents are regulated two times of the negative sequence voltages. Simulation results showing the positive and negative sequence active power and reactive power are provided in Fig. 3-34 (a) from top to bottom and the negative sequence voltages and currents are provided in Fig. 3-34 (b) from top to bottom. This case is provided to clearly show the effectiveness of the negative sequence current regulation in phasor domain simulation. As shown in Fig. 3-34, the inverter delivers constant positive active power while the positive reactive power is increased due to the drop of the voltage. When the event is applied, the positive sequence voltage magnitude drops to 0.9 pu while the negative sequence voltage magnitude increases to 0.1 pu. The big portion of the negative sequence voltage is from the d-axis. By regulating to the commands proportional to the voltage, the negative d-axis current is -0.2 pu while the negative q-axis current is almost zero. The EMT emulation results are also provided in Fig. 3-34. It should be noted that the spikes at the first several switching cycles of EMT results are partially relevant to transient current limiting control logics applied to the inverter switches.

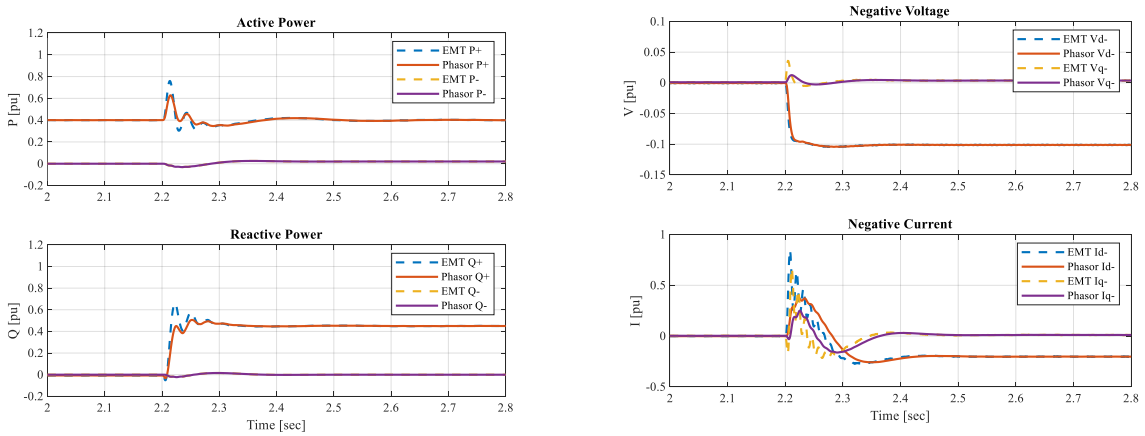

(a) P and Q (b) Angle difference and internal voltage

Fig. 3-34 Case I: Results of unbalanced grid voltage drop in PSCAD and GridLAB-D models. The grid phase A voltage drops from 1 to 0.7 pu. Reactive power is regulated proportional to negative sequence voltage.

The same fault event is applied in GFM inverter while the negative sequence current commands are zero, as shown in Fig. 3-35. Compared to the negative q-axis current of -0.2 pu under the previous event, the q-axis current is 0. The inverter outputs balanced currents as shown in Fig. 3-35 (b). Both power, voltage and current results in these two tests match well among different platforms.

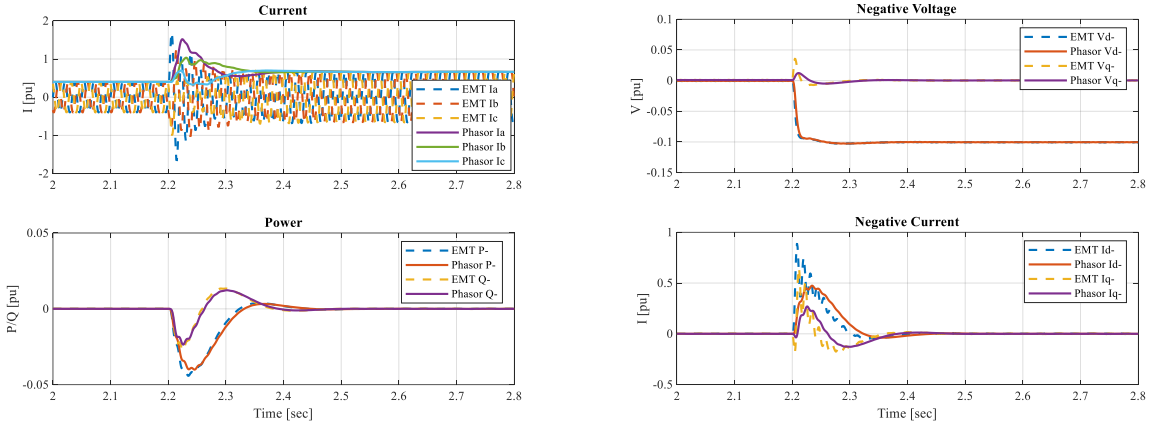

(a) P and Q (b) Angle difference and internal voltage

Fig. 3-35 Case II: Results of unbalanced grid voltage drop in PSCAD and GridLAB-D models. The grid phase B and phase C voltages drop from 1 to 0.7 pu. Reactive power is regulated to be zero.

In this scenario, grid voltages v_{gb} and v_{gc} fall to 0.7 pu at t = 2.2 s. The negative sequence currents are regulated two times of the negative sequence voltages. Fig. 3-36 shows the response when this event is applied. It can be seen that with the regulation, the GFM inverter delivers unbalanced current with phase C current lower than phase A and B. On the other hand, the inverter negative d-axis and q-axis currents are twice of their negative voltages, respectively. From the results, it can be seen that the phasor model can capture distribution system dynamics in fault events closer to the EMT switching model.

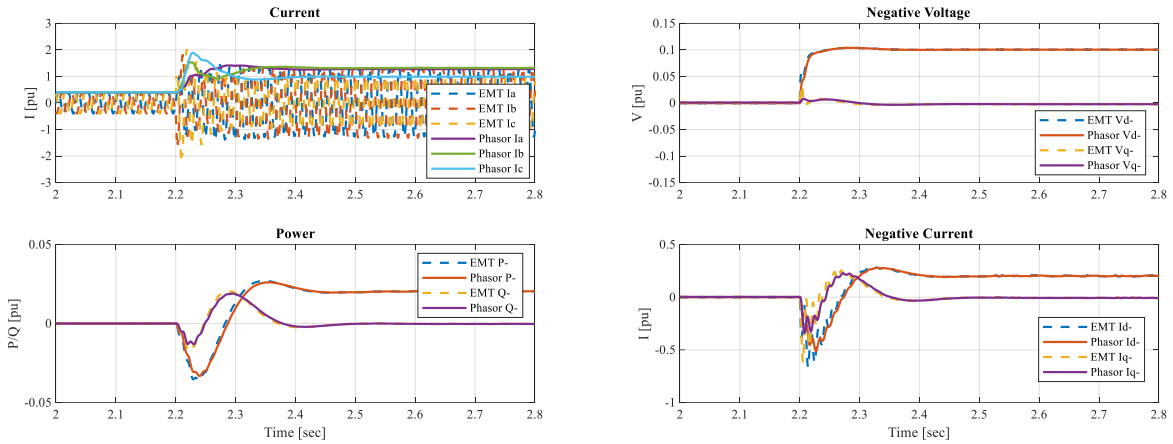

(a) P and Q (b) Angle difference and internal voltage

Fig. 3-36 Case III: Results of unbalanced grid voltage drop in PSCAD and GridLAB-D models. The grid phase B and phase C voltages drop from 1 to 0.7 pu. Reactive power is regulated to be two times of negative sequence voltage.

3.3.4 Black-Box IBR Model and Validation

Our research concentrated on the development, validation, and assessment of black-box models (BBMs) for grid-connected inverter-based resources (IBRs). The methodology commenced with an exhaustive literature review encompassing various black-box modeling techniques, culminating in the adoption of a data-driven ML approach—specifically, a convolutional neural network—owing to its demonstrated superior precision.

The AI-based BBM was formulated, trained, and validated within the GridLAB-D simulation environment, leveraging empirical field data and incorporating validation with an additional commercial IBR product. The validation process adhered to the standard test cases established under **M 3.5.12**, ensuring that the model accurately captured both steady-state and dynamic performance characteristics when integrated into a GridLAB-D software. The models were rigorously tested under disturbance events including balanced and unbalanced faults, voltage and frequency ride through, and short-circuit ratio assessments. A significant achievement was the successful integration of the BBM of IBR into an open-source power distribution system simulation software while achieving active power, reactive power, voltage, and output current predictions with an accuracy greater than 95%. This evaluation in a distribution feeder setup helped assess the applicability and limitations of black-box modeling compared to white- and gray-box approaches.

Therefore, the final milestone was successfully achieved with the validation of the black-box model against multiple IBR products, rigorous model quality testing under standard scenarios, and development of user guide to provide clarity on the intended applications, advantages, limitations, and best practices for using black-box modeling approach. These efforts contribute to a more reliable framework for black-box modeling in distribution system studies, enhancing simulation accuracy and applicability for real-world grid integration studies.

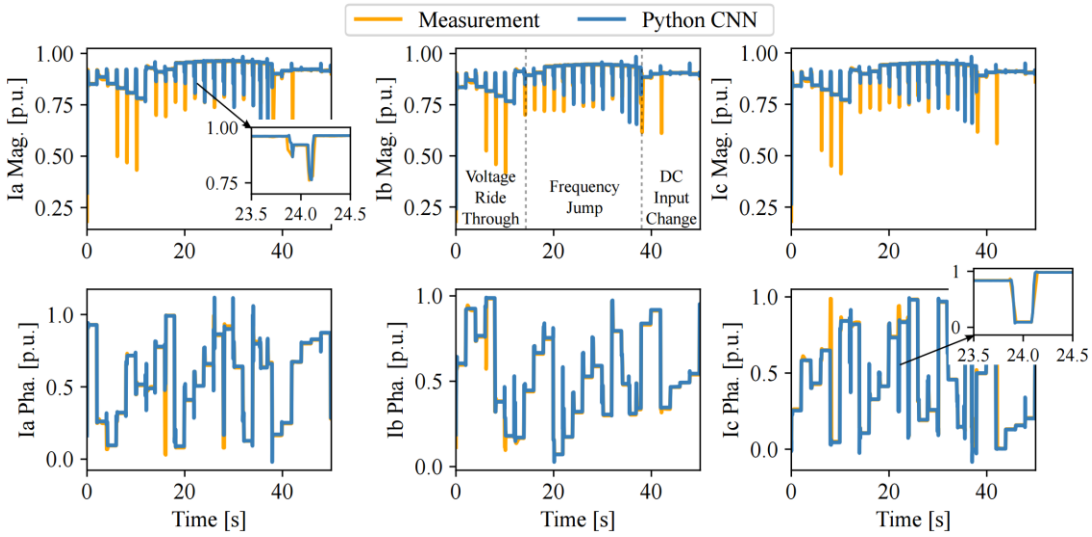

Fig. 3-37 Three-phase output current magnitudes and phase angles measurement from the commercial inverter (IBR-1) versus the outputs from the DL CNN model with the training data from IBR-1.

Fig. *3-37* shows the performance of the trained model in representing the dynamics of IBR-1 using training data. The results indicate that the trained DL model accurately represents the wide dynamic operating range of the commercial IBR with minimal error, achieving NRMSE of below 4.5%.

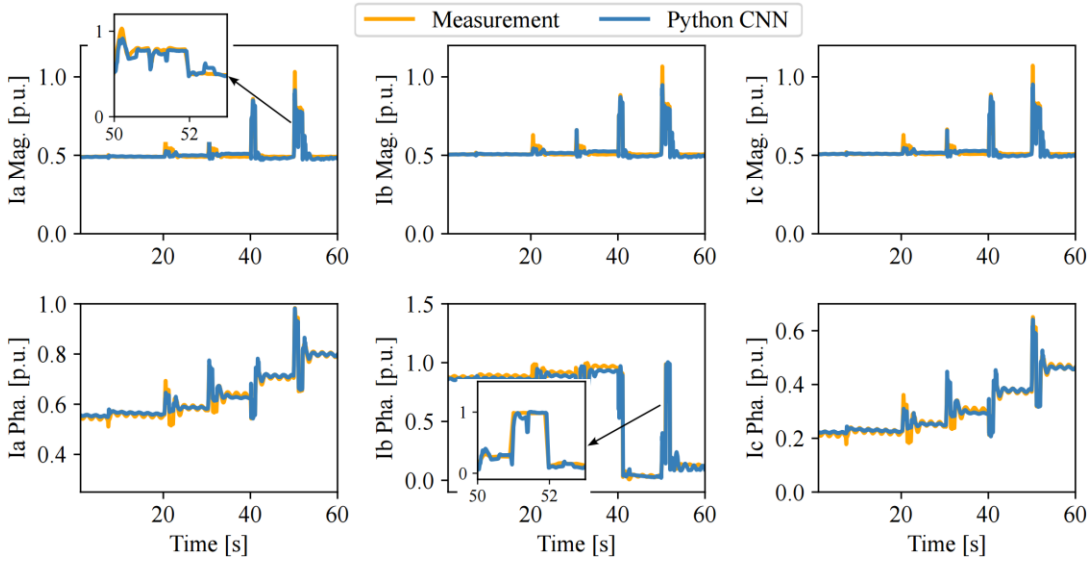

Fig. 3-38 Three-phase output current magnitudes and phase angles measurement from the commercial inverter (IBR-2) versus the outputs from the DL CNN model with the validation data from IBR-2.

Fig. 3-38 shows the validation performance of the tuned model with new data from the new commercial IBR. The results confirm that the model accurately represents the dynamics of the new commercial IBR product under various operating scenarios, with a minimal validation NRMSE below 5%.

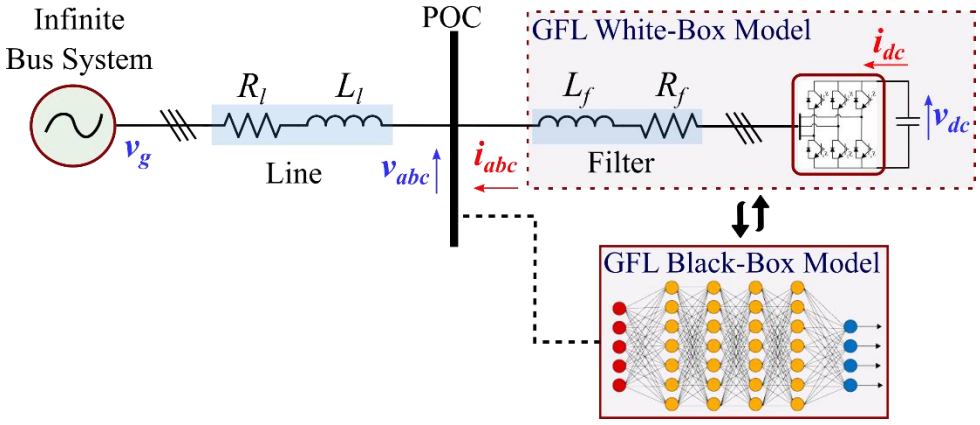

Fig. 3-39 CNN-BBM integration to the infinite bus system in GridLAB-D framework.

The CNN-BBM was then integrated with an infinite source in the GridLAB-D framework, as shown in Fig. 3-39. Its performance was compared against both the Python CNN-BBM and original measurement data demonstrating that the CNN-BBM accurately represents the dynamics of commercial GFL IBRs.

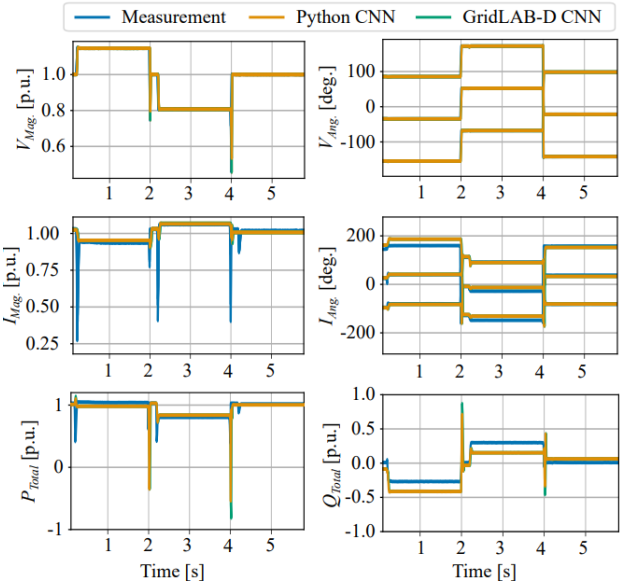

Fig. 3-40 Three-phase input voltage magnitude and angle, output current magnitude and angle, and active and reactive power measurement from the commercial IBRs versus the response from the CNN model in python versus the CNN model integrated into the open-source solver (GridLAB-D).

Fig. 3-40 displays the magnitude of the output current from the GE inverter, GridLAB-D model, and CNN-based black-box model during voltage-ride through and DC input change. The performance suggests that the GridLAB-D model closely follows the response observed in the black-box model and HIL measurement data, with NRMSE of below 4.5%.

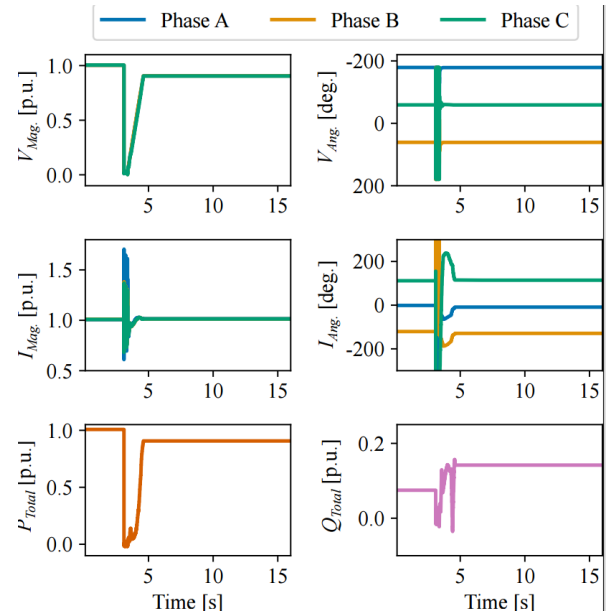

Fig. 3-41 Outputs of the proposed DL model during LVRT when integrated into a infinite bus system within GridLAB-D software framework.

Fig. 3-41 presents the output of the GridLAB-D DL model during a low voltage ride-through (LVRT) test, where the voltage at the point of interconnection (POI) is reduced from 1.0 p.u. to 0.9 p.u. As expected, when the POI voltage dropped to zero, both active and reactive power at the POI dropped to zero. The active power recovered shortly after the voltage ramped up from zero. When the POI voltage stabilized at 0.9 p.u., a small reduction in active power was observed due to the reactive power injection. Overall, the DL model remained stable and closely mirroring the dynamic behavior of a real IBR.

Therefore, this work developed a CNN-based deep learning model for GFL-controlled IBRs, addressing gaps in accuracy and flexibility. Trained on data from commercial IBRs under diverse grid conditions, including voltage and frequency ride-through events, it was successfully integrated into GridLAB-D for large-scale stability simulations. The model was validated against ERCOT standards, achieving an NRMSE under 5% for P and Q while meeting steady-state and dynamic performance expectations. This marks the first successful integration of a data-driven, ML-based IBR model into GridLAB-D, demonstrating its potential for power system stability and planning studies. However, the accuracy and robustness of black-box models depend on diverse training datasets, especially for extreme events like frequency jumps. This work paves the way for more advanced data-driven ML approaches for grid modeling and simulation frameworks.

3.3.5 Gray-Box Model and Validation

In recent years, the increased incorporation of renewable energy resources into distribution systems has emphasized the necessity for dynamic modeling of inverter-based resources (IBRs). Therefore, it has become essential to aggregate the modeling of distribution feeders, especially in behind-the-meter (BTM) sections, incorporating diverse IBRs. However, the integration of IBRs and load fluctuations has led to highly complex dynamical behaviors, presenting a significant challenge in modeling distribution systems.

3.3.5.1 Gray-box Modeling

To address the aforementioned challenge, we developed a gray-box modeling framework by encoding prior physical knowledge of the system in an optimization-based model and then embedding the output of the optimization-based model into the input of a data-driven model. We have tested the gray-box model algorithm for the BTM feeder in the MATLAB environment and demonstrated the effectiveness of the gray-box modeling approach. In addition, we have extracted the derived neural network that represents the gray-box model for the behind-the-meter (BTM) feeder and integrated the detailed codes into GridLAB-D.

To model a BTM feeder, we aim to capture a map between the inverter terminals and the service transformer. For the BTM feeder with IBRs, multiple inverters are usually connected to each other in complex and even unknown topologies. This makes it challenging to model and analyze the system. Kron reduction is known as a powerful method that can simplify the electrical network in power systems. With Kron reduction, the complex electrical network between inverters can be replaced with a simpler

equivalent one, in which every two nodes are connected with an impedance line. To show the process of Kron reduction for the BTM feeder with IBRs, we give the figure below,

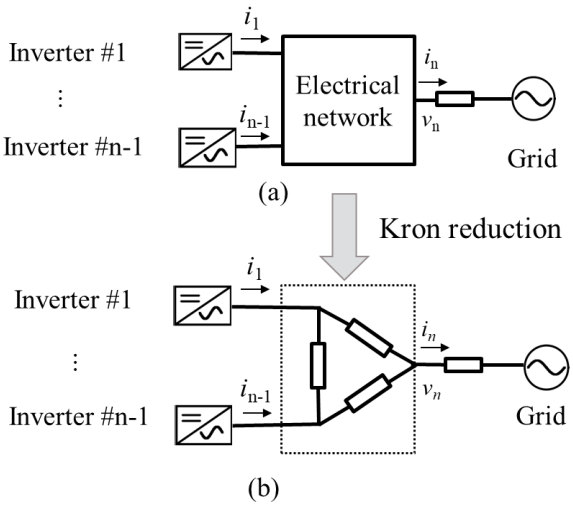

Fig. 3-42 (a) BTM feeder with IBRs (b) Equivalence model using Kron reduction.

In our gray-box modeling framework, we encode prior physical knowledge of the system in an optimization-based model and then incorporate the optimization-based model into a data-driven model. Without loss of generality, we select voltage and current at the service transformer as input u and output y, i.e., $u = v_n$, $y = i_n$. Input and output can also be reversed in some cases. Note that complete knowledge of the distribution system may not be available. For example, we only have information on the structures of the inverters and their control diagrams. To give a mathematical model for the BTM feeder, we use the Kron reduction technique to construct an equivalent model for the coupling network between inverters and service transformers. Then, with the prior knowledge and equivalence model, mathematical equations for the model are given as

$$y_w = f(U,p)$$

where y_w is the output from the optimization-based model, which provides an estimation for i_n. $f(\cdot)$ is a function constructed by the system dynamics. U is the input of the optimization-based model. Not only it includes the measured voltage at the service transformer, but it also includes measured current from the inverters, i.e., $U = [i_1, \cdots, i_{n-1}, vn]$. p is the parameters in the optimization-based model, such as the control parameters of the inverters and resistance and inductance of the impedance network in the equivalence model derived through Kron reduction. The parameters are identified by using the input-output data. Specifically, the parameters are optimized by solving a least-square optimization problem to minimize estimation errors.

Next, the output y_w from the optimization-based model and the input u are both used as the input of a data-driven model to form a gray-box model. That is, the estimated i_n from the optimization-based model and the measured voltage at the service transformer are both used as the input of the gray-box model. Then we have

$$\hat{y} = g([y_w, U]),$$

where $\hat{y}$ is the output of the gray-box model, which is the estimated value of i_n. $g(\cdot)$ is a data-driven model structure, which can be a linear time-invariant model, Hammerstein-Wiener model, or neural network. Without loss of generality, we use a neural network (NN) as the model structure. Thus, we complete the design of the gray-box modeling algorithm.

The framework of the gray-box modeling algorithm can be summarized below:

(1) Collect the input and output data for the BTM feeder with IBRs and divide them into a training dataset and a test dataset
(2) Complement prior knowledge with the equivalent network model using Kron reduction
(3) Determine mathematical equations with unknown parameters for the optimization-based model
(4) Estimate parameters in the optimization-based model using the training dataset
(5) Embed the output of the optimization-based model as an additional input of the data-driven model (represented using a NN), and train the NN with the training dataset
(6) Test the performance of the gray-box model using the test dataset

To integrate the developed gray-box model into GridLAB-D, we extract its mathematical equations below,

$$y = w_2\tanh(w_1u+b_1)+b_2,$$

where u and y are input and output vectors, respectively; w_1 and w_2 are weighting matrices, b_1 and b_2 are bias; $\tanh(\cdot)$ is the activation function. Typically, the input u includes the voltage at the service transformer and the estimated output from the optimization-based model; y is the estimated current from the developed gray-box model.

Fig. 3-43 shows the overall structure of the gray-box modeling algorithm. For the gray-box integration process in GridLAB-D, we initially collected the output voltage and current data in the phasor domain. We then trained the neural network in MATLAB, incorporating the output current from the optimization-based physical model as additional inputs. Eventually, we extracted the weights and the biases from the trained neural network and input them into the GridLAB-D environment for the gray-box model integration

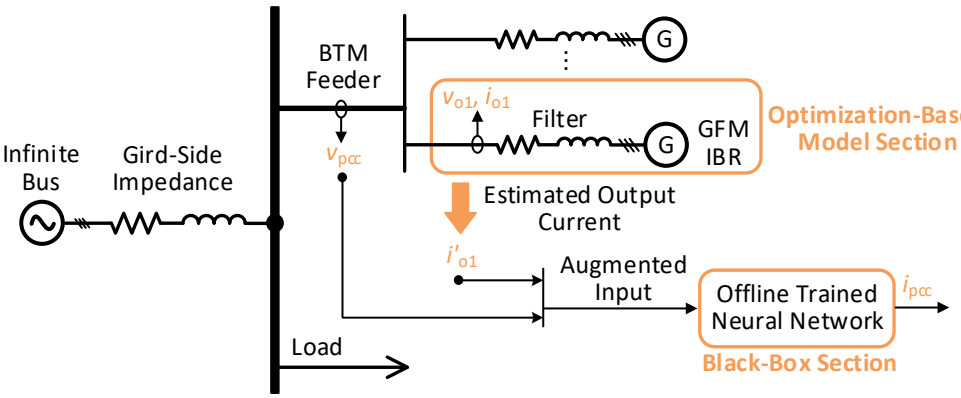

Fig. 3-43 The structure of the gray-box modeling algorithm.

3.3.5.2 Estimating NREL Data with Gray-Box Model

In this subsection, we tested the gray-box model to estimate the NREL data collected from NREL hardware testbed. Three different test scenarios are designated, as shown below:

(1) Scenario 1: Voltage magnitude change: The grid voltage magnitude changes from 1 pu to 1pu + Δpu (0.01, 0.02, 0.03, 0.04, 0.05).
(2) Scenario 2: Phase angle change: The grid voltage phase changes from the current phase to the current phase + Δθ (5°, 10°, 15°, 20°, 30°).
(3) Scenario 3: Frequency change: The grid voltage frequency changes from 60 Hz to 60+Δf (0.1, 0.2, 0.3, 0.4, 0.5).

The test results shown in Fig. *3-44*, it can be observed that the developed gray-box model can accurately estimate the dynamic behaviors of the NREL GFM IBR. Furthermore, the NRMSE error between the estimated values and the actual values is calculated with an average NRMSE of 5%.

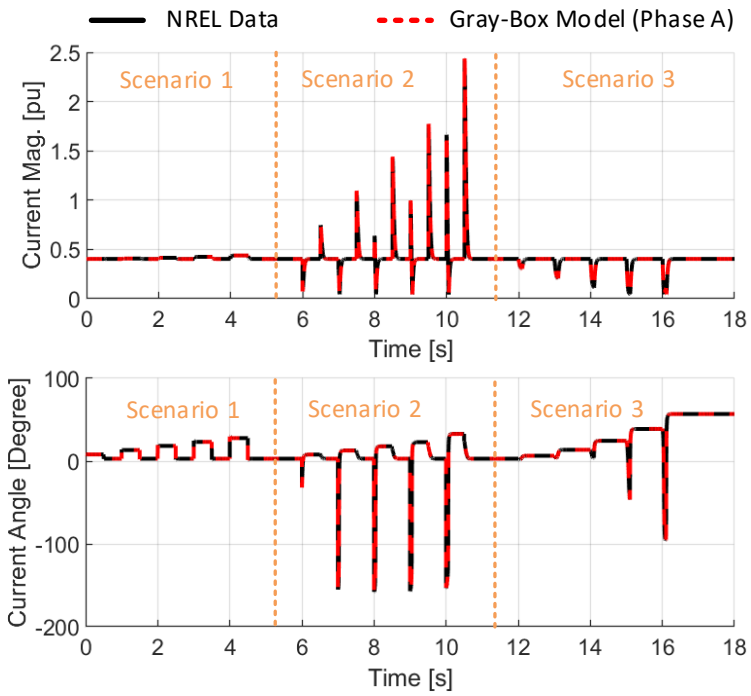

Fig. 3-44 Comparison of current phasor between gray-box model and NREL data under the grid voltage magnitude, phase, and frequency changes.

3.3.5.3 Testing Gray-Box Model in GridLab-D

We tested the gray-box model in GridLab-D under seven required test scenarios: small voltage disturbance, phase-angle-jump, small frequency disturbance, high voltage ride-through, low voltage ride-through, system strength, unbalanced and balanced fault. The detailed testing results are shown below.

In the small voltage disturbance case, we tested the gray-box model for the BTM GFM IBR under the small voltage magnitude disturbance condition. The line impedance is

adjusted to calculate SCR = 10. The neural network includes one hidden layer with two neurons. The grid voltage magnitude changes +/- 3% and returns to initial conditions. Specifically, as shown in Fig. *3-45*, the grid voltage magnitude increases from 1 pu to 1.03 pu at *t* = 2 s and returning to 1 pu at *t* = 3 s, followed by a decrease from 1 pu to 0.97 pu at *t* = 8 s and a return to 1 pu at *t* = 9 s.

In the phase angle jump case, we tested the gray-box model for the BTM GFM IBR under the phase angle jump condition. The line impedance is adjusted to calculate SCR = 10. The neural network includes one hidden layer with two neurons. The grid voltage phase angle changes +/- 25 degrees and returns to initial conditions. Specifically, as shown in Fig. *3-46*, the grid voltage phase angle increases 25 degrees at *t* = 2 s and returns at *t* = 3 s, followed by a decrease of 25 degrees at *t* = 8 s and a return to 1 pu at *t* = 9 s.

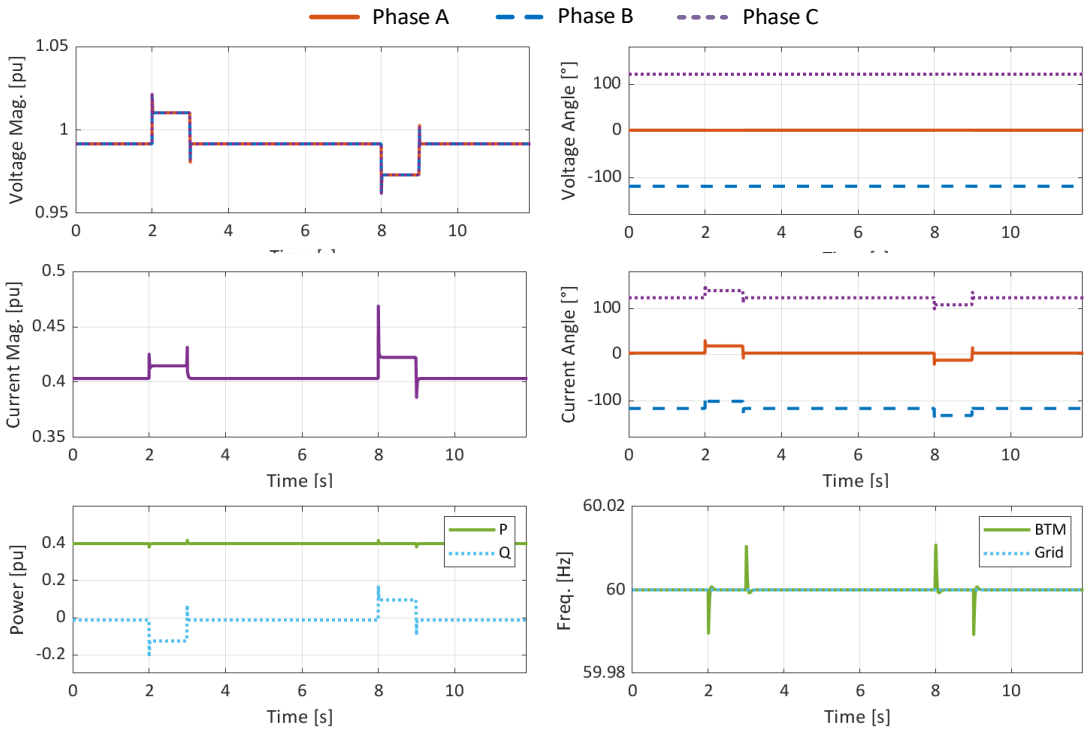

Fig. 3-45 GridLab-D test results under small voltage disturbance condition.

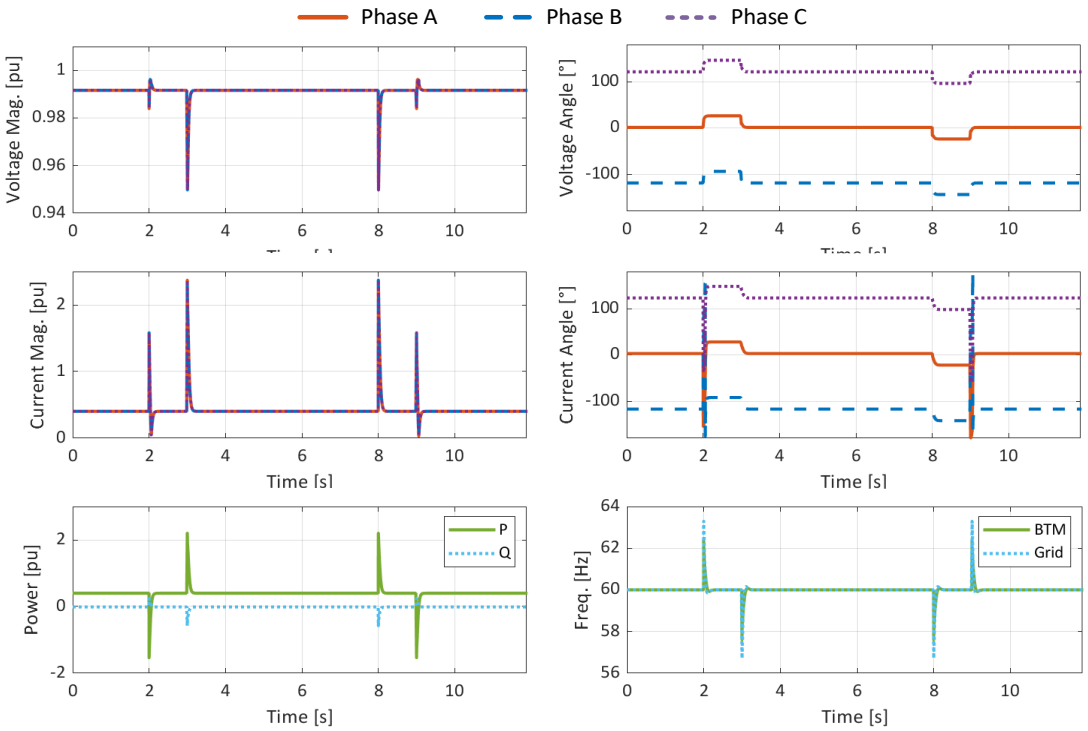

Fig. 3-46 GridLab-D test results under phase angle jump condition.

In the small frequency disturbance case, we tested the gray-box model for the BTM GFM IBR under the small frequency disturbance condition. The line impedance is adjusted to calculate SCR = 10. The neural network includes one hidden layer with two neurons. The grid voltage frequency changes +/- 0.3 Hz and returns back to 60 Hz. Specifically, as shown in Fig. 3-47, the grid voltage frequency increases from 60 Hz to 60.3 Hz at t = 2 s and returns to 60 Hz at t = 3 s, followed by a decrease from 60 Hz to 59.7 Hz at t = 8 s and a return to 60 Hz at t = 9 s.

In the high voltage ride-through case, we tested the gray-box model for the BTM GFM IBR under a high voltage ride-through profile. The line impedance is adjusted to calculate SCR = 10. The neural network includes one hidden layer with two neurons. The grid voltage magnitude increases from 1 pu to 1.2 pu and then decreases to 1.17 pu, 1.14 pu, and 1.1 pu. Specifically, as shown in Fig. *3-48*, the grid voltage magnitude increases from 1 pu to 1.2 pu at *t* = 2 s and then decreases to 1.17 pu at *t* = 3 s, 1.14 pu at *t* = 4 s, and 1.1 pu at *t* = 4.2 s. Eventually, the grid voltage magnitude returns back to 1 pu at *t* = 4.5 s.

In the low voltage ride-through case, we tested the gray-box model for the BTM GFM IBR under a low voltage ride-through profil. The line impedance is adjusted to calculate SCR = 10. The neural network includes one hidden layer with two neurons. The grid voltage magnitude decreases from 1 pu to 0 and then gradually increases to 0.9 pu. Specifically, as shown in Fig. *3-49*, the grid voltage magnitude decreases from 1 pu to 0 at *t* = 2 s and then gradually increases to 0.9 pu at *t* = 3.5 s. Eventually, the grid voltage magnitude returns back to 1 pu at *t* = 5 s.

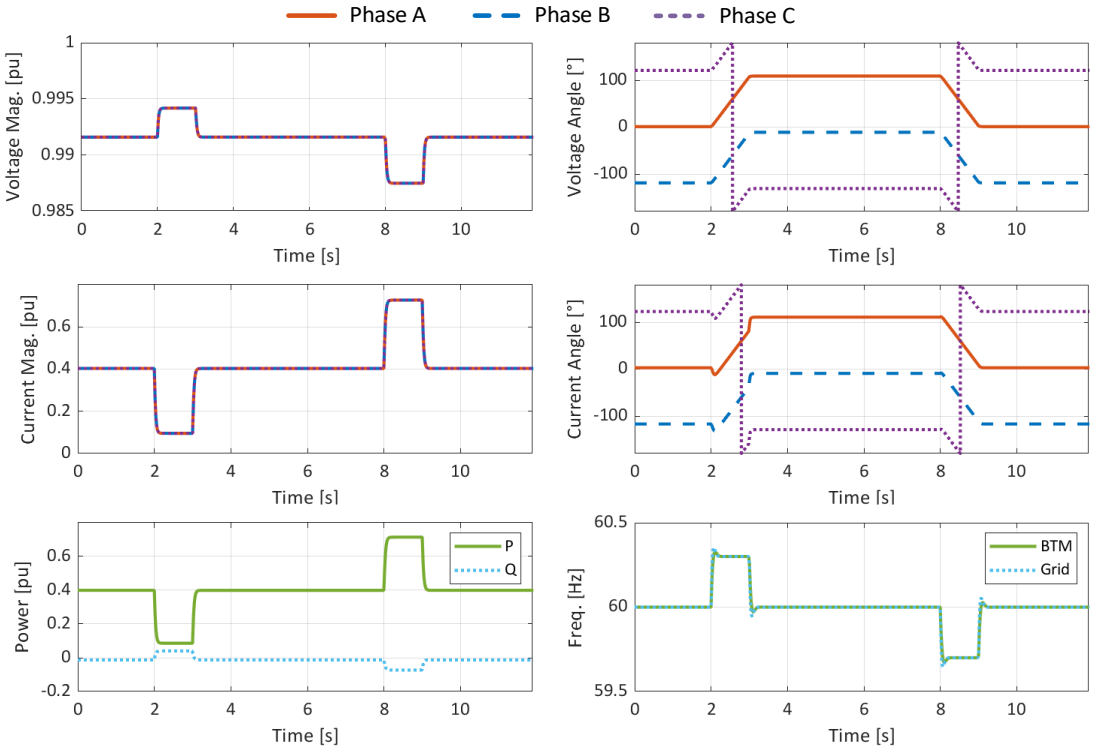

Fig. 3-47 GridLab-D test results under small frequency disturbance condition.

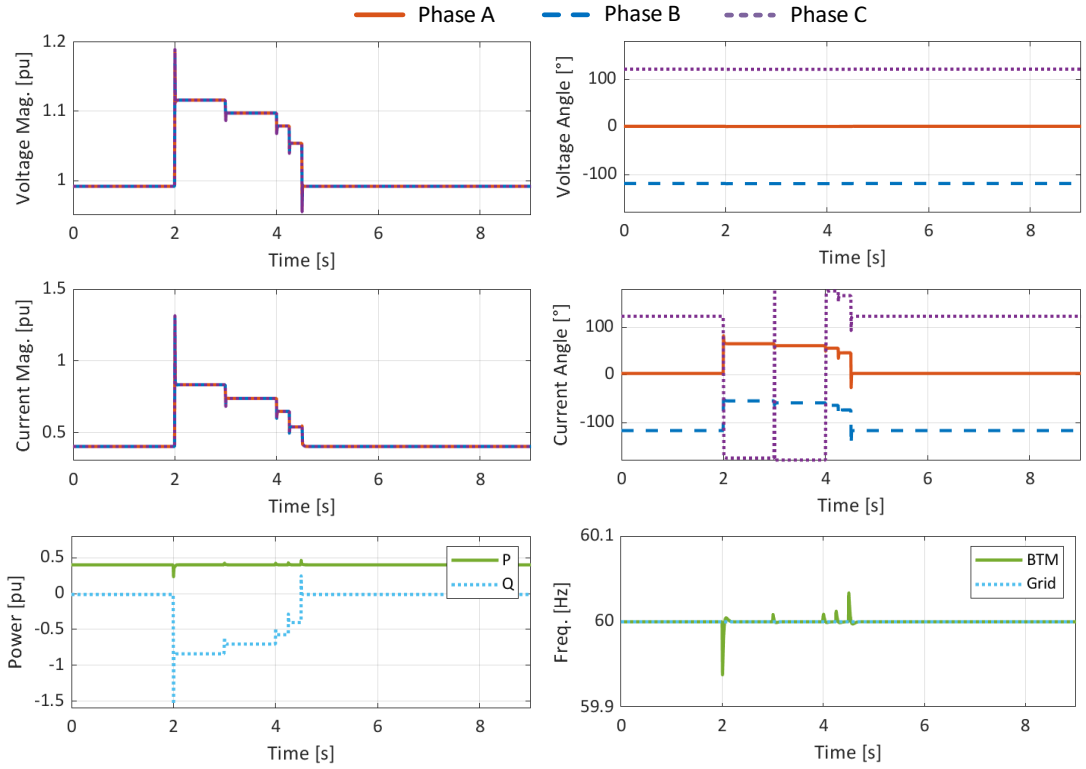

Fig. 3-48 GridLab-D test results under high voltage ride-through condition.

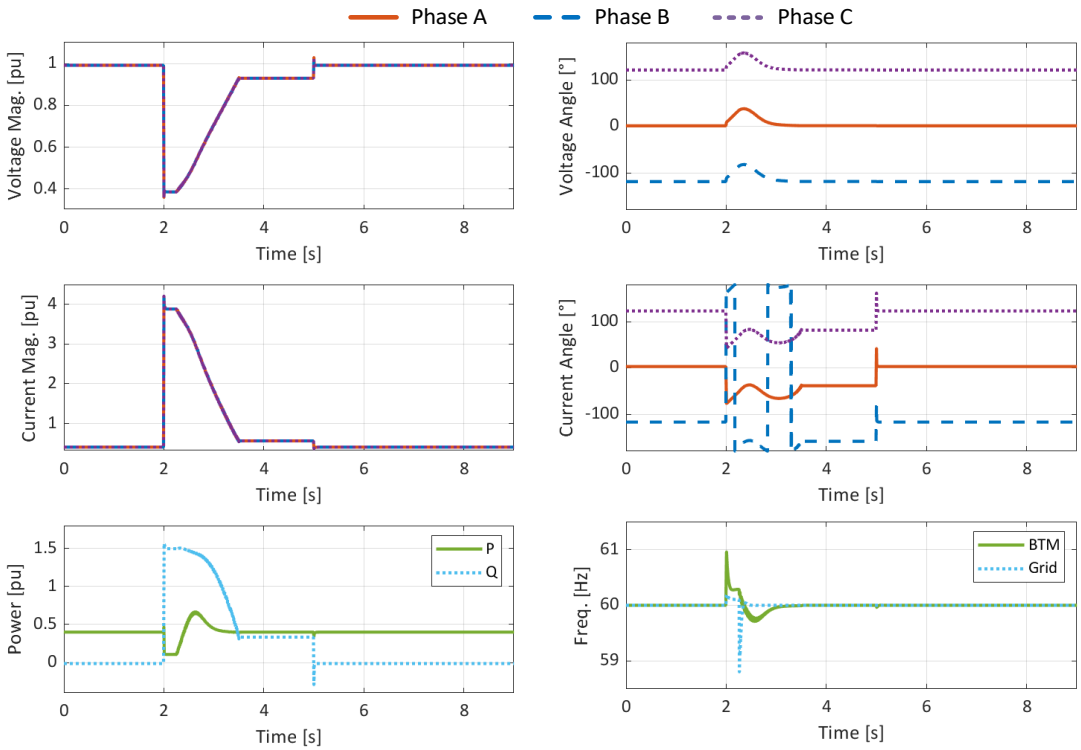

Fig. 3-49 GridLab-D test results under low voltage ride-through condition.

In the grid strength case, we tested the gray-box model for the BTM GFM IBR under the system strength test. The line impedance is adjusted to identify the threshold SCR = 7, meaning that SCR < 7 indicates the system instability. The neural network includes one hidden layer with two neurons. The small voltage disturbance testing scenario is selected as an example to show the results. Specifically, as shown Fig. *3-50*, the grid voltage magnitude increases from 1 pu to 1.03 pu at t = 2 s and returning to 1 pu at t = 3 s, followed by a decrease from 1 pu to 0.97 pu at t = 8 s and a return to 1 pu at t = 9 s.

Furthermore, we tested the gray-box model for the BTM GFM IBR when SCR = 6. The neural network includes one hidden layer with two neurons. The small voltage disturbance testing scenario is selected as an example to show the results. When the SCR is low, potential numerical issues may become worse when integrating data-driven models with physics-based models, which are typically represented using ordinary differential equations (ODEs). These issues often show up as numerical oscillations. Future work should focus on further developing the interface algorithms and numerical solvers capable of simultaneously handling both data-driven and physics-based models.

In the unbalanced and balanced fault case, we tested the gray-box model for the BTM GFM IBR under the fault test condition. The line impedance is adjusted to calculate SCR = 7. The neural network includes one hidden layer with two neurons. The unbalanced and balanced faults, i.e., Phase A fault, Phases A, B fault, Phases A, B, and C fault, are triggered. Specifically, as shown in Fig. 3-51, the load in phase A is shorted at t =2 s and connected back at t = 2.2 s. The loads in phases A and B are shorted at t = 4 s and

connected back at t = 4.2 s. The loads in phases A, B, and C are shorted at t = 6 s and connected back at t = 6.2 s.

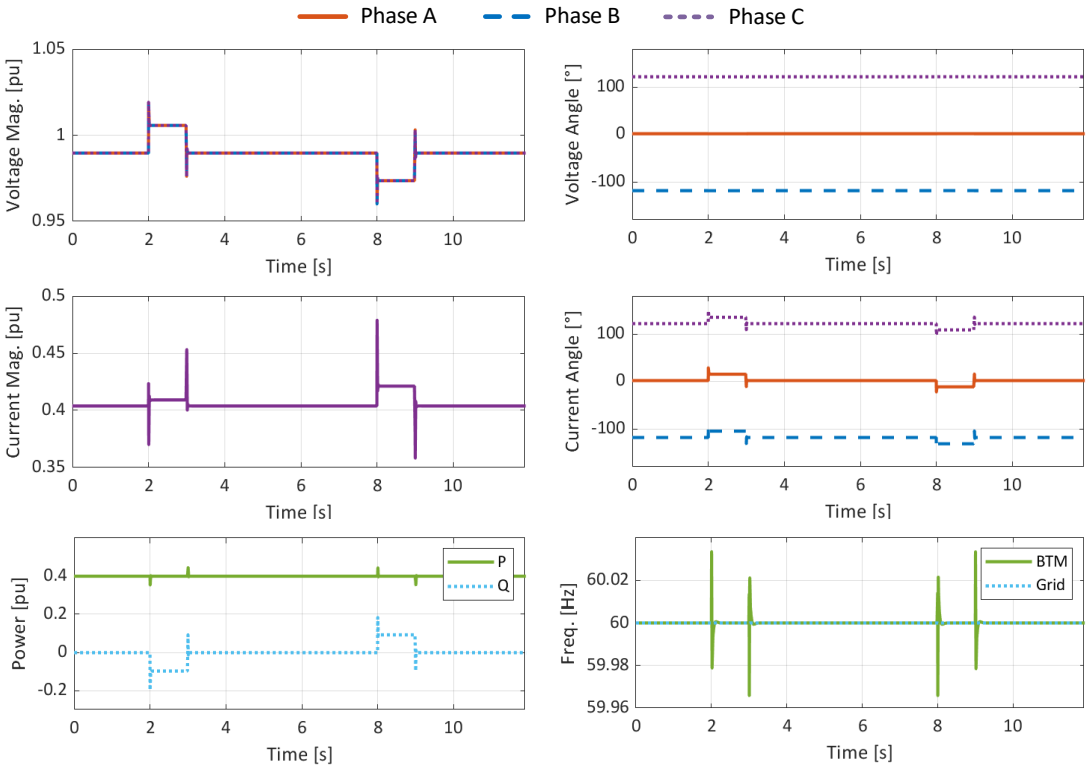

Fig. 3-50 GridLab-D test results under higher SCR condition.

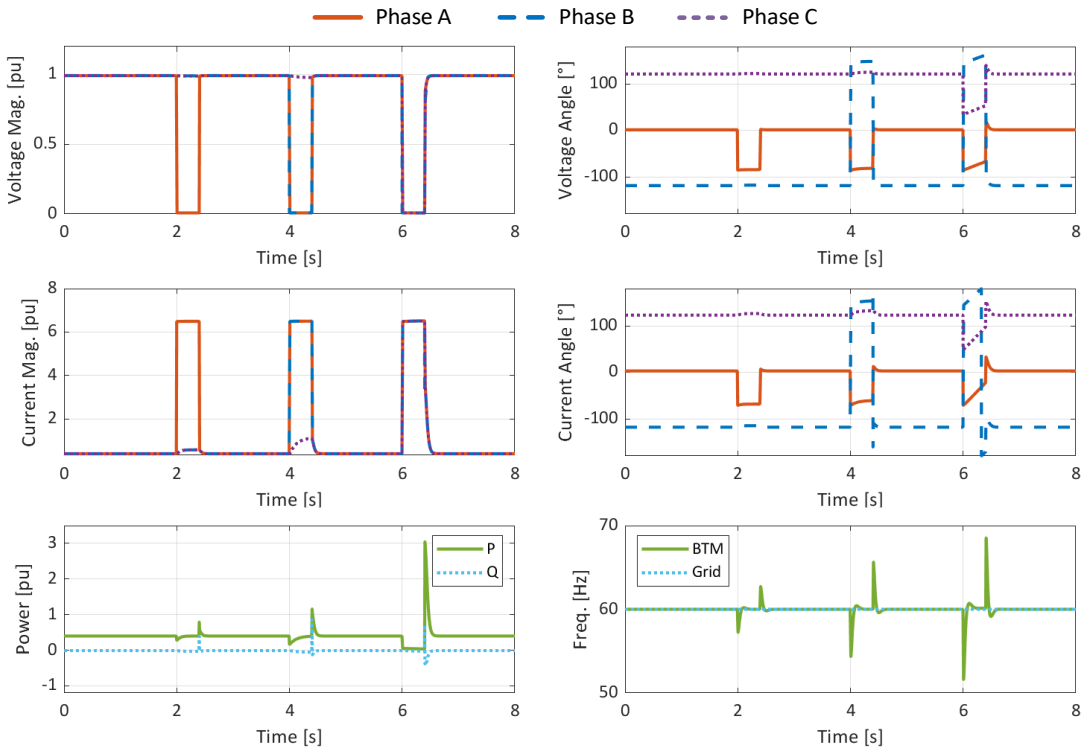

Fig. 3-51 GridLab-D test results unbalanced and balanced fault condition.

3.3.5.4 Subsection Conclusion and Discussion

Gray-box models are essentially physics-informed data-driven models, which present higher feasibility with reduced model complexity, and know more about the physical systems rather than purely relying on data-intensive approaches. Meanwhile, it is found that data diversity is critical to explore various scenarios for model training and validation; data preprocessing is also necessary to ensure a computationally efficient model training and validation process. The developed gray-box models have been fully integrated into GridLab-D and tested and validated with various test cases, including small voltage disturbance, phase-angle-jump, small frequency disturbance, high voltage ride-through, low voltage ride-through, system strength, unbalanced and balanced fault. Furthermore, the derived and integrated gray-box models show a high accuracy in terms of estimating the dynamic behaviors of BTM systems. Finally, the integrated models in GridLab-D exhibit expected behaviors in various test cases.

3.3.6 Motor Load Modeling

To study the interactive behaviors between the power grid and buildings, we first proposed the integrated thermal-electrical modeling for accurate characterization of the coupling between the electrical and mechanical components of behind-the-meter motor-driven building loads. The proposed modeling aims to enable and promote the detailed studies of the impacts of building loads on the power grid operations.

We first developed a thermal-electrical model in Modelica to effectively integrate the mechanical model of air-source heat pump with the electric model of doubly-feed induction motor. The proposed model will simulate the dynamics of electrical motor and interact with building devices, such as compressors, fans, and pumps, through transitional device model and variable frequency driven (VFD) model if VFD is used.

Then we performed model simplification over the proposed detailed thermal-electrical models to reduce the model complexities for fast simulation and enable scalable building load aggregation. After that, we defined a set of representative heat pump sizes that can be modeled and used in the integrated power grid simulation.

Finally, we proposed a load aggregation model that can determine a combination of heat pumps and refrigerators randomly so that the total electric power of such a combination will closely match the specified size of motor under a given feeder node. This approach will ensure the diversity of building loads under each feeder node.

We successfully integrated the aggregate motor-driven load models that into GridLAB-D including heat pump and refrigerator. Multiple load models were connected in each bus to account for different loads while operating the motor models in different operating conditions. To model the real dynamics of variable loads more accurately, it is necessary to account for operating scenarios within the aggregate model under the same bus. Therefore, the resulting implementation has been completed and tested to be successful.

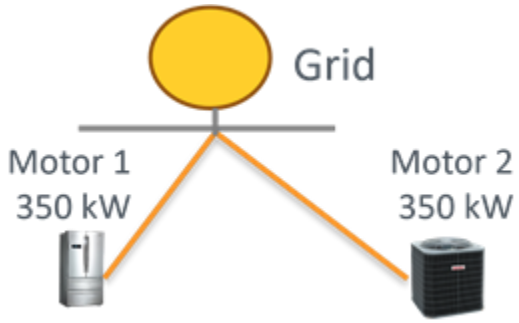

Fig. 3-52 Representation of single motor loads under each bus.

Motor 1: 350 kW	*Motor 2: 350 kW*
▪ ***00:00, OFF***	▪ *00:00, OFF*
▪ ***2.001, ON***	▪ *1.001, ON*
▪ ***5.001, OFF***	▪ *7.001, OFF*
▪ ***8.001, ON***	▪ *10.001, ON*
▪ ***12.001, OFF***	
▪ ***16.001, ON***	
▪ ***19.001, OFF***	

Fig. 3-53 ON—OFF mode of operation for Motor Model.

The code has been thoroughly debugged, and the simulation results are shown below. Fig. 3-52 shows the single motor connected to each bus. Two motors of equal size of 350 kW were connected in each bus and the ON-OFF operating scenario was created to test the motor model dynamics. Fig. 3-54 shows the stator voltage and current of phase-A, measured active and reactive power during ON—OFF instances as shown in Fig. 3-53.

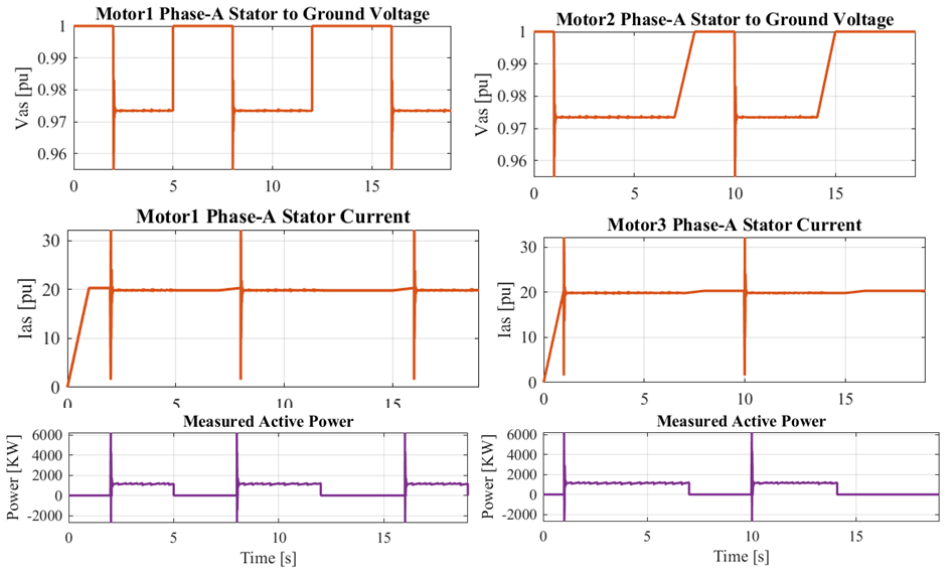

Fig. 3-54 Stator voltage and current of phase-A and measured active and reactive power when a single motor is connected to each bus.

Therefore, different operating scenarios within the aggregate model under the same/different bus are tested, resulting in the successful testing and completion of the implementation.

3.4 Model Validation, Integration, and Evaluation in a Realistic Feeder Environment in GridLAB-D

3.4.1 Distribution Feeder Model Development and Validation

To achieve the milestone of CYME model to GridLAB-D model conversion the team had first converted the CYME source file received from the ComED into a CYME data base file and then utilized a conversion script written in Python to generate the GridLaB-D model. The CYME model includes fifteen feeders among which two feeders cover the Bronzeville area. The rated voltage of both feeder is 12.50 kV.

During GridLAB-D model conversion the line capacitance information is captured which enables the inclusion of line charging in the GridLAB-D simulation as needed. The GridLAB-D model has all load objects in 100% constant power as a default setting. In addition, all load objects use the ZIP format. Macros are defined and incorporated for adjusting the ZIP components of load objects, which can change the feeder CVR factor.

The scripts used for the model conversion, power flow comparison, and ZIP load formatting are available from GitHub repositories. Here are the links:

- https://github.com/gridlab-d/tools/tree/master/conversion_scripts
- https://github.com/gridlab-d/tools/blob/master/python_scripts/GlmParser/parse_glm.py

To validate the model conversion process, the power flow results of the GridLAB-D model and the original CYME model are compared. Comparison results of the voltage magnitude in each phase are shown in Table 3-12. The average error of node voltages is much less than 0.1%, which meets the requirements specified in Milestone 1.2.2. Thus, the accuracy of the converted GridLAB-D model is validated.

Table 3-12 Comparison of voltage magnitude in each phase.

Feeder ID		Z13757	Z17455
Rated VLL (kV)		12.50	12.50
Number of Energized Nodes		440	125
Phase A Node Voltage Magnitude	Max	0.0021661202%	0.0004295394%
	Min	0.0000050576%	0.0000050576%
	Avg	0.0015553105%	0.0003538406%
Phase B Node Voltage Magnitude	Max	0.0026118322%	0.0002781408%
	Min	0.0000219017%	0.0000219017%
	Avg	0.0018014466%	0.0002247935%
Phase C Node Voltage Magnitude	Max	0.0033066077%	0.0002565626%
	Min	0.0000092686%	0.0000092686%
	Avg	0.0022924205%	0.0002010034%

3.4.2 Micro-PMU and PQ Meter Data Collection:

ComEd has deployed 25 Phasor Measurement Units (PMUs) and 3 Power Quality (PQ) meters in the Bronzeville Community Microgrid (BCM) footprint. Fig. 3-55 shows the simplified single-line diagram of the BCM. It consists of two feeders connected to two substations via two point-of-interconnection switches—POI-1 and POI-2. These two feeders can be interconnected via three tie-switches—T1, T2, and T3—to transfer load from one feeder to another. BCM is fed by a mixture of 3 distributed energy resources (DERs)—a 4.8 MW gas generator, a 750 kW photovoltaic (PV) system, and a 500 kW/2000 kWh battery energy storage system (BESS). The 26 micro-PMUs and 3 PQ meters are strategically installed in the BCM to capture the dynamics of events in the BCM, including the dynamics of the DERs. The team has compared the field measurements of voltage and frequency for the PMUs with the GridLAB-D simulation results. The team has ensured that the NRMSE of the voltage and frequency measurements is less than 5% for those 17 PMUs, which satisfies the requirements in Milestone M.3.4.11.

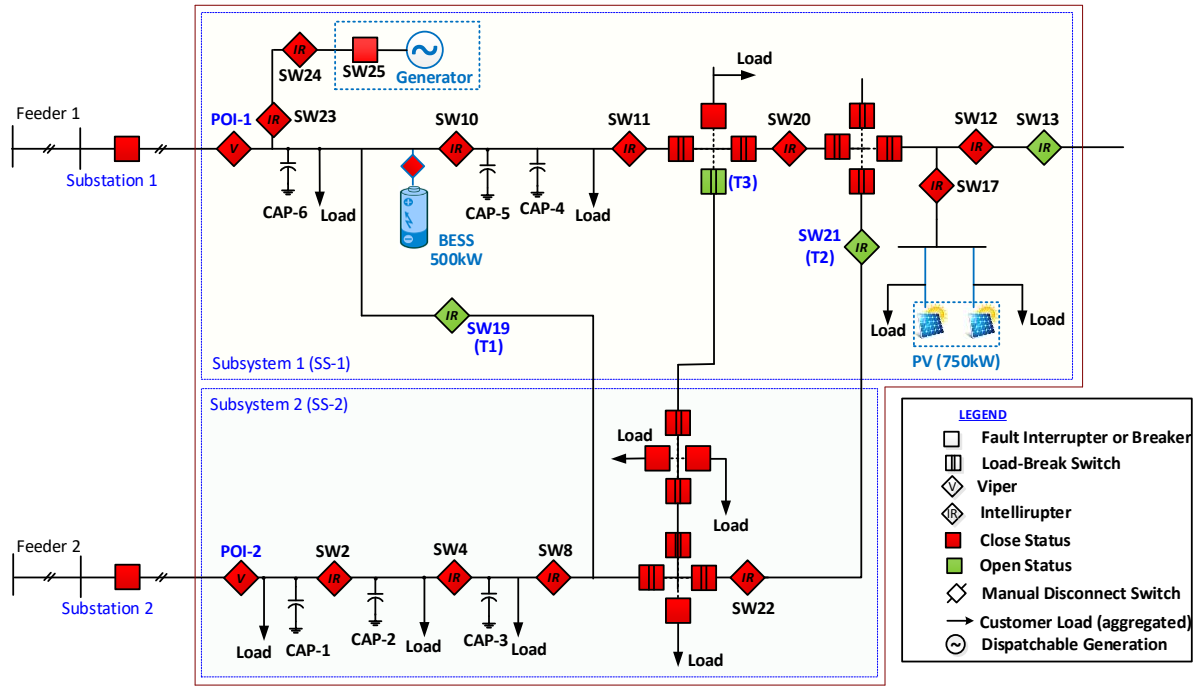

Fig. 3-55: Simplified single line diagram of Bronzeville Community Microgrid (BCM).

The single line diagram of the selected feeders Z13757 and Z17455 considered for this study is given in Fig. 3-55. Equivalent models of these feeders are developed in the GridLAB-D software. There are total 25 PMUs in these feeders. The field measurements selected for the comparison are collected on May 31, 2023. Among the 25 PMUs, PMU 34 could not be located in CYME and GridLAB-D model and therefore excluded from the comparison. Data from the PMUs P15, P12, P13, P30, and P37 were missing from the field measurements. Additionally, data from PMUs P28 and P27 were corrupted and because of that these PMUs are also excluded from the comparison.

Table 3-13 NRMSE of Voltage and Frequency measurements.

PMU Name	Voltage NRMSE (%)	Frequency NRMSE (%)	PMU Name	Voltage NRMSE (%)	Frequency NRMSE (%)
P14	V_a = 1.5	0.23	P7	V_a = 3.1	0.23
	V_b = 0.53			V_b = 2.12	
	V_c = 0.5			V_c = 2.8	
P16	V_a = 1.46	0.23	P2	V_a = 3.8	0.23
	V_b = 0.58			V_b = 4.02	
	V_c = 0.54			V_c = 3.47	
P17	V_a = 1.4	0.23	P29	V_a = 0.02	0.23
	V_b = 0.65			V_b = 0.014	
				V_c = 0.17	
P18	V_a = 0.64	0.23	P8	V_a = 1.5	0.23
	V_b = 0.7			V_b = 0.5	
	V_c = 0.7				
	V_a = 0.6			V_a = 1.71	

P19	$V_b = 0.6$	0.23	P23	$V_b = 0.6$	0.23
				$V_c = 0.5$	
P38	$V_a = 0.1$	0.23	P26	$V_a = 1.81$	0.23
	$V_b = 0.06$			$V_b = 0.03$	
	$V_c = 0.03$			$V_c = 0.09$	
P4	$V_a = 1.6$	0.23	P25	$V_a = 0.19$	0.23
	$V_b = 0.7$			$V_b = 0.2$	
	$V_c = 0.4$			$V_c = 0.19$	
P5	$V_a = 1.84$	0.23	P3	$V_a = 1.39$	0.23
	$V_b = 0.7$			$V_b = 0.4$	
	$V_c = 0.48$			$V_c = 0.2$	
P6	$V_a = 0.7$	0.23			
	$V_b = 0.09$				
	$V_c = 0.6$				

Table *3-13* presents the NRMSE of the voltage and frequency measurements from the 17 PMUs. For the selected PMUs, the GridLAB-D results closely match the field measurement data, with the NRMSE for voltage and frequency measurements within 5% and a confidence level exceeding 90% **[M 3.4.11]**. Although some differences can be observed, they can be attributed to (a) a lack of information regarding the actual load at the time the field measurements were captured and (b) the fact that the GridLAB-D models were developed based on a CYME model that is over a year old, during which time changes in the actual feeder configuration may have occurred.

3.4.3 Dynamic Simulation Results

To evaluate the response of the developed IBR models in a realistic feeder, the IBR models were connected to the ComEd feeder at specific nodes. A single-line diagram of the selected feeders (1 and 2) are depicted in Fig. 3-55. Features of the selected feeders are outlined in Table 3-14. Note that the IBR models used in this study have been previously validated through EMT simulations and field data in small-scale systems. Therefore, in this work, the validated models are applied to analyze a large-scale system.

Table 3-14 Features of the selected feeders: 1 and 2.

Feeder ID	1	2
Peak kW	5719.5	4343.8
Peak kVAR	2770.1	2103.8
Number of Energized Nodes	440	125
Spot Load	94	43
Overhead Line	219	113
Underground Cable	383	195

Switch	34	44
Breaker	4	1
Fuse	42	19
Recloser	12	12
Shunt Capacitor	7	8

3.4.3.1 Simulation Results

The black-box, gray-box, PNNL's white-box GFL, PNNL's white-box GFM (droop-based), and GE's white-box GFL inverter models are connected to the ComEd feeder. Fig. 3-56 illustrates the feeder configuration for the scenario involving a balanced fault event with the black-box and gray-box IBRs located close to the source node. Fig. 3-57 illustrates the responses of the different IBRs during a balanced three-phase fault in Feeder 1. The results in Fig. 3-57 indicate that the IBRs reach the pre-fault steady-state conditions when the fault event is cleared. Similar other case studies are also considered, which are not provided in this document due to restrictions in page limits. These results demonstrate the completion of Milestone **[M 3.5.15]**, which requires the integration of white-, black-, and gray-box IBR models in the ComEd feeder model in GridLAB-D.

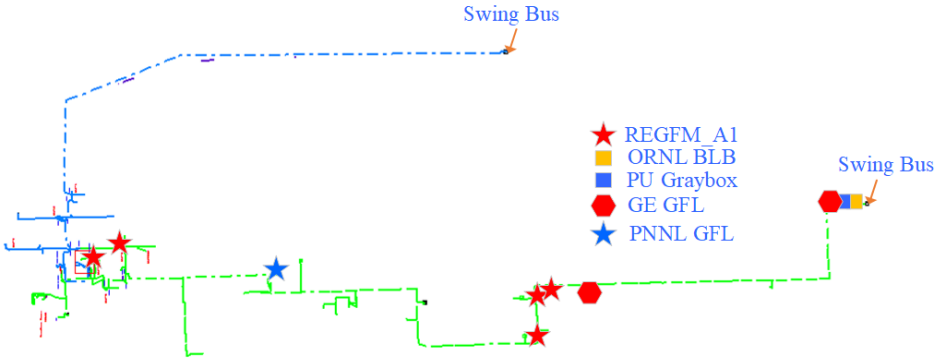

Fig. 3-56: Feeder configuration. Black-Box and Gray-Box IBRs are connected to nodes close to the source (swing) node.

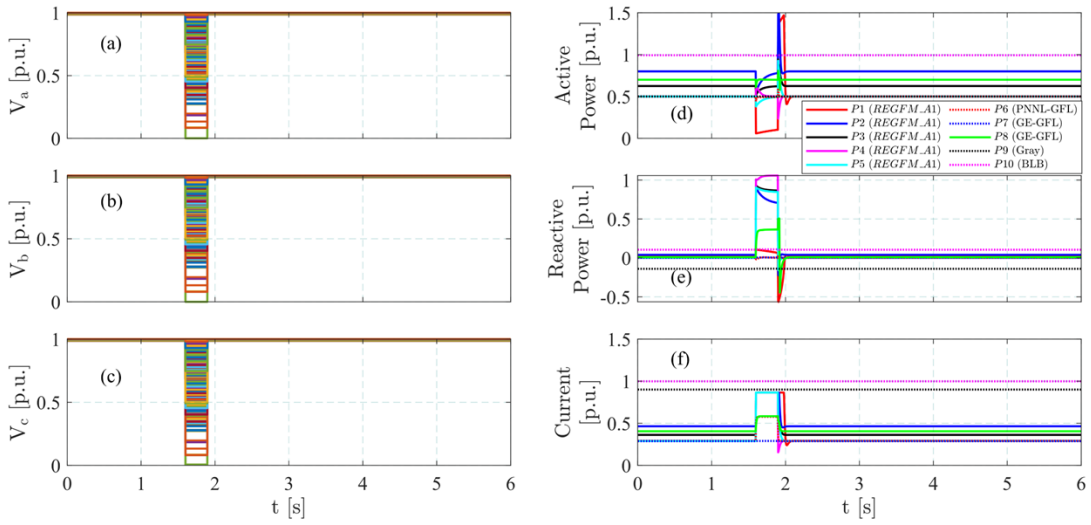

Fig. 3-57: Balanced fault event in feeder 1 with black-box and gray-box IBRs close to the swing node. (a)-(c) feeder nodes voltages, (d) IBRs active power, (e) IBRs reactive power, and (f) IBRs current.

3.4.4 Subsection Conclusion and Discussion

Ten IBR models, including white-, black-, and gray-box models with GFMs and GFLs, were added to the ComEd feeder model, which has about 565 nodes. The IBRs were tested under various fault events, including balanced and unbalanced faults, load changes, and voltage and frequency step changes at different feeder locations. The simulation results met the expected requirements and aligned with milestone **M 3.5.15.** Notably, the simulations were very fast. For example, a 10-second simulation with 4ms time steps took about 50 seconds. It is important to note that GridALB-D can simulate the phasor dynamics of unbalanced distribution systems. However, it cannot replace the EMT solver. For example, GridLAB-D cannot capture harmonics and high-frequency oscillations (e.g., >30Hz) that may result from improper control design of IBRs. EMT solvers are needed to simulate those behaviors.

4 Significant Accomplishments and Conclusions

The major accomplishments of this project are summarized as follows.

(a) **GridLAB-D network solver enhancement for handling short-circuit faults**. The project team has updated GridLAB-D's solver, which previously could only handle high impedance fault conditions, and even then still had periodic convergence problems. The underlying solver was converted to a fixed-point iterative approach, which enabled solutions with very low impedance connections to the ground. With some further modifications, this enabled GridLAB-D to model both balanced and unbalanced faults for studying large-signal disturbances of distribution systems.

(b) The project team has developed **an integrated co-simulation platform** for studying distribution system transients and dynamics by leveraging and enhancing open-source and commercial simulation tools including GridLAB-D, HELICS, and PSCAD.

- **EMT & per-phase phasor co-simulation.** The project team has achieved the EMT & per-phase phasor co-simulation using GridLAB-D, HELICS, and PSCAD, enabling the black-box PSCAD inverter models developed by OEMs to be connected to a realistic distribution feeder environment in GridLAB-D to examine their impacts on large-scale systems. Specifically, an enhanced interface model was developed to prevent false tripping of the vendor-specific, black-box inverter models during disturbances, and an initialization algorithm was developed to ensure a seamless transition from the power flow mode to the dynamic co-simulation mode for feeder models that comprises both grid-forming and grid-following inverters.

(c) The project team has developed *white-, black-, and gray-box models* for IBRs and loads by using physics-based and data-driven ML approaches. These models have been validated using a variety of data sources, including EMT simulations, controller-hardware-in-the-loop testing, and hardware experimental results, and have been integrated into the open-source tool GridLAB-D.

- **White-box per-phase phasor grid-forming and grid-following IBR models.** This project team has developed the white-box per-phase phasor grid-forming and grid-following IBR models. The grid-following IBR model is embedded with grid-support functions including volt-var and frequency-watt that are specified in the IEEE Std. 1547. The grid-forming IBR model is based on the recently developed WECC standard library virtual synchronous machine grid-forming inverter model—REGFM_B1. Both models work for a variety of disturbances, including balanced and unbalanced faults in distribution systems.
- **Black-box grid-following IBR model.** The project team has developed a convolutional neural network (CNN)-based deep learning model for grid-following IBRs. The model was trained on based data from commercial IBRs under diverse grid conditions, including voltage and frequency ride-through events.
- **Gray-box BEM feeder models with IBRs and loads.** The project team has developed a gray-box behind-the-meter (BTM) feeder model that incorporates IBRs and loads by integrating physics-based modeling with data-driven neural

networks (NNs). The physics-based component, represented by ordinary differential equations, captures the fundamental control characteristics of inverters located in the BTM feeder and serves as the structural backbone of the model. The data-driven component, implemented via simplified NNs, corrects the discrepancies between measured data and the physical model outputs, enhancing overall model accuracy while enabling fast training.

(d) The project team has applied the co-simulation platform and IBR models to a realistic distribution feeder model provided by ComEd for planning studies. Specifically, ten IBR models, including white-, black-, and gray-box models for GFMs and GFLs, were added to the ComEd feeder model that has around 565 nodes. The power flow of the feeder model has been calibrated using data from 20+ micro-PMUs deployed in the field. The feeder model with IBRs has been tested under various disturbances in GridLAB-D, such as balanced and unbalanced faults, load switching, and voltage and frequency step changes. The utility partner ComEd has also conducted various simulations using the model and provided user feedback to the team. The results show that the developed co-simulation platform and IBR models allow engineers and researchers to simulate the transients and dynamics of distribution systems with a high penetration of distributed energy resources.

The outcomes of this project significantly advance transient and dynamic modeling capabilities for distribution systems and increase the confidence of utilities and operators in planning and operating systems with high levels of inverter-based DERs and variable loads.

5 Path Forward

Future R&D plans

- **System-level studies with enhanced IBR models**. This project mainly focuses on IBR model development and validation and has limited scope on system level studies. For the next step, it would be beneficial to perform a more comprehensive system-level studies using the developed models to better understand how the high penetration of DERs will impact distribution systems under various disturbances, especially for those severe faults such as evolving faults, multiple reclosing, and high-speed reclosing with no intentional delay, etc. In addition, it would also be beneficial to investigate how distribution systems interact with transmission systems through a T&D co-simulation using the developed models.
- **Distribution protection studies consider various IBR fault responses**. The high-fidelity IBR models and simulation platforms not only can be used to study the transient and dynamic behavior of distribution systems, but also can be used to study the distribution system protection. In the future, it would be beneficial to model different types of protective relays in GridLAB-D and investigate whether those relays can effectively protect the distribution feeder with a high penetration of IBRs. The simulation platform can also be used to test and analyze new protection algorithms, protection coordination, and Fault Location, Isolation, and Service Restoration (FLISR) strategies, etc.
- **Enhance the usability of GridLAB-D through improved user interface and visualization capabilities.** Currently, GridLAB-D offers limited user interface and data visualization, which may pose challenges for utility users. To facilitate broader industry adoption in the future, it would be beneficial to develop a more intuitive user interface and visualization capabilities.
- **Update GridLAB-D solver to handle ungrounded distribution feeders**. Under this project, the GridLAB-D solver has been updated to handle balanced and unbalanced short-circuit faults, however, one remaining limitation is that GridLAB-D can only model grounded distribution systems. Although this assumption is valid for most distribution systems in North America, it would be beneficial to further update the GridLAB-D solver and relevant component models such as lines and transformers to handle ungrounded distribution systems such as floating wye and delta-connected systems, which can further enlarge GridLAB-D's application scenarios.
- **EMT & per-phase phasor co-simulation enhancements**. The project team has developed an EMT & per-phase phasor co-simulation platform. However, more research work is still needed, such as to better understand when per-phase phasor simulation, full EMT simulation, or EMT & per-phase phasor co-simulation should be used for distribution system simulation with high DER penetration, and to explore iterative approaches for improving the accuracy of EMT & per-phase phasor co-simulation, etc. In addition, it would also be valuable to develop a methodology to determine the boundary for the EMT & per-phase phasor co-simulation. It is also important to understand the differences between distribution systems and transmission systems when selecting the co-simulation boundary.

- **Expand white-box IBR models in the GridLAB-D model library**. The project team has developed white-box, per-phase phasor grid-following and grid-forming IBR models in GridLAB-D, and validated them against some manufacturers' products. This work has set up the foundation of IBR modeling in GridLAB-D. However, different commercial IBRs may have different dynamic behaviors, especially under large-signal disturbances. This is mainly because today's IBR controls are not standardized yet, and different manufacturers may implement the IBR controls differently, resulting in different dynamic responses. Therefore, it would be important to further expand the white-box IBR models in the GridLAB-D model library to reflect the diverse dynamic behaviors of IBRs from a variety of commercial products, and the collaboration with IBR manufacturers would be very important to develop such models. In addition, it would also be beneficial to investigate whether the dynamics of the primary energy sources at the dc side should be modeled in the phasor domain or not, such as photovoltaic panels, battery energy storage, and wind turbines, etc., and how the dynamics at the dc side may impact the stability.
- **Further research on data-driven, ML-based black-/gray-box modeling**. The project team has integrated both the data-driven, ML-based black-box and gray-box IBR models into GridLAB-D. This work marks the first data-driven, ML-based IBR models that are integrated into phasor-based simulation tools, and demonstrates their potential for the power system stability simulations. However, this technology is still at its early stage, and further research is needed to advance this approach and better understand its applicability and limitations. Key research questions include **a)** determining how many test scenarios should be designed and what types of data should be collected to effectively train such models, **b)** identifying which AI algorithms are most appropriate for developing these models, and **c)** understanding the difference in computational time between data-driven, ML-based black-/gray-box models and physical models, and **d)** addressing the potential numerical stability issues that may arise from integrating both physics-based and data-driven, ML-based IBR models within the same network model, and developing new interface algorithms to improve numerical stability in simulations.

Commercialization and Technology Transfer plan

- **Enhance the usability of GridLAB-D to Facilitate Broader Industry Adoption.** To facilitate broader industry adoption of GridLAB-D in the future, it would be beneficial to develop a more intuitive user interface and visualization capabilities. The project team could work with more utility partners to collect their suggestions on designing such interfaces and visualization tools.
- **Integrate the white-box IBR models into commercial distribution system planning and simulation tools.** The white-box IBR models developed under this project have been rigorously tested and validated. For the next step, the project team will seek opportunities to integrate the models into commercial distribution planning tools such as CYME and Synergi to enable broader access.

- **Open-source the data-driven, ML-based black- and gray-box modeling approaches.** These methods are still in the early stages of development and are not yet ready for commercialization. However, as they mature, the team may consider collaborating with software vendors for licensing or open-sourcing them to enable broader technology transfer and public use.

6 Products

Publication

[1] Z. Chen, H. Liu, P. J. Hart, W. Du, F. Tuffner and U. C. Nwaneto, "Per-phase Phasor Modeling of GFL and GFM Inverters for Distribution System Dynamic Studies," *2024 IEEE Power & Energy Society Innovative Smart Grid Technologies Conference (ISGT)*, Washington, DC, USA, 2024, pp. 1-5.
[2] Z. Chen, H. Liu, P. J. Hart, W. Du, F. Tuffner and U. C. Nwaneto, "Phasor-Domain Modeling of Inverter Based Resources Considering Unbalanced Grid Faults," *2024 IEEE Power & Energy Society General Meeting (PESGM)*, Seattle, WA, USA, 2024, pp. 1-5.
[3] S. Subedi, L. Qiao, Y. Gui, Y. Xue, F. Tuffner and W. Du, "Deep Learning-Based Dynamic Modeling of Three-Phase Voltage Source Inverters," *2024 IEEE Energy Conversion Congress and Exposition (ECCE)*, Phoenix, AZ, USA, 2024, pp. 4450-4456, doi: 10.1109/ECCE55643.2024.10861015.
[4] S. Subedi, Y. Gui and Y. Xue, "Applications of Data-Driven Dynamic Modeling of Power Converters in Power Systems: An Overview," in *IEEE Transactions on Industry Applications*, doi: 10.1109/TIA.2025.3529797.
[5] J. Zhang, Y. Men, L. Ding, X. Lu and W. Du, “Gray-Box Modeling for Distribution Systems with Inverter-Based Resources: Integrating Physics-Based and Data-Driven Approaches,” *IEEE Transactions on Industry Applications,* vol. 60, no. 4, pp. 5490-5498, July-Aug. 2024.
[6] J. Zhang, Y. Men, L. Ding, X. Lu and W. Du, “Gray-Box Modeling for Distribution Systems with Inverter-Based Resources,” *in Proc. of IEEE Energy Conversion Congress and Exposition (ECCE)*, pp. 3124-3130, 2023.
[7] Y. Liu, W. Du and S. G. Abhyankar, "An Electromagnetic Transient and Three-Phase Phasor Co-Simulation Platform for Studying Distribution System Transients with High Penetration of DERs," *2023 IEEE Power & Energy Society General Meeting (PESGM)*, Orlando, FL, USA, 2023, pp. 1-5.
[8] L. Qiao, Y. Xue, Y. Gui, W. Du and F. F. Wang, "Comparative Study of Nonlinear Black-Box Modeling for Power Electronics Converters," *2023 IEEE Energy Conversion Congress and Exposition (ECCE)*, Nashville, TN, USA, 2023, pp. 1446-1452.
[9] U. C. Nwaneto, Y. Liu, W. Du, F. K. Tuffner, Z. Chen and H. Liu, "Improvement of the Interface Models of a Per-Phase Phasor/EMT Co-Simulation Platform for Studying Transients and Dynamics in Distribution Grids With IBRs," in *IEEE Transactions on Smart Grid*, doi: 10.1109/TSG.2025.3592672.
[10] S. Subedi, J. Choi, and Y. Xue, ‘Dynamic Modeling and Validation of AI Models of IBRs Within Open-Source Solver’, in *IEEE Transactions on Sustainable Energy*. (submitted).

Conference Panel and Special Session

[1] ‘Transient and Dynamic Modeling and Control of Large-Scale, Resilient Distribution Systems with High Penetration of Inverter-based Distributed Energy Resources and Loads’, *2023 IEEE Energy Conversion Congress and Exposition (ECCE)*, Nashville, TN, USA.
[2] ‘Simulating Transients and Dynamics of Distribution Systems with High Penetration of Inverter-based Resources’, 2024 IEEE Power & Energy Society General Meeting (PESGM), Seattle, WA, USA.

Technical Presentation

[1] W. Du, ‘Integrated Multi-Fidelity Modeling and Co-Simulation Platform for Distribution System Transients with High Penetration of Inverter-Based Resources’, *2023 IEEE Energy Conversion Congress and Exposition (ECCE)*, Nashville, TN, USA.
[2] R. Sharma, ‘Advanced Sensor Deployment and Use Cases at ComEd’, *2023 IEEE Energy Conversion Congress and Exposition (ECCE)*, Nashville, TN, USA.
[3] H. Liu and Z. Chen, ‘Generic Grid-Following (GFL) and Grid-Forming (GFM) Inverter Models for Distribution System Studies’, *2023 IEEE Energy Conversion Congress and Exposition (ECCE)*, Nashville, TN, USA.

[4] Y. Xue, 'Black-Box Modeling of Solar PV Inverters Using Recurrent Neural Network', *2023 IEEE Energy Conversion Congress and Exposition (ECCE)*, Nashville, TN, USA.
[5] F. Tuffner, 'Power System Modeling of Electric Vehicles, Motors, and Other Complex Loads – What Level of Detail and When Is It Needed?', *2023 IEEE Energy Conversion Congress and Exposition (ECCE)*, Nashville, TN, USA.
[6] X. Lu, 'Gray-box Modeling of Behind-the-Meter (BTM) Distribution Feeders with High Penetration of Inverter-Based Resources (IBRs) and Varying Loads', 2023 IEEE Energy Conversion Congress and Exposition (ECCE), Nashville, TN, USA.
[7] W. Du, 'Integrated Multi-Fidelity Model and Co-Simulation Platform for Distribution System Transient and Dynamic Analysis (DistribuDyn Project Overview)', 2024 IEEE Power & Energy Society General Meeting (PESGM), Seattle, WA, USA.
[8] R. Sharma, 'Utility Perspective on the Need to Understand the Transient Behavior of Distribution Systems with a High Penetration of IBRs and DERs', 2024 IEEE Power & Energy Society General Meeting (PESGM), Seattle, WA, USA.
[9] F. Tuffner, 'Dynamic Simulation Capability of GridLAB-D', 2024 IEEE Power & Energy Society General Meeting (PESGM), Seattle, WA, USA.
[10] Z. Chen, 'Per-phase Phasor Domain Modeling and Validation for Distribution System Studies: Generic Grid-Following and Grid-Forming IBRs', 2024 IEEE Power & Energy Society General Meeting (PESGM), Seattle, WA, USA.
[11] U. Nwaneto, 'EMT and Per-phase Phasor Co-Simulation for Distribution System Transients Using GridLAB-D and PSCAD', 2024 IEEE Power & Energy Society General Meeting (PESGM), Seattle, WA, USA.
[12] X. Lu, 'Data-Driven Modeling of Distribution Feeders with A High Penetration Level of Inverter-Based Resources', 2024 IEEE Power & Energy Society General Meeting (PESGM), Seattle, WA, USA.
[13] S. Subedi, 'Data-Driven IBR Black-Box Modeling', 2024 IEEE Power & Energy Society General Meeting (PESGM), Seattle, WA, USA.

Model Source Code and User Guide

[1] Gray-Box IBR Model

User Guide: https://gridlab-d.shoutwiki.com/wiki/Spec:ibr_grayboxmodels

Source Code: https://github.com/gridlab-d/gridlab-d/issues/1443

[2] Black-Box IBR Bodel

User Guide: https://gridlab-d.shoutwiki.com/wiki/Spec:ibr_blackboxmodels

Source Code: https://github.com/gridlab-d/gridlab-d/issues/1443

[3] White-Box GFM and GFL IBR Models

User Guide: https://gridlab-d.shoutwiki.com/wiki/Spec:ibr_whiteboxmodels

Source Code: https://github.com/gridlab-d/gridlab-d/issues/1443

7 Project Team and Roles

The project team includes PNNL, ORNL, GE Vernova, Purdue University, and ComEd. The role and contributions of each team member are summarized as follows.

DOE: **JJ Dai** served as the initial technology manager for this project, which was later taken over by **Yi Yang** after JJ Dai left the DOE. **Bob Reedy** serves as the backup technology manager for this project.

PNNL: **Wei Du** is the PI and is responsible for the overall project progress and deliverables. **Frank Tuffner** is the co-PI and led the GridLAB-D network update work. He also helped other team members to get familiar with GridLAB-D modeling and simulation. **Yuan Liu** has developed the initial EMT & per-phase co-simulation platform using GridLAB-D, PSCAD, and HELICS. **Udoka Nwaneto** further improved the co-simulation platform by implementing an enhanced interface and an initialization algorithm. He also tested the white-box grid-forming IBR model developed by GE Vernova. **Shrirang Abhyankar** implemented modularized functions for typical control blocks in GridLAB-D to improve modeling efficiency. **Jing Xie** converted the ComEd feeder model from CYME to GridLAB-D. **Sheik Mohiuddin** calibrated the power flow of the ComEd feeder model using field micro-PMU data, and performed dynamic simulations for the ComEd feeder with high DER penetration using GridLAB-D. He also tested the black-box and gray-box models developed by ORNL and Purdue University.

ORNL: **Yaosuo Xue** is the ORNL co-PI and leads the development of IBR black-box modeling efforts and verified the model performance within the open-source environment. **Liang Qiao** developed the initial model training algorithms, compared different neural network structures, and selected the CNN structure and tested the developed CNN model of IBRs with advanced grid support functions such as IEEE 1547. **Sunil Subedi** further optimized the deep-learning network structure and training algorithms, converted the python model to C++ model, programmed and implemented the method in GridLAB-D, and tested the black-box model with multiple commercial and utility field data sets. He also tested the quality of the black-box models with ERCOT and NERC guidelines such as for voltage/frequency ride through, fault, short-circuit ratio., etc. **Jamie Lian** is the ORNL co-PI and is responsible for the load modeling work. **Jian Sun** developed the integrated thermal-electrical modeling for accurate characterization of the coupling between the electrical and mechanical components of behind-the-meter motor-driven building loads. **Yanfei Li** defined a set of representative heat pump sizes and calibrated the model parameters of these representative heat pump models.

GE Vernova: **Hanchao Liu** leads GE Vernova's project progress and deliverables, delivered black-box EMT model of grid-following IBR for co-simulation using GridLAB-D, PSCAD, and HELICS, and leads the efforts to improve model accuracy for white-box grid-following and grid-forming IBR models. **Zhe Chen** developed the white-box phasor domain IBR models in GridLAB-D, benchmarked dynamic simulations against control hardware-in-the-loop, PSCAD, Matlab/Simulink simulations as well as other commercial IBR products, and tested model quality covering the ERCOT and WECC criteria.

Purdue University: Xiaonan Lu serves as the PI from Purdue University and leads the efforts on gray-box modeling, testing, and integration into the open-source software tool GridLAB-D. **Yuxi Men** and **Lizhi Ding** are Ph.D. students at Purdue under Dr. Lu's supervision. Their contributions include developing the full suite of the gray-box modeling algorithms in MATLAB, validating the models using test measurements, and integrating the models into GridLAB-D. They are also involved in disseminating the gray-box modeling approach, including developing a dedicated wiki page on the GridLAB-D website. **Junhui Zhang** is a postdoctoral researcher at Purdue also under Dr. Lu's supervision, contributed to the initial literature review, conceptual design of the gray-box modeling framework, and preliminary algorithm testing.

ComEd: **Brooks Glisson** is the Senior Manager of the Smart Grid Emerging Technology Team at ComEd, responsible for overseeing the overall project progress and deliverables from ComEd's side. **Honghao Zheng** was the Manager of Grid Analytics, overseeing project execution, resource allocations, and coordinating with several internal and external teams. In April 2024, **Sri Raghavan Kothandaraman** took over Honghao's role. **Lindsay Vacek** was the Program Manager responsible for the financial aspects of the project, with **Guillermo Diaz Jr** transitioning into this role in 2023. **Roshan Sharma** is an engineer executing the project SOW, which includes collecting and sharing PMU and PQ meter data from Bronzeville Community Microgrid (BCM) feeders, installing and performing motor tests at ComEd's lab facility to capture the dynamic response of the IBRs, and conducting simulation tests of the developed GridLAB-D models of BCM feeders and the IBRs.

8 References

[1] ERCOT Dynamics Working Group, "ERCOT Dynamics Working Group Procedure Manual," Rev. 20, Oct. 5, 2023. [Online]. Available: https://www.ercot.com/files/docs/2023/05/25/dwg_procedure_manual_revision_19-ros-approved-05042023.docx. Accessed: Feb. 3, 2024.

[2] WECC Modeling and Validation Work Group, "WECC Criteria for Acceptance of New Dynamic Models." Feb. 2009 [Online]. Available: https://www.wecc.org/sites/default/files/documents/program/2024/WECC%20Criteria%20for%20Acceptance%20of%20New%20Dynamic%20Models.pdf. Accessed: May 13, 2025.

[3] North American Electric Reliability Corporation, " White Paper: Grid Forming Functional Specifications for BPS-Connected Battery Energy Storage Systems," Sept. 2023. [Online]. Available: https://www.nerc.com/comm/RSTC_Reliability_Guidelines/White_Paper_GFM_Functional_Specification.pdf. Accessed: May 13, 2025.

[4] IEEE Standards Association, " P2800.2™/D0.6 Draft Recommended Practice for Test and Verification Procedures for Inverter-Based Resources Interconnecting with Bulk Power Systems," unpublished, Dec. 2023.

[5] L. Fan, Z. Miao, S. Shah, P. Koralewicz, V. Gevorgian and J. Fu, "Data-Driven Dynamic Modeling in Power Systems: A Fresh Look on Inverter-Based Resource Modeling," in *IEEE Power and Energy Magazine*, vol. 20, no. 3, pp. 64-76, May-June 2022.

[6] B. Wang and G. Verbič, "Stability Analysis of Low-Voltage Distribution Feeders Operated as Islanded Microgrids," in IEEE Transactions on Smart Grid, vol. 12, no. 6, pp. 4681-4689, Nov. 2021.

[7] M. Ghazavi Dozein, B. C. Pal and P. Mancarella, "Dynamics of Inverter-Based Resources in Weak Distribution Grids," in IEEE Transactions on Power Systems, vol. 37, no. 5, pp. 3682-3692, Sept. 2022.

[8] J. Zhang, Y. Men, L. Ding, X. Lu and W. Du, "Gray-Box Modeling for Distribution Systems With Inverter-Based Resources: Integrating Physics-Based and Data-Driven Approaches," in *IEEE Transactions on Industry Applications*, vol. 60, no. 4, pp. 5490-5498, July-Aug. 2024.

[9] F. Dorfler and F. Bullo, "Kron Reduction of Graphs With Applications to Electrical Networks," in *IEEE Transactions on Circuits and Systems I: Regular Papers*, vol. 60, no. 1, pp. 150-163, Jan. 2013.

[10] Y. Zhang, A. Gole, W. Wu, B. Zhang, and H. Sun, “Development and analysis of applicability of a hybrid transient simulation platform combining TSA and EMT elements,” *IEEE Trans. Power Syst.*, vol. 28, no. 1, pp. 357–366, Feb. 2013.

[11] F. Plumier, P. Aristidou, C. Geuzaine, and T. Van Cutsem, “Co-simulation of electromagnetic transients and phasor models: A relaxation approach,” *IEEE Trans on Power Del.*, vol. 31, no. 5, pp. 2360–2369, 2016.

[12] HELICS, “*HELICS User Guide*,” Feb 25, 2025. [Online]. Available: https://docs.helics.org/en/latest/user-guide/fundamental_topics/federates.html. Accessed: May 16, 2025.

[13] W. Du *et al.*, "Modeling of Grid-Forming and Grid-Following Inverters for Dynamic Simulation of Large-Scale Distribution Systems," in *IEEE Transactions on Power Delivery*, vol. 36, no. 4, pp. 2035-2045, Aug. 2021.

[14] Du, Wei, Sebastian Achilles, Deepak Ramasubramanian, *et al.*, 2024. *Virtual Synchronous Machine Grid-Forming Inverter Model Specification (REGFM_B1)*. UNIFI-2024-6-1.

[15] Du, Wei, *Model specification of droop-controlled, grid-forming inverters (REGFM_A1)*. Pacific Northwest National Laboratory (PNNL), Richland, WA (United States); 2023 Sep 29.

Pacific Northwest National Laboratory

902 Battelle Boulevard
P.O. Box 999
Richland, WA 99354

1-888-375-PNNL (7665)

www.pnnl.gov